

Modern Astronomy

Part 1. Interstellar Medium (ISM)

Week 3

March 21 (Thursday), 2023

updated 03/18, 10:39

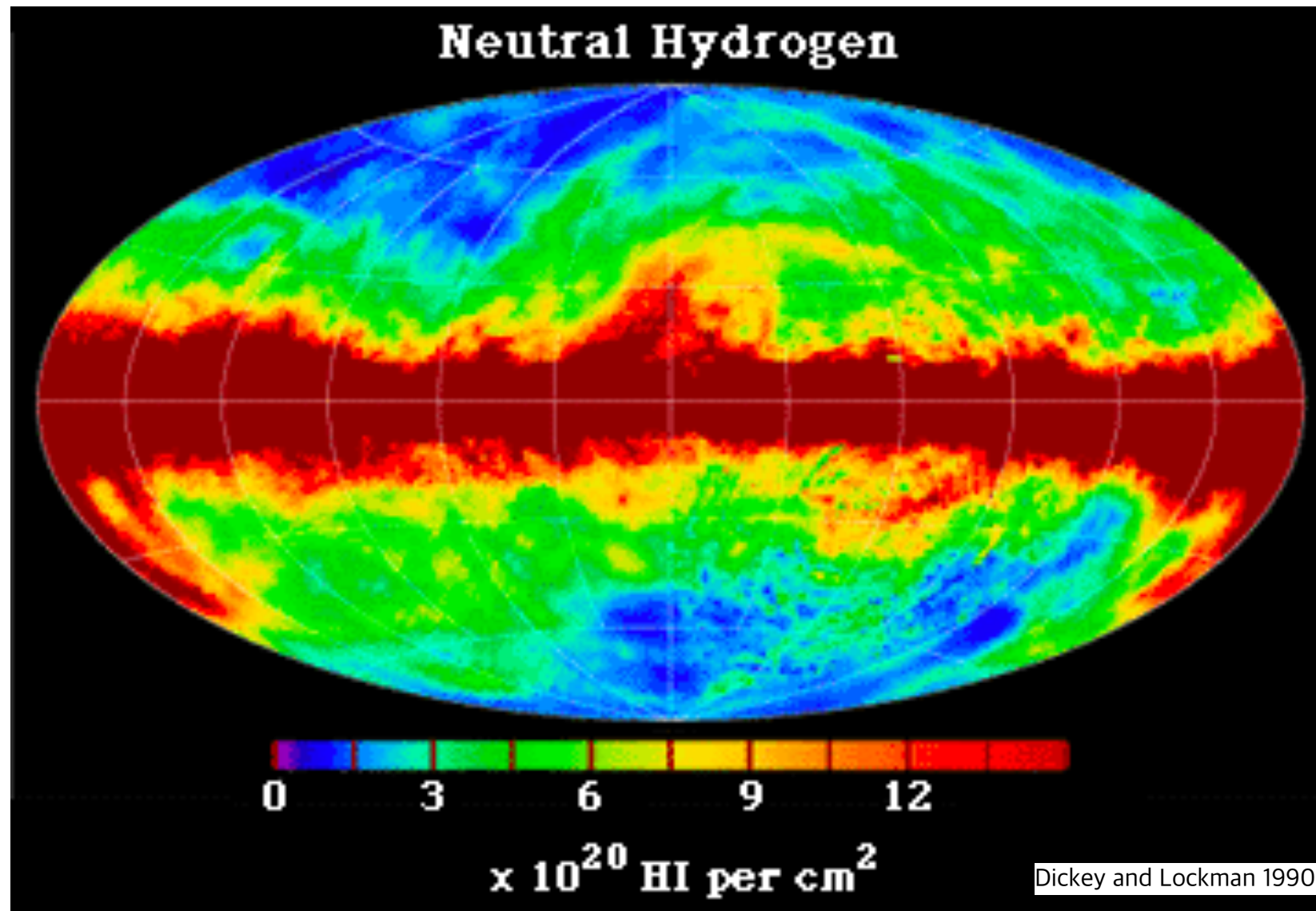
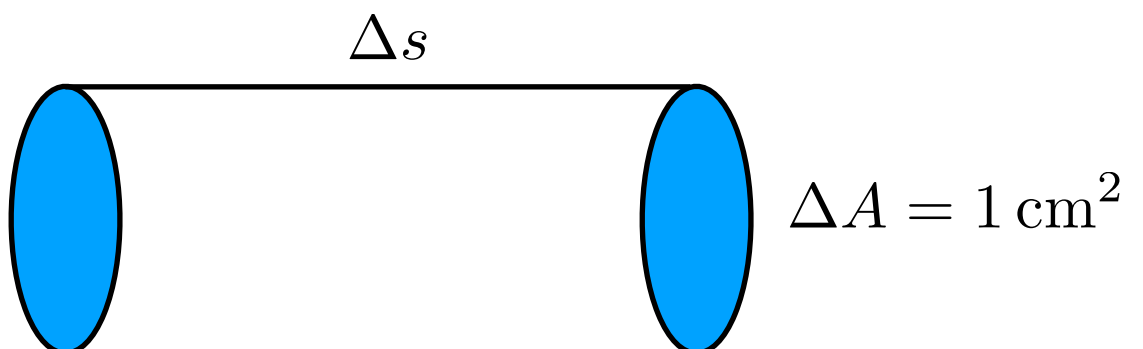
선광일 (Kwang-Il Seon)

UST / KASI

Typical H I column density in our Galaxy

- Column density

$$N_{\text{HI}} = n_{\text{HI}} \Delta s \text{ [cm}^{-2}\text{]} \iff N_{\text{HI}} = \frac{n_{\text{HI}} V}{\Delta A}$$



$$N_{\text{HI}} = 10^{20} - 10^{22} \text{ cm}^2$$

in our Galaxy, except for the Lockman hole

The Lockman hole is an area of the sky in which minimal amounts of neutral hydrogen gas are observed.

Column density in Lockman hole

$$N_{\text{HI}} \approx 5 \times 10^{19} \text{ cm}^2$$

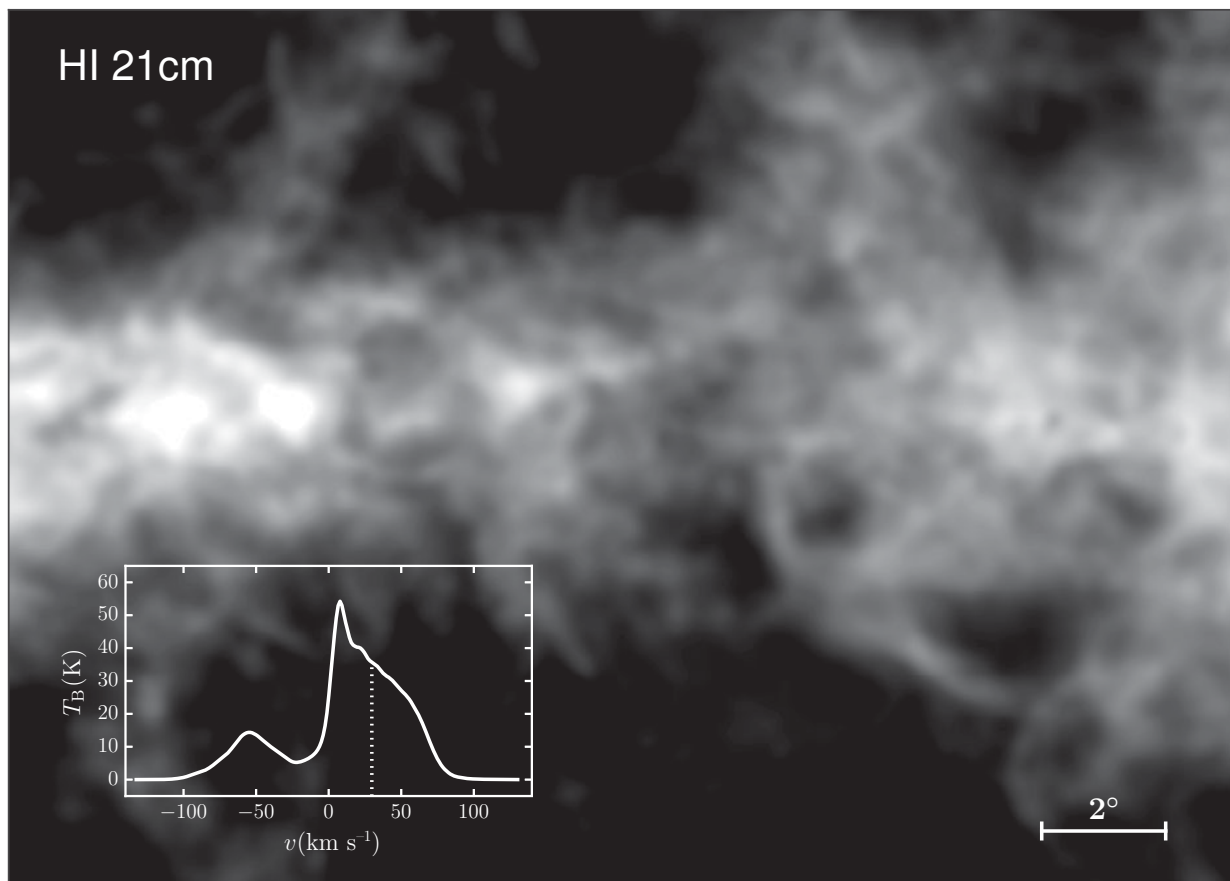
Coordinates:

$$(l, b) = (149.77, 52.03)$$

$$(\text{RA, dec}) = (10\text{h}45\text{m}, +58\text{deg})$$

Size: ~ 15 square degrees

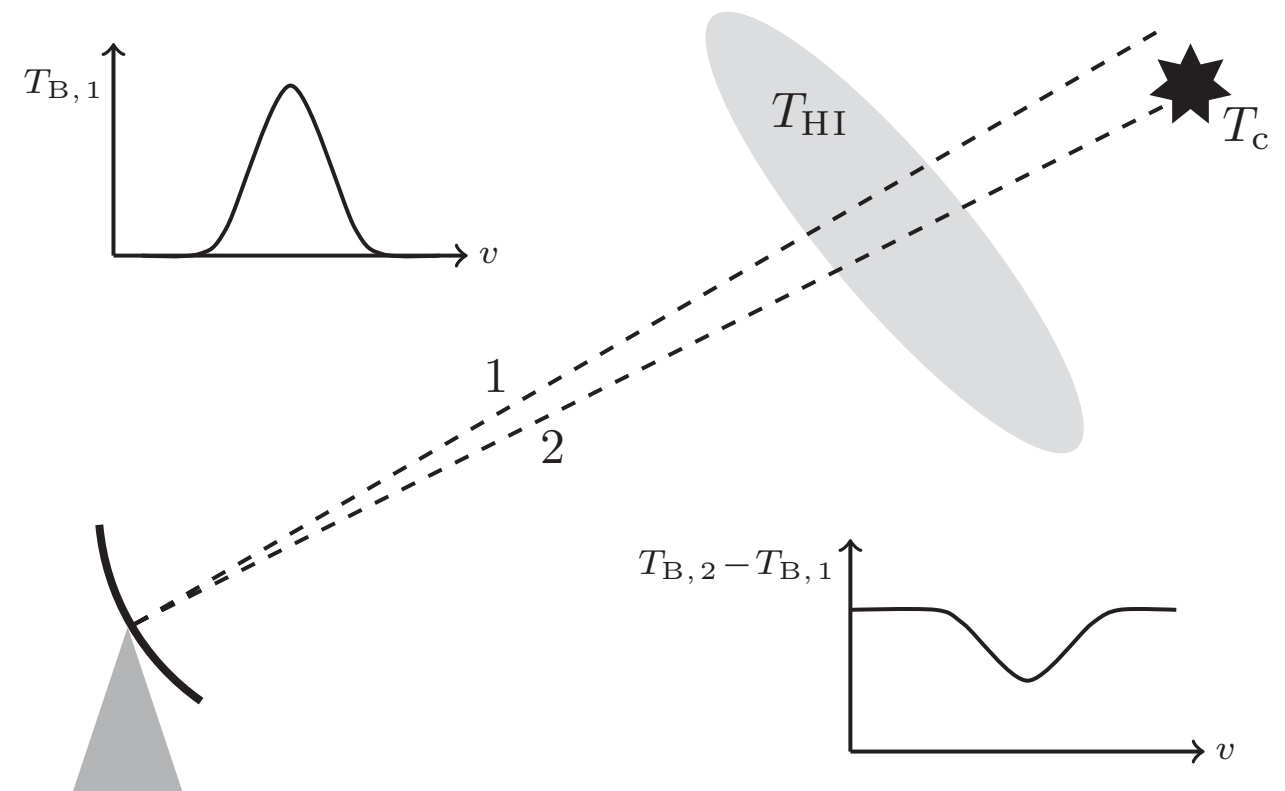
21 cm emission & absorption lines



Galactic 21 cm H I line emission from the HI4PI survey.

The inset shows the mean spectrum of this region in units of brightness temperature versus velocity.

The vertical dotted line shows the velocity slice shown in the image.



Schematic of an absorption experiment to measure the temperature of an atomic cloud.

The first line of sight measures the emission from the cloud only.

The second line of sight contains a background source with continuum (brightness) temperature T_c .

The difference between the two lines of sight reveals a dip in the continuum due to absorption by the cloud.

Ionized Gas - Ionization Equilibrium

- ***Photoionization Equilibrium:***
 - ▶ Balance between photo-ionization and the process of recombination.
- ***Collisional Ionization Equilibrium (CIE)*** or coronal equilibrium
 - ▶ Balance at a given temperature between collisional ionization from the ground states of the various atoms and ions, and the process of recombination from the higher ionization stages.
 - ▶ In this equilibrium, effectively, all ions are in their ground state.

H II regions: Photoionization and Recombination of Hydrogen

- Interstellar medium (ISM), which is primarily composed of hydrogen, is transparent to $h\nu < 13.6 \text{ eV}$ photons, but is very opaque to ionizing photons with $h\nu > 13.6 \text{ eV}$.
 - Ionized atomic hydrogen regions, broadly termed “H II regions”, are composed of gas ionized by photons with energies above the hydrogen ionization energy of 13.6 eV.



- Sources of ionizing photons include massive, hot young stars, hot white dwarfs, and supernova remnant shocks.

- The photoionization cross-section of H depends strongly on frequency and is reasonably approximated by a power-law:

$$\sigma_{\text{pi}}(\nu) \approx \sigma_0 \left(\frac{h\nu}{I_{\text{H}}} \right)^{-3} \quad \text{for } I_{\text{H}} \lesssim h\nu \lesssim 100I_{\text{H}}$$

$(I_{\text{H}} = 13.6 \text{ eV})$

$$\sigma_0 \equiv \frac{2^9 \pi}{3e^4} \alpha \pi a_0^2 = 6.304 \times 10^{-18} \text{ cm}^2$$

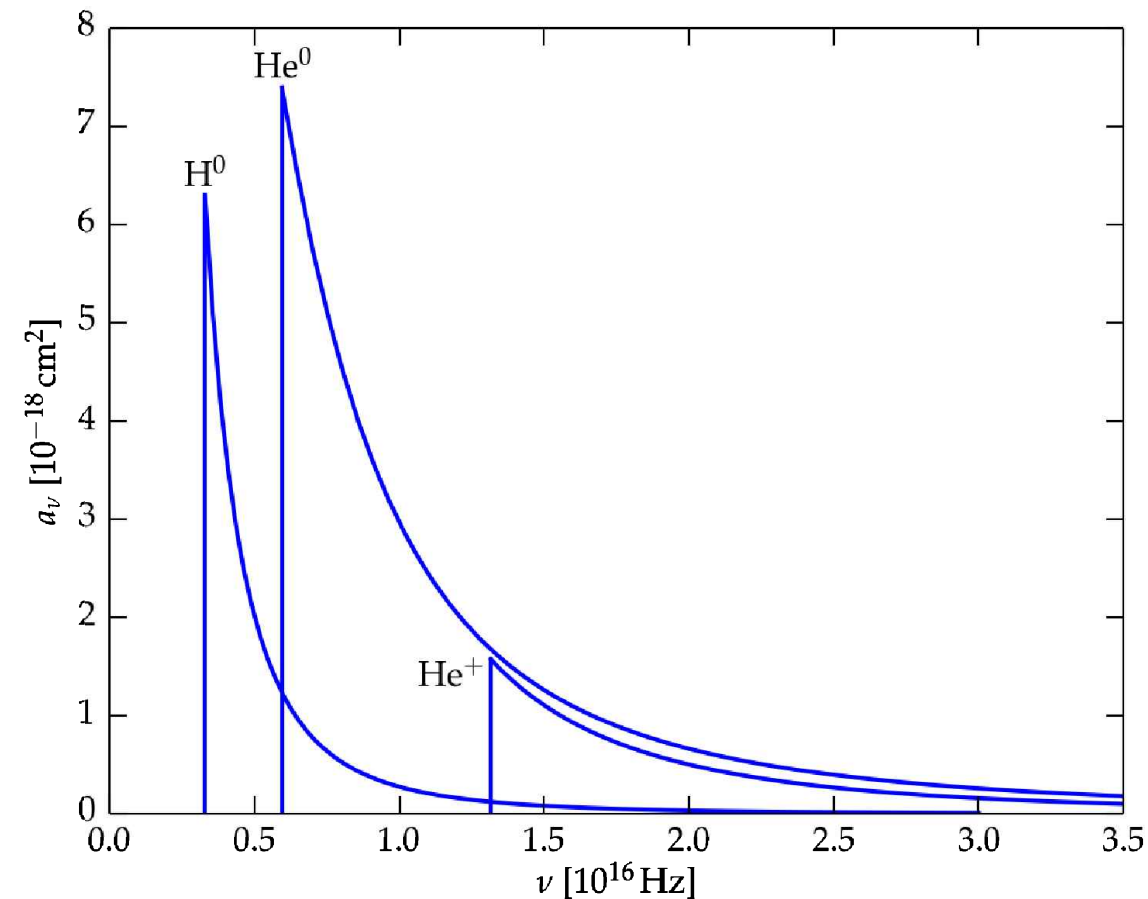
fine-structure constant

$(\alpha \equiv e^2/hc = 1/137.04, e = 2.71828\dots)$

- The recombination rate coefficient (recombination to levels $n \geq 2$) is given in an approximate power law form,

$$\alpha_{\text{B}}(T) \equiv \sum_{n=2}^{\infty} \sum_{\ell=0}^{n-1} \alpha_{n\ell}(T)$$

$$\approx 2.59 \times 10^{-13} T_4^{-0.833 - 0.034 \ln T_4} [\text{cm}^3 \text{s}^{-1}] \quad \text{for } 0.3 \lesssim T_4 = T/10^4 \text{ K} \lesssim 3$$



Photoionization cross section for hydrogen(H^0), hydrogenic helium (He^+), and neutral helium (He^0). [Fig. 4.1 in Ryden]

The Strömgren Sphere: A Uniform, Pure Hydrogen Nebula

- ***Strömgren Sphere:***
 - Following Strömgren (1939), we consider the simple idealized problem of a fully ionized, spherical region of uniform medium plus a central source of ionizing photons.
 - The ionization is assumed to be maintained by absorption of the ionizing photons radiated by a central hot star. The central source produces ionizing photons (Lyman continuum; LyC), with energy $\nu > \nu_0 = I_{\text{H}}/h$ at a constant rate $Q_0 \equiv \dot{N}_{\text{ionize}}$ [photons s⁻¹].
- **O star** temperatures, masses, and ionizing photon rates
 - The emission of the most massive (O-type) stars can be approximated as a blackbody with a peak energy $E \sim 5hc/kT \approx 12.9$ eV, very close to the hydrogen ionization potential.
 - O stars produce enough ionizing photons to create large ionized, or H II, regions.

SpT	T_* (K)	$M_*(M_\odot)$	$\log_{10}(L_*/L_\odot)$	$\log_{10}(\dot{N}_{\text{ionize}})$
O3	44600	58.3	5.83	49.63
O4	43400	46.2	5.68	49.47
O5	41500	37.3	5.51	49.26
O6	38200	31.7	5.30	48.96
O7	35500	26.5	5.10	48.63
O8	33380	22.0	4.90	48.29
O9	31500	18.0	4.72	47.90

- Ionization and Recombination rates:

- Ionization rate per neutral hydrogen atom at a radius $r = 1 \text{ pc}$ from an O star is

$$R_{\text{ionize}} = \frac{\dot{N}_{\text{ionize}}}{4\pi r^2} \sigma_0 \approx 3 \times 10^{-7} \text{ s}^{-1}$$

$\dot{N}_{\text{LyC}} = 5 \times 10^{48} \text{ s}^{-1}$
 $\sigma_0 = 6.3 \times 10^{-18} \text{ cm}^2$
 $r = 1 \text{ pc} = 3.1 \times 10^{18} \text{ cm}$

- This is much greater than the recombination rate per hydrogen ion,

$$R_{\text{recombine}} = \alpha_B n_e \approx 3 \times 10^{-12} \left(\frac{n_e}{10 \text{ cm}^{-3}} \right) \text{ s}^{-1} \quad \text{at } T = 10^4 \text{ K}$$

- This implies a neutral hydrogen atom near the center of the nebula would survive a few months before being ionized but then, once ionized, would have to wait about ten thousand years before recombining with a free electron. We conclude that, at 1 pc, the nebula is almost fully ionized.
- As we move outwards in the nebula away from the O star the ionization rate decreases as $1/r^2$ and eventually will match the recombination rate. This defines the boundary of the H II region.

-
- The transition from ionized to neutral will occur at a length scale of the mean free path of photoionization in the neutral gas.

$$\lambda_{\text{mfp}} = \frac{1}{n_{\text{H}} \sigma_{\text{pi}}} \sim 5 \times 10^{-4} \text{ pc} \left(\frac{n_{\text{H}}}{10^2 \text{ cm}^{-3}} \right)^{-1} \left(\frac{\sigma_{\text{pi}}}{6.304 \times 10^{-18} \text{ cm}^2} \right)^{-1}$$

- This length scale is over a thousand times smaller than the observed size of the nebula.
- Therefore, the gas is either fully ionized or neutral.
- This tells us that the transition from ionized gas to neutral gas at the boundary of the H II region will occur over a distance that is very small compared to the Strömgren radius.

- Assuming that ***the ionization is nearly complete*** ($n_p = n_e = n_{\text{H}}$) ***within*** R_s , and nearly zero ($n_{\text{H}^0} = n_{\text{H}}$, $n_e = 0$) outside R_s , we obtain the size of the ionized region by simply equating the rate of ionization to the rate of recombination (over the whole volume of the ionized region):

$$Q_0 = (n_{\text{H}}^2 \alpha_B) \frac{4\pi}{3} R_s^3 \quad \longleftarrow \quad Q_0 = \dot{N}_{\text{LyC}}$$

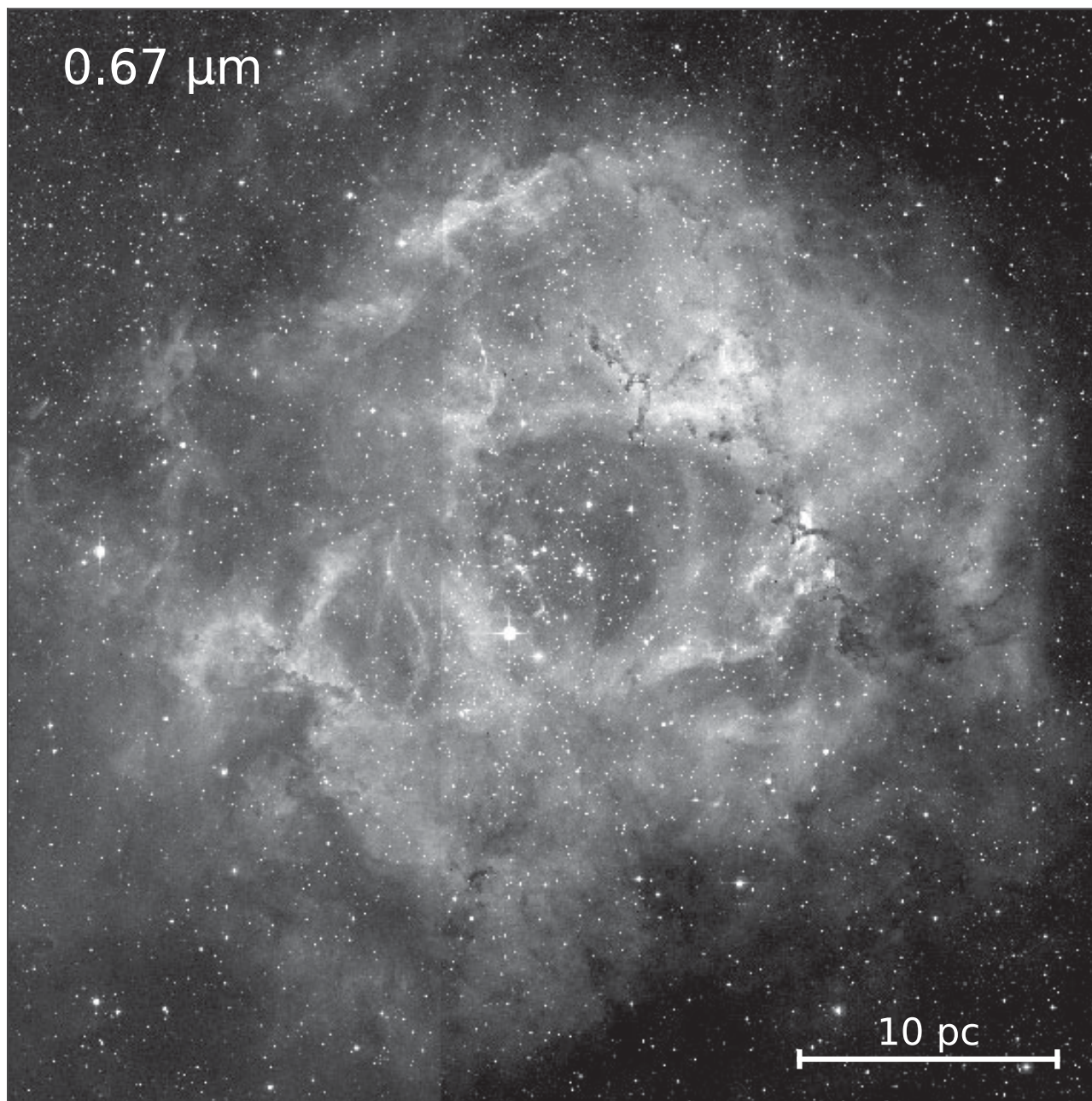
- This gives the Stromgren radius:

$$\begin{aligned} R_s &= \left(\frac{3}{4\pi} \frac{Q_0}{\alpha_B n_{\text{H}}^2} \right)^{1/3} \\ &= 3.17 \left(\frac{Q_0}{10^{49} \text{ photons s}^{-1}} \right)^{1/3} \left(\frac{n_{\text{H}}}{10^2 \text{ cm}^{-3}} \right)^{-2/3} \left(\frac{T}{10^4 \text{ K}} \right)^{0.28} \text{ [pc]} \end{aligned}$$

The physical meaning of this is that ***the total number of ionizing photons emitted by the star balances the total number of recombinations within the ionized volume*** $(4\pi/3)R_s^3$, often called the Strömgren sphere. Its radius R_s is called the Strömgren radius.

H II region - Rosette nebula

- For the Rosette, we find $R_S = 40$ pc which is about a factor of 2 larger than its observed extent. The discrepancy is because some of the ionizing photons are absorbed by dust.

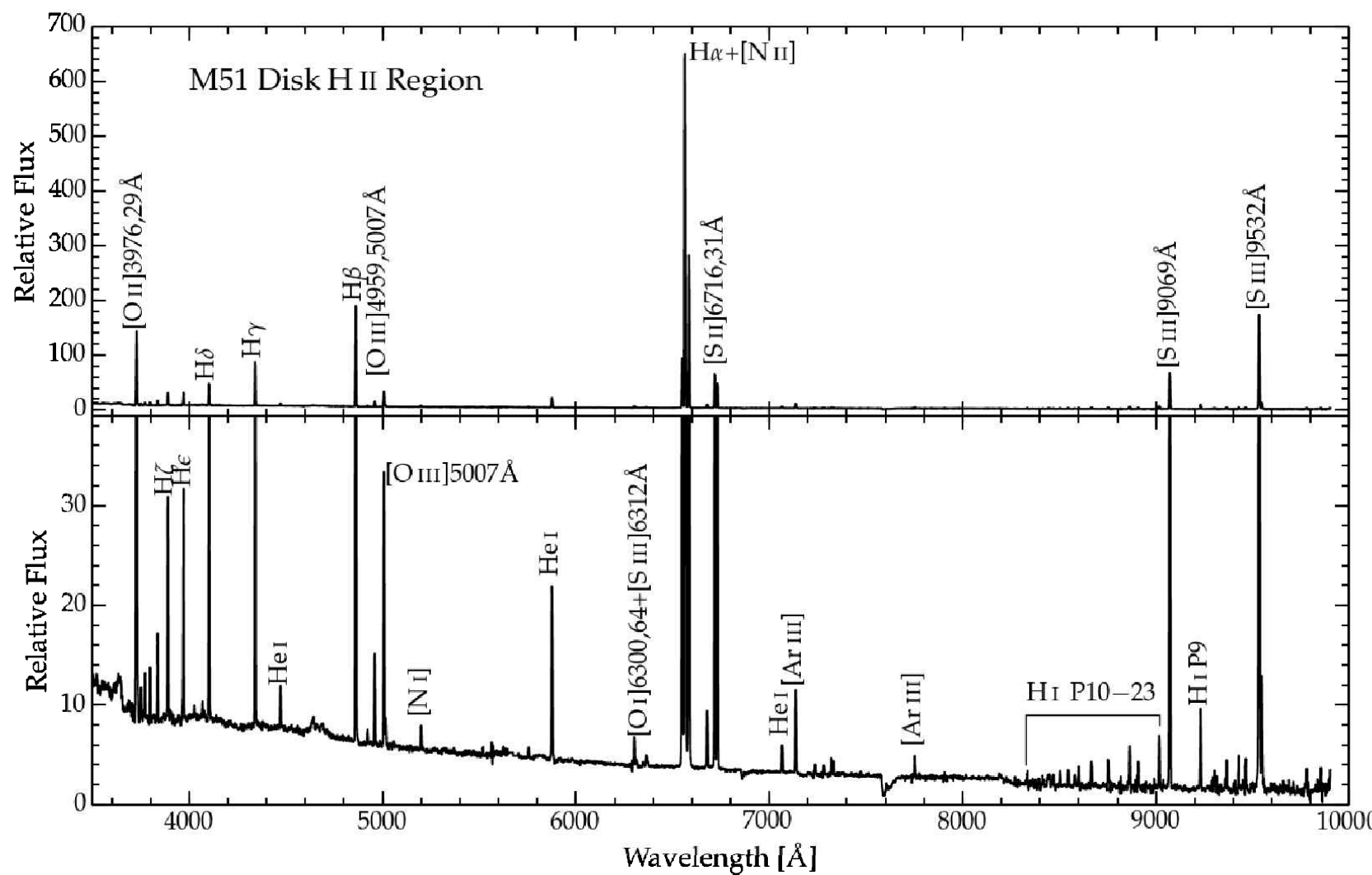


Optical (DSS2 Red) image of the Rosette nebula.

[Fig 6.1, J. P. Williams]

Nebular Emission Lines

- In the figure, the continuum is a mixture of free-bound continuum (from radiative recombination), free-free emission (thermal bremsstrahlung), and two-photon emission.
- The ***collisionally excited emission lines*** are much stronger than the continuum spectrum. The collisional emission lines are utilized to measure the temperature and density of the medium.



Spectrum of a disk HII region in the Whirlpool galaxy (M51).

(top) bright lines

(bottom) scaled to show faint lines.

Figure 4.6 [Ryden]

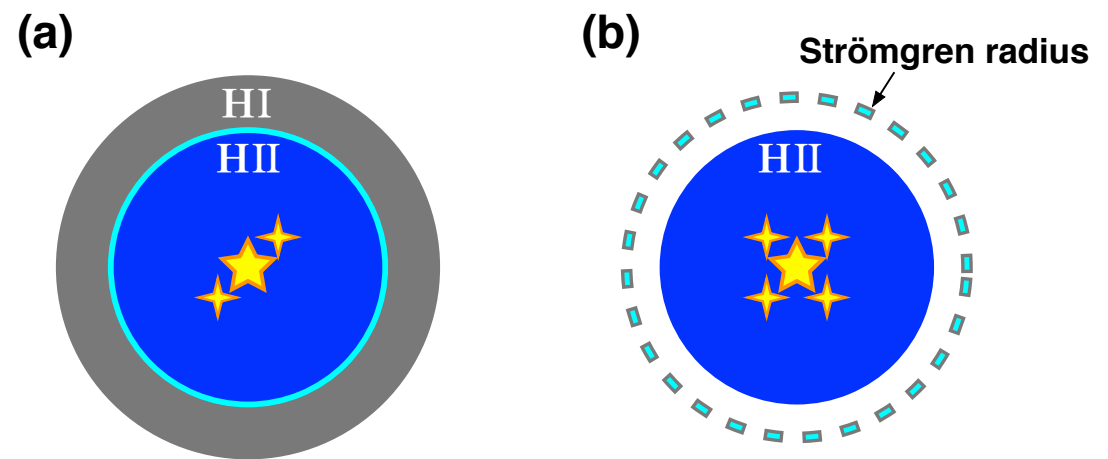
Case A and B (Radiative Recombination of Hydrogen)

- **On-the-spot approximation:**
 - In optically thick regions, it is assumed that every photon produced by ***radiative recombination to the ground state*** of hydrogen is immediately, then and there, destroyed in photoionizing other hydrogen atom.
 - In the on-the-spot approximation, recombination to the ground state has no net effect on the ionization state of the hydrogen gas.
- Baker & Menzel (1938) proposed two limiting cases:
 - **Case A: Optically thin** to ionizing radiation, so that every ionizing photon emitted during the recombination process escapes. For this case, we sum the radiative capture rate coefficient α_{nl} over all levels nl .
 - **Case B: Optically thick** to radiation just above $I_H = 13.60 \text{ eV}$, so that ionizing photons emitted during recombination are immediately reabsorbed, creating another ion and free electron by photoionization. In this case, the recombinations directly to $n = 1$ do not reduce the ionization of the gas: ***only recombinations to $n \geq 2$ act to reduce the ionization.***
 - **Case B in photoionized gas:** Photoionized nebulae around OB stars (H II regions) usually have large enough densities of neutral H. For this situation, case B is an excellent approximation.
 - **Case A in collisionally ionized gas:** Regions where the hydrogen is collisional ionized are typically very hot ($T > 10^6 \text{ K}$) and contain a very small density of neutral hydrogen. For these shock-heated regions, case A is an excellent approximation.

Properties of Ionized Hydrogen Regions

- Ionized atomic hydrogen regions, broadly termed “H II regions”, are composed of gas ionized by photons with energies above the hydrogen ionization energy of 13.6 eV.
 - Ionization Bounded:** These objects include “*classical H II regions*” ionized by hot O or B stars (or clusters of such stars) and associated with regions of recent massive-star formation, and “planetary nebulae”, the ejected outer envelopes of AGB stars photoionized by the hot remnant stellar core.
 - Density Bounded: Warm Ionized Medium / Diffuse Ionized Gas:** Ionized Gas in the diffuse ISM, far away from OB associations.

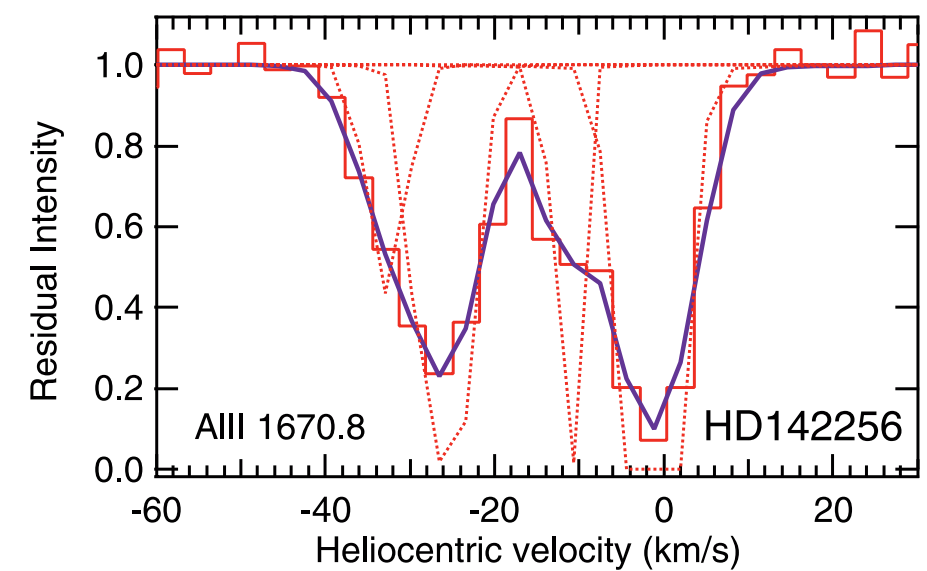
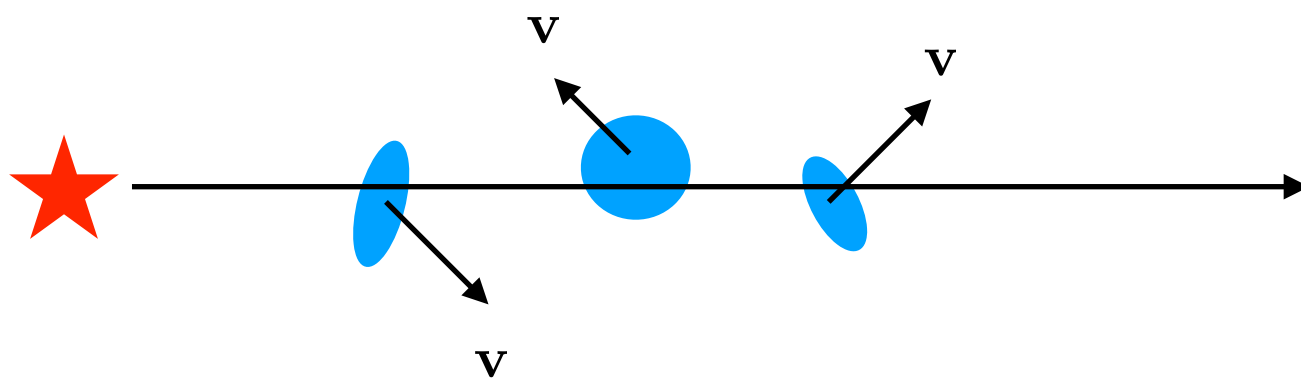
- (a) An ionization-bounded nebula whose radius is determined by the ionization equilibrium. The LyC is entirely consumed to ionize the surrounding H I gas.
- (b) In a density-bounded nebula, the amount of the surrounding H I gas is not enough to consume all LyC photons. Some of the LyC escapes from the cloud, which is called the LyC leakage.



- Three processes govern the physics of H II regions:
 - Photoionization Equilibrium:** the balance between photoionization and recombination. This determines the spatial distribution of ionic states of the elements in the ionized zone.
 - Thermal Balance** between heating and cooling. Heating is dominated by photoelectrons ejected from hydrogen and helium with thermal energies of a few eV. Cooling is mostly dominated by electron-ion impact excitation of metal ion followed by emission of “forbidden” lines from low-lying fine structure levels. It is these cooling lines that give H II regions their characteristic spectra.
 - Hydrodynamics**, including shocks, ionization and photodissociation fronts, and outflows and winds from the embedded stars.

Observations of Metallic Absorption Lines Toward the CNM

- The composition and excitation of interstellar gas can be studied using absorption lines that appear in the spectra of background stars (or other sources).
 - The most prominent absorption lines at visible wavelengths are Ca II K and H lines at $\lambda = 3933, 3968 \text{ \AA}$, and Na I D₁ and D₂ doublet lines at $\lambda = 5890, 5896 \text{ \AA}$.
- Absorption lines (and emission lines) contains a lots of information about number density, temperature, chemical abundances, ionization states, and excitation states.
 - However, interpreting the information requires understanding the ways in which light interacts with baryonic matter, radiative transfer.
 - We need to know the line profile to analyze absorption lines.**



- The interstellar absorption lines are typically narrow compared to spectral features produced by absorption in stellar photospheres, and in practice can be readily distinguished.
- It is normally possible to detect absorption only by the ground state (and perhaps the excited fine-structure levels of the ground electronic state) - the populations in the excited electronic states are too small to be detected in absorption.
- The widths of absorption lines are usually determined by Doppler broadening, with line widths of a few km s⁻¹ (or $\Delta\lambda/\lambda \approx 10^{-5}$) - often observed in cool clouds.
- However, interpreting the information requires understanding the ways in which light interacts with baryonic matter, radiative transfer.
- **We need to know the line profile to analyze absorption lines.**

Absorption & Emission Line Profile

- In the classical / quantum theory of spectral lines,**

we obtain a Lorentzian line profile:

$$\sigma_\nu = f_{nn'} \frac{\pi e^2}{m_e c} \frac{\gamma/4\pi^2}{(\nu - \nu_0)^2 + (\gamma/4\pi)^2}$$

$$\int_0^\infty \sigma_\nu d\nu = f_{nn'} \frac{\pi e^2}{m_e c}$$

m_e = electron mass
 e = electric charge

where $f_{nn'}$ is called the **oscillator strength** or **f-value** for the transition between states n and n' .

$\gamma = A$ is the **damping constant (or Einstein A-coefficient)**.

Selected Resonance Lines ^a with $\lambda < 3000 \text{ \AA}$						
	Configurations	ℓ	u	$E_\ell/hc(\text{ cm}^{-1})$	$\lambda_{\text{vac}}(\text{ \AA})$	$f_{\ell u}$
C IV	$1s^2 2s - 1s^2 2p$	$^2S_{1/2}$	$^2P_{1/2}^o$	0	1550.772	0.0962
		$^2S_{1/2}$	$^2P_{3/2}^o$	0	1548.202	0.190
N V	$1s^2 2s - 1s^2 2p$	$^2S_{1/2}$	$^2P_{1/2}^o$	0	1242.804	0.0780
		$^2S_{1/2}$	$^2P_{3/2}^o$	0	1242.821	0.156
O VI	$1s^2 2s - 1s^2 2p$	$^2S_{1/2}$	$^2P_{1/2}^o$	0	1037.613	0.066
		$^2S_{1/2}$	$^2P_{3/2}^o$	0	1037.921	0.133
C III	$2s^2 - 2s 2p$	1S_0	$^1P_1^o$	0	977.02	0.7586
C II	$2s^2 2p - 2s 2p^2$	$^2P_{1/2}^o$	$^2D_{3/2}^o$	0	1334.532	0.127
		$^2P_{3/2}^o$	$^2D_{5/2}^o$	63.42	1335.708	0.114
N III	$2s^2 2p - 2s 2p^2$	$^2P_{1/2}^o$	$^2D_{3/2}^o$	0	989.790	0.123
		$^2P_{3/2}^o$	$^2D_{5/2}^o$	174.4	991.577	0.110
CI	$2s^2 2p^2 - 2s^2 2p 3s$	3P_0	$^3P_1^o$	0	1656.928	0.140
		3P_1	$^3P_2^o$	16.40	1656.267	0.0588
		3P_2	$^3P_2^o$	43.40	1657.008	0.104
N II	$2s^2 2p^2 - 2s 2p^3$	3P_0	$^3D_1^o$	0	1083.990	0.115
		3P_1	$^3D_2^o$	48.7	1084.580	0.0861
		3P_2	$^3D_3^o$	130.8	1085.701	0.0957
NI	$2s^2 2p^3 - 2s^2 2p^2 3s$	$^4S_{3/2}^o$	$^4P_{5/2}$	0	1199.550	0.130
		$^4S_{3/2}^o$	$^4P_{3/2}$	0	1200.223	0.0862
OI	$2s^2 2p^4 - 2s^2 2p^3 3s$	3P_2	$^3S_1^o$	0	1302.168	0.0520
		3P_1	$^3S_1^o$	158.265	1304.858	0.0518
		3P_0	$^3S_1^o$	226.977	1306.029	0.0519
Mg II	$2p^6 3s - 2p^6 3p$	$^2S_{1/2}$	$^2P_{1/2}^o$	0	2803.531	0.303
		$^2S_{1/2}$	$^2P_{3/2}^o$	0	2796.352	0.608
Al III	$2p^6 3s - 2p^6 3p$	$^2S_{1/2}$	$^2P_{1/2}^o$	0	1862.790	0.277
		$^2S_{1/2}$	$^2P_{3/2}^o$	0	1854.716	0.557

Table 9.4 in [Draine]
See also Table 9.3

Line Broadening Mechanisms

- **Atomic levels are not infinitely sharp**, nor are the lines connecting them.
 - (1) Doppler (Thermal) Broadening
 - (2) Natural Broadening
 - (3) Collisional Broadening
 - (4) Thermal Doppler + Natural Broadening
- **Voigt profile : Thermal + Natural broadening**
 - Atoms shows both a Lorentz profile plus the Doppler effect.
 - In this case, we can write the profile as an average of the Lorentz profile over the various velocity states of the atom:
 - ***Voigt profile = convolution of a Lorentz function (natural broadening) and Gaussian function (thermal broadening).***

- The profile can be written using the Voigt function.

$$\phi(\nu) = \frac{1}{\Delta\nu_D \sqrt{\pi}} H(u, a)$$

$$H(0, a) \approx 1$$

$$\phi(\nu = 0) \approx \frac{1}{\Delta\nu_D \sqrt{\pi}}$$

Here, Voigt function is defined as

$$H(u, a) \equiv \frac{a}{\pi} \int_{-\infty}^{\infty} \frac{e^{-y^2} dy}{(u - y)^2 + a^2}$$

$$a \equiv \frac{\Gamma}{4\pi\Delta\nu_D}$$

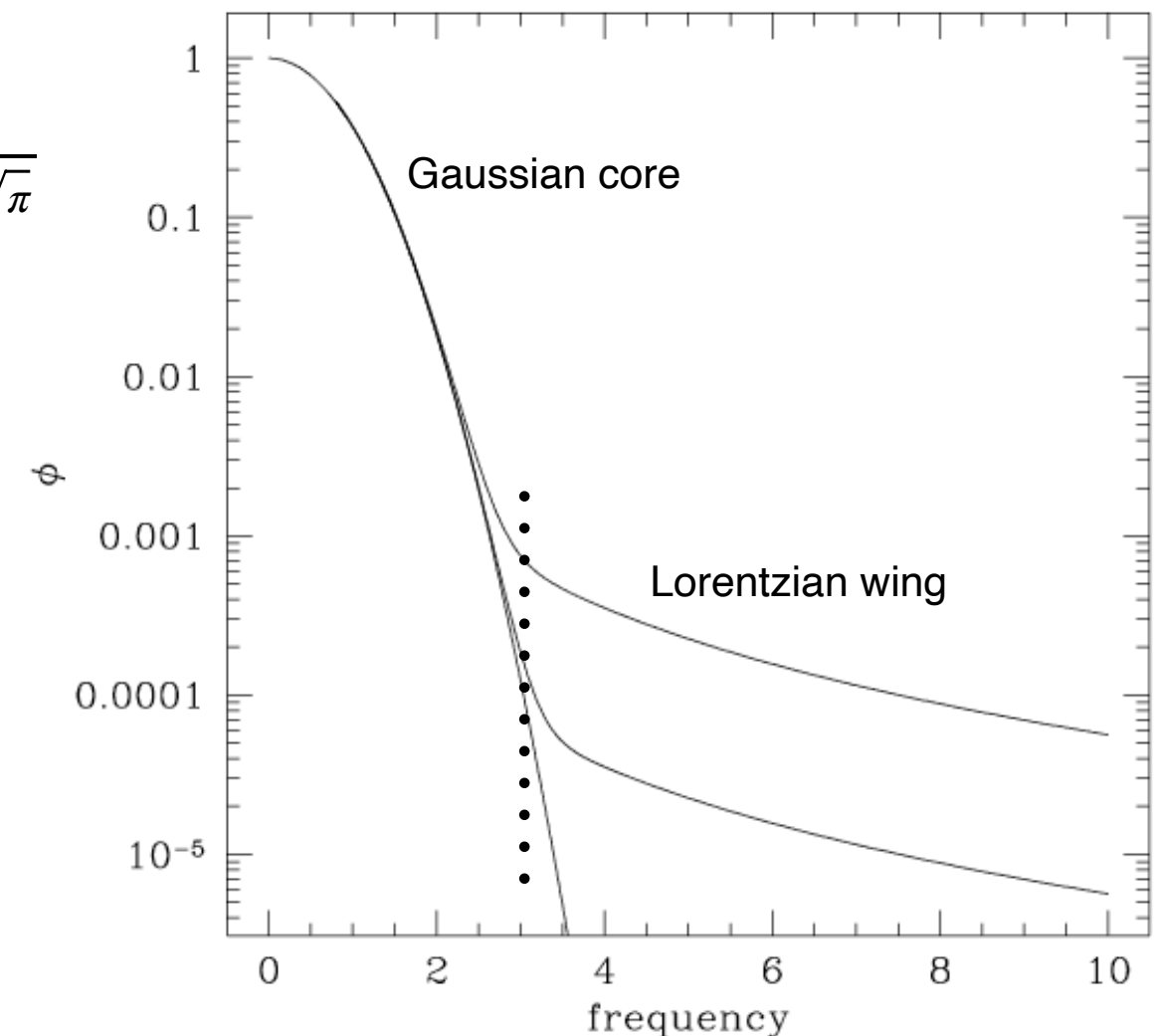
$$u \equiv \frac{\nu - \nu_0}{\Delta\nu_D}$$

Thermal Doppler broadening parameter:

$$\Delta\nu_D = \nu_0 \frac{v_{\text{th}}}{c} = \frac{\nu_0}{c} \sqrt{\frac{2kT}{m}} = \frac{v_{\text{th}}}{\lambda_0}$$

Here, a is a ratio of the intrinsic broadening to the thermal broadening.

u is a measure of how far you are from the line center, in units of thermal broadening parameter.



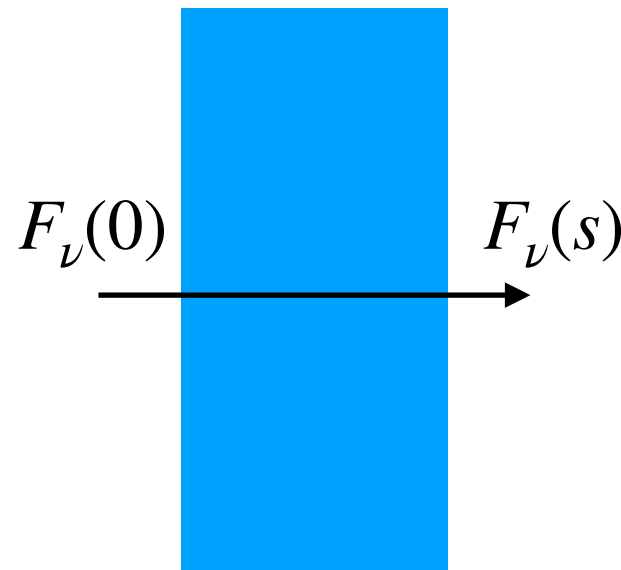
Including the turbulent motion, the Doppler parameter is

$$\Delta\nu_D = \nu_0 \frac{v_{\text{th}}}{c} \rightarrow \Delta\nu_D = \nu_0 \frac{b}{c} = \frac{b}{\lambda_0}$$

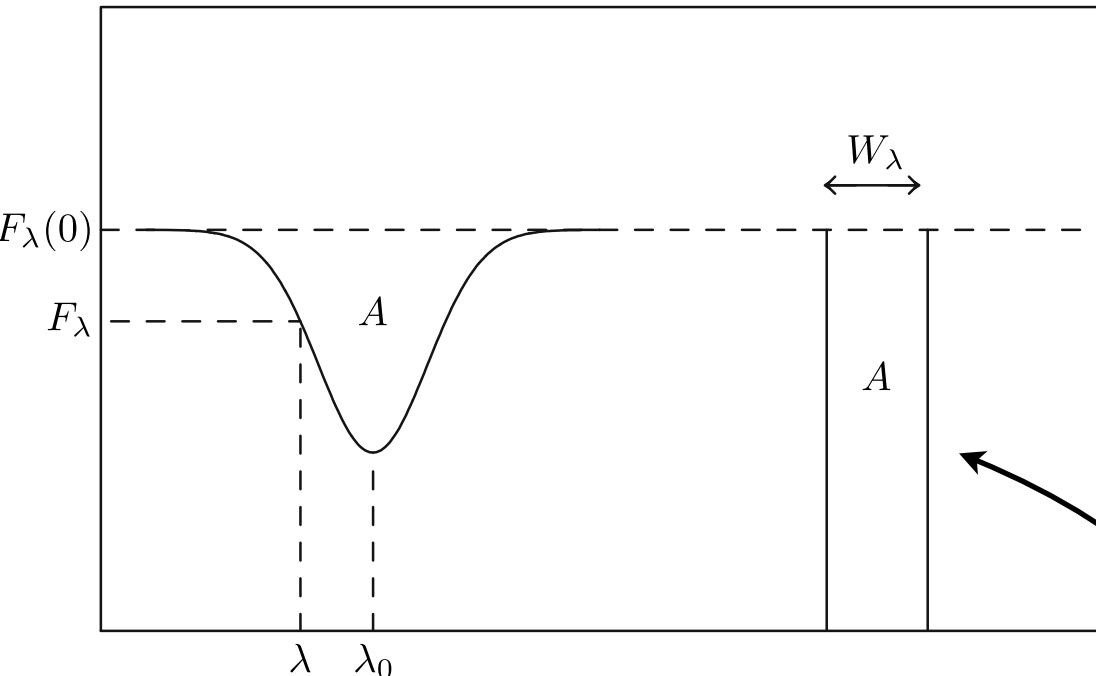
$$\text{where } b = \sqrt{v_{\text{th}}^2 + v_{\text{turb}}^2}, \quad v_{\text{th}} = \sqrt{\frac{2kT}{m}}$$

v_{turb} is the rms velocity of the turbulent motion.

Absorption Line & Equivalent Width



$$F_\nu = F_\nu(0)e^{-\tau_\nu}$$



$$\tau_\nu = \tau_0 H(u, a)$$

$$\tau_0 = \frac{\sqrt{\pi} e^2}{m_e c} f_{\ell u} \frac{\lambda_{\ell u}}{b} N_\ell$$

cross section at line center : $\sigma_0 = \frac{\pi e^2}{m_e c} f_{\ell u} \frac{\lambda_{\ell u}}{\sqrt{\pi} b}$

(wavelength) equivalent width

- **Equivalent width**

Here, τ_0 is the optical depth at the line center.
 N_ℓ is the column density of the atoms in the lower (ground) level.

$$W_\lambda \equiv \int d\lambda \left[1 - \frac{F_\lambda}{F_\lambda(0)} \right] = \int d\lambda (1 - e^{-\tau_\lambda})$$

- The spectrograph often lack the spectral resolution to resolve the profiles of narrow lines, but can measure the total amount of “missing power” resulting from a narrow absorption line.
- *The equivalent width is the width of a straight-sided, perfectly black absorption line that has the same integrated flux deficit as the actual absorption line.*

Variation of Line Profiles & Curve of growth

- The absorption line profiles for $b = 10 \text{ km s}^{-1}$**

- When $\tau_0 < 1$, $F_\nu/F_\nu(0) \approx 1 - \tau_\nu$ and thus the shape of an absorption line resembles an upside-down Voigt function.
- When $\tau_0 \gg 1$, the absorption line saturates at its center and becomes increasingly “box-shaped.”

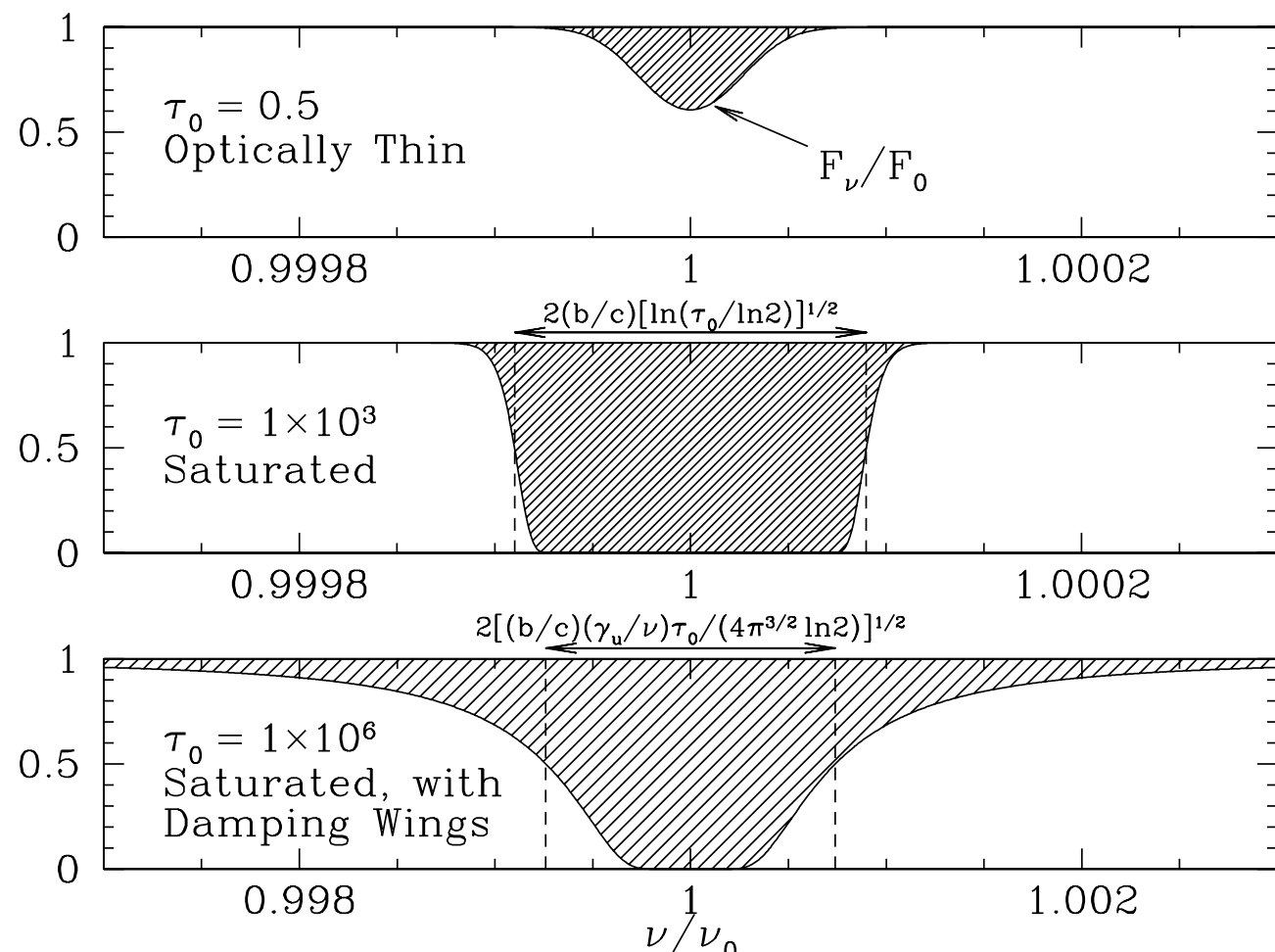
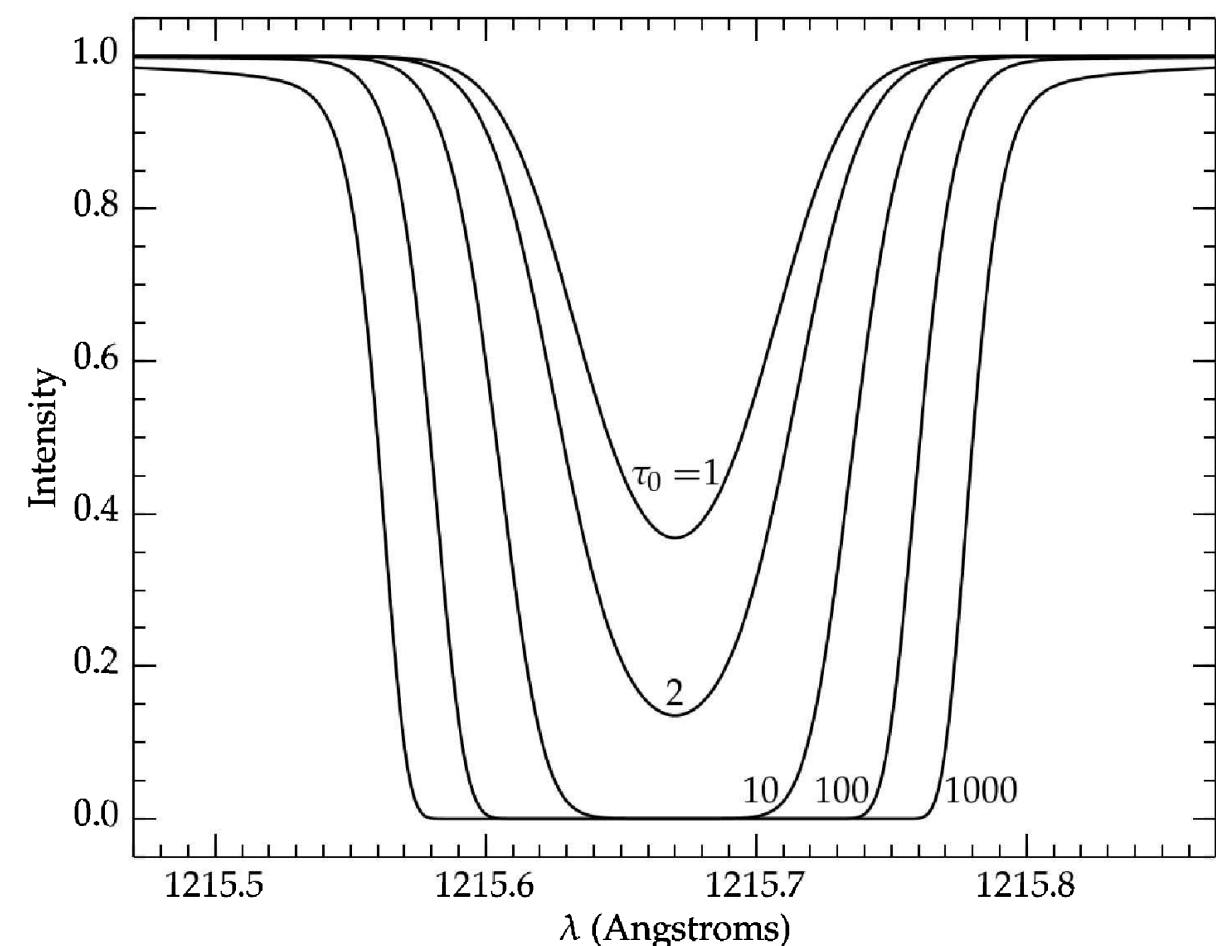


Figure 9.1 in [Draine]

Note the different abscissa in the lowest panel.



Lyman α absorption lines for $b = 10 \text{ km s}^{-1}$.

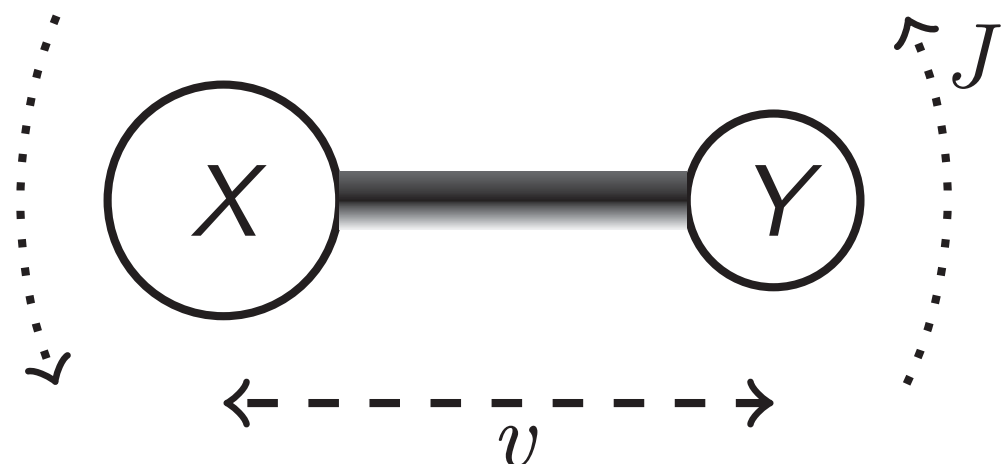
Figure 2.6 in [Ryden]

- Curve of growth**

- The curve of growth refers to the numerical relation between the observed equivalent width and the underlying optical depth (or the column density) of the absorber.

Molecular Clouds

- In dense regions (away from energetic sources of radiation), atoms can combine to form molecules.
 - **Electronic states:** The electrons share orbitals around two or more nuclei with transitions that produce UV and optical lines analogous to those in atoms.
 - **Vibrational and rotational states:** In addition, the interactions of the nuclei themselves have quantized vibrational and rotational states, though at much lower energies. The corresponding lines lie in the IR and mm wavelength regime.



Schematic of the vibrational and rotational modes of a diatomic molecule, with quantum numbers v and J respectively.

- Classically, the vibration and rotation can be viewed as an accelerating charge.
- Observations reveal a rich spectrum from multiple species that tells us about the physical and chemical properties of the molecular ISM, which is the coldest parts of the Universe and the sites of stellar birth.

Molecular Structure: Bohn-Oppenheimer Approximation

- **Bohn-Oppenheimer approximation:**

- The motions of the electrons and nuclei could be treated separately.

This come about because of the great difference between the masses of the electron and a typical nuclei.

- The slowly moving nuclei only sense the electrons as a kind of smoothed-out cloud. As the nuclei move, the electrons have sufficient time to adjust to adiabatically the new nuclear positions. The nuclei then feel only an equivalent potential that depends on the internuclear distance and on the particular electronic state.
 - Due to very different energies of the **electronic, vibrational, and rotational states**, these interactions can be assumed to be decoupled. The separation of wavefunctions is referred to as the Born-Oppenheimer approximation. Under the Born-Oppenheimer approximation, the total wavefunction is a product of the nuclear, electronic, vibrational, and rotational wavefunctions.

$$\psi_{\text{tot}} = \psi_{\text{nuc}} \psi_{\text{el}} \psi_{\text{vib}} \psi_{\text{rot}}$$

Order of magnitude of energy levels

- Energy Levels

$$E_{\text{elect}} : E_{\text{vib}} : E_{\text{rot}} = 1 : \left(\frac{m_e}{M}\right)^{1/2} : \left(\frac{m_e}{M}\right)$$

- Since $M \approx 10^4 m_e$ ($m_p/m_e = 1836$), the relative strengths of electronic, vibrational, and rotational transitions are

$$E_{\text{elect}} : E_{\text{vib}} : E_{\text{rot}} \sim 1 : 10^{-2} : 10^{-4}$$

- Typical values are

$$E_{\text{elect}} : E_{\text{vib}} : E_{\text{rot}} \sim 10 \text{ eV} : 0.1 \text{ eV} : 0.001 \text{ eV}$$

UV IR IR or radio

- Typical wavelengths are

$$\lambda_{\text{elect}} : \lambda_{\text{vib}} : \lambda_{\text{rot}} \sim 100 \text{ nm} : 10 \mu\text{m} : 1 \text{ mm}$$

- That is, electronic transitions are in the optical/ultraviolet, vibrational in the near/mid-infrared, and rotational in the (sub-)millimeter.

[Energy Levels, Pure rotational & ro-vibrational transitions]

- **Energy Levels**

$$E_q(v, J) = V_q(r_0) + h\nu_0 \left(v + \frac{1}{2} \right) + B_v J(J+1)$$

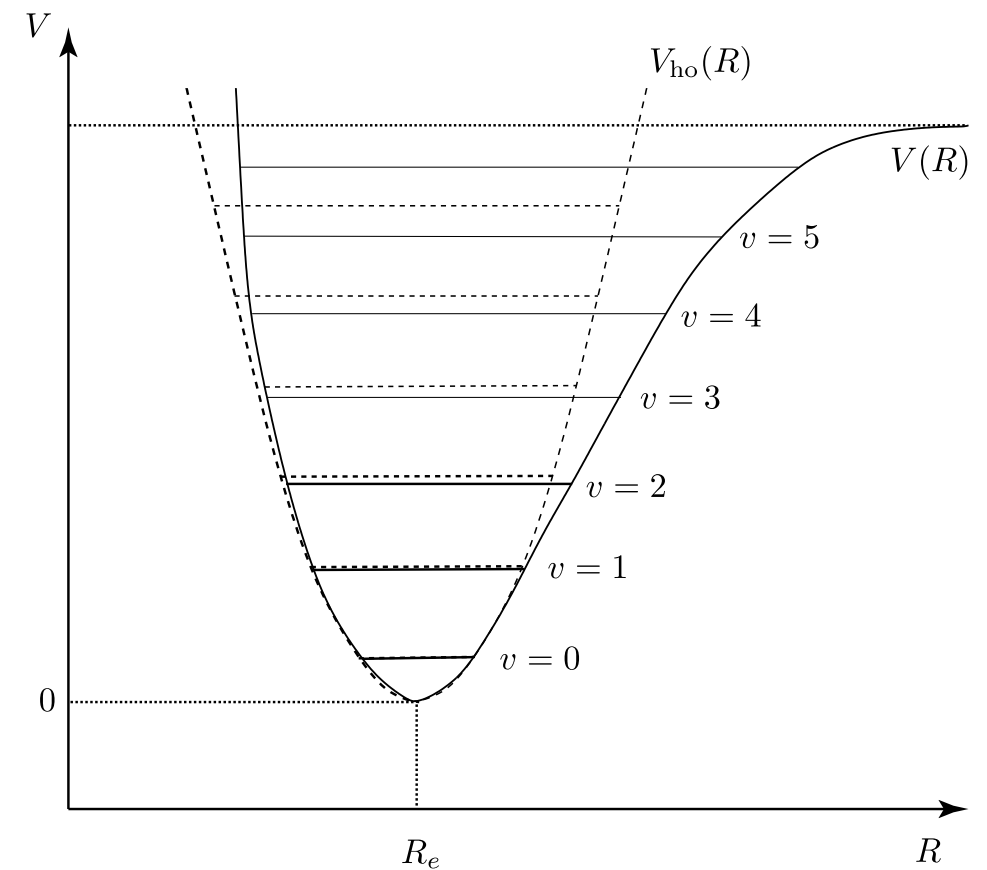
$$\begin{aligned} v &= 0, 1, 2, \dots \\ J &= 0, 1, 2, \dots \end{aligned}$$

$$\nu_0 \equiv \frac{\omega_0}{2\pi} \quad B_v = \frac{\hbar^2}{2I} \quad I = \mu r_0^2 \quad = \text{moment of inertia of the molecule.}$$

Here, q denotes an electronic state.

- **Pure rotational spectrum:** In the lowest vibrational and electronic states, it is possible to have transitions solely among the rotational states. Such transitions give rise to a pure rotational spectrum.
- **Rotational-vibration spectrum:** Because the energies required to excite vibrational modes are much larger than those required to excite rotation, it is unlikely to have a pure vibrational spectrum.

The transitions then yield a rotation-vibrational spectrum, in which both the vibrational state and the rotational state can change together.



[Selection Rules]

- Electric-dipole selection rule for the ro-vibrational transitions:

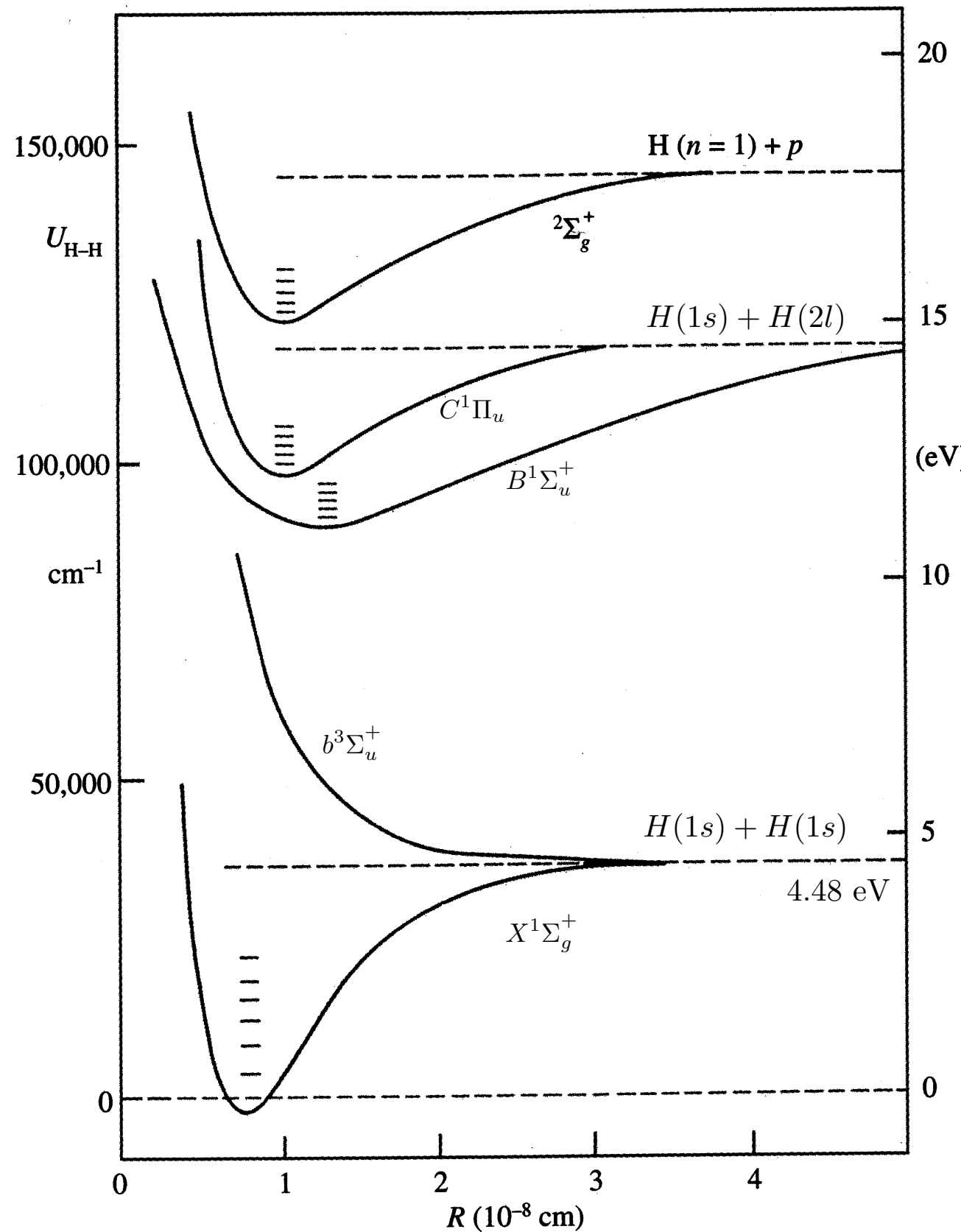
$$\Delta v = \text{any}$$

$$\Delta J = 0, \pm 1 \text{ not } J = 0 \leftrightarrow 0$$

- But, note that H_2 has no permanent electric-dipole moment.

The electric-quadrupole are allowed for $\Delta J = \pm 2$ within the ground electronic state.

[Energy levels of Molecular Hydrogen]

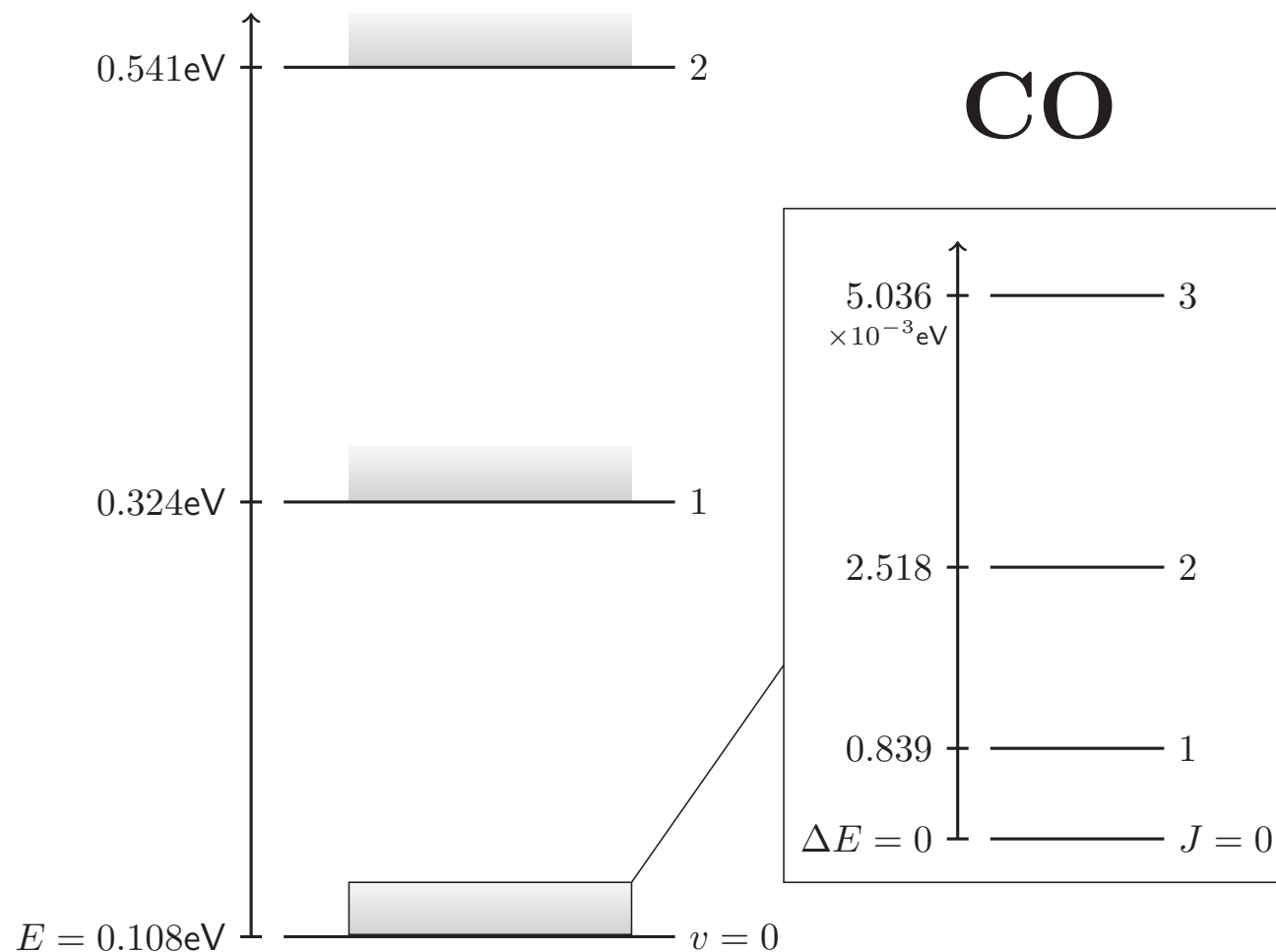


- The short horizontal lines in each of the bound states indicate the vibrational levels.
- The transition from the ground state $X^1\Sigma_g^+$ to the excited states $B^1\Sigma_u^+$ and $C^1\Pi_u$ are called **Lyman and Werner bands**.

Werner band: $C^1\Pi_u - X^1\Sigma_g^+$ at about 1100 Å;
Lyman band: $B^1\Sigma_u^+ - X^1\Sigma_g^+$ at about 1010 Å.

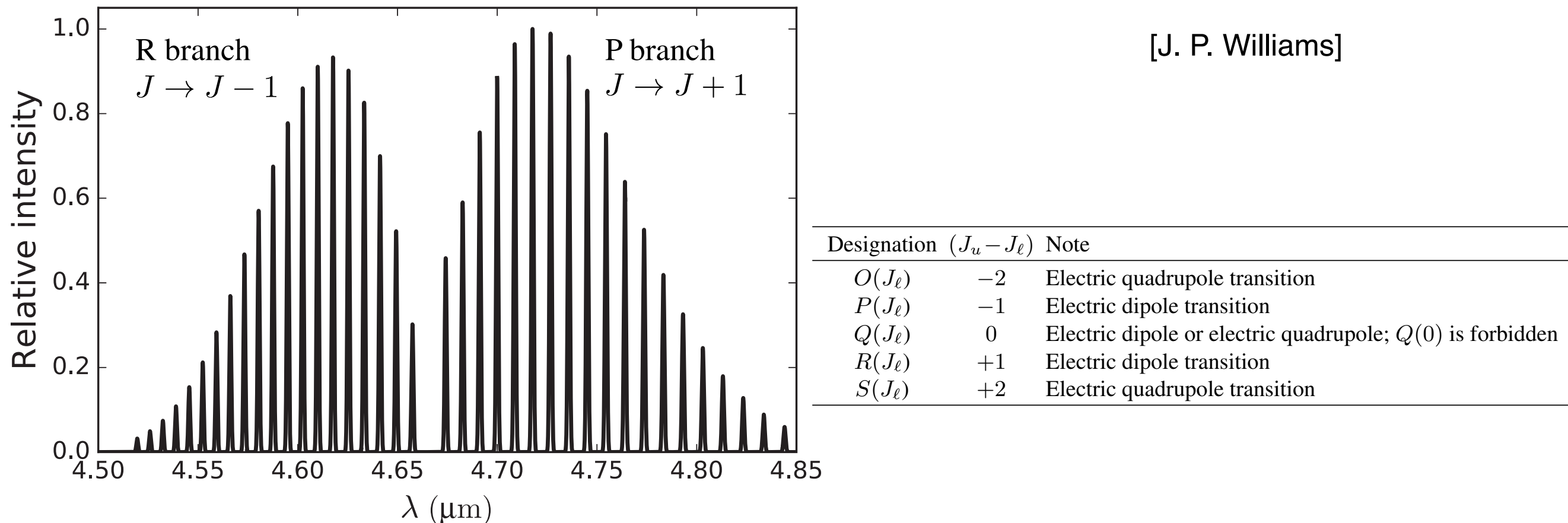
In principle, states are labelled alphabetically in ascending energy order. However, there are many exceptions. The lowest triplet state of H_2 is the $b^3\Sigma_u^+$ with the $a^3\Sigma_g^+$ lying somewhat higher.

[Energy levels of CO]



- The rotational and vibrational energy levels for carbon monoxide.
 - The left side shows the vibrational energy for each level v .
 - The rotational transitions are illustrated by the gray shading at each level.
 - The rotational energies are about 100 times smaller than the vibrational.
 - The inset on the right hand side shows a zoomed-in region of J-ladder.

[Energy levels of CO]



- Model spectrum of ro-vibrational lines for CO $v = 1 - 0$, illustrating the two branches corresponding to a positive or negative change in J and a central gap at $\Delta J = 0$.
 - The symmetry comes from the sign of the $\Delta J = \pm 1$ jump and produces two branches in the spectrum.
 - The R branch corresponds to a higher energy jump, $J \rightarrow J - 1$, and lies at shorter wavelengths.
 - The P branch is a smaller jump, $J \rightarrow J + 1$, and is at longer wavelengths.
 - The envelope shape arises from the population level distribution that is small at low levels due to the degeneracy $g_J = 2J + 1$, and at high levels due to the Boltzmann exponential $e^{E/kT_{\text{ex}}}$.
 - The difference between the relative intensity of the P and R branches is due to different values in the Einstein A coefficient.

- The extra bonds and degrees of freedom in molecules with three or more atoms allow many more transitions.
 - This requires additional quantum numbers to describe the vibrational modes and axes of rotation, and different selection effects.
 - Possibilities include a Q-branch with $\Delta J = 0$.
 - Water, for example, has thousands of lines in the infrared-millimeter region.
 - The range of transitions provides many ways for the molecular ISM to radiate and effectively cool across a temperature continuum from > 1000 K to 10 K.

The invisibility of H₂ in the Cold ISM

- Hydrogen is, by far, the most common element in the Universe and molecular hydrogen is the most common molecule in the ISM.
 - However, its symmetry prevent pure rotational transitions. From a quantum standpoint, the two hydrogen atoms are identical so there is no change in state in a 180 degree rotation. Because there is not separation of charge from the center of the system, it is also said to have **zero dipole moment**.
 - In cold regions, it will not radiate and is effectively invisible.
- Tracers of Cold Molecular Gas
 - To diagnose the properties of these regions requires observations of other constituents: dust and molecules such as CO.
 - The offset between the charge distribution and center of mass in asymmetric molecules such as CO produces a dipole moment and a series of rotational energy levels that can be populated through collisions in cold gas.
 - Although the abundances of these molecules are very low relative to H₂, **they provide the only means for the gas to radiate** and result in a rich line spectrum at millimeter wavelengths.

- A sample of molecular rotational transitions
 - The following table shows a small set of commonly observed, low-lying, rotation transitions, $J + 1 \rightarrow J$, in the ground vibrational level, $v = 0$.
 - The Einstein A coefficients are extremely small compared to (permitted) vibrational and electronic transitions.
 - Higher transitions are excited by slightly warmer and denser gas.

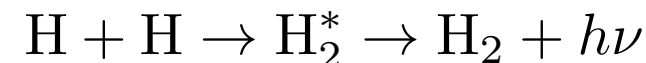
- The table includes the isotopologue, ^{13}CO of CO.
- Isotopologues are molecules that differ only in their isotopic composition. At least one atom has a different number of neutrons than the parent.
- They have the same transitions at nearby frequencies with similar decay and excitation rates.
- Observations of these rare species help diagnose conditions in dense regions where lines from the primary species are optically thick.

Molecule	Transition	ν (GHz)	E_u/k (K)	A (s^{-1})
CO	1–0	115.271	5.5	7.20×10^{-8}
	2–1	230.538	16.6	6.91×10^{-7}
	3–2	345.796	33.2	2.50×10^{-6}
	^{13}CO	1–0	110.201	5.3
		2–1	220.399	6.03×10^{-7}
		3–2	330.588	2.18×10^{-6}
CS	1–0	48.991	2.4	1.75×10^{-6}
	2–1	97.981	7.1	1.68×10^{-5}
	3–2	146.969	14.1	6.07×10^{-5}
HCN	1–0	88.633	4.3	2.41×10^{-5}
	2–1	177.261	12.8	2.31×10^{-4}
	3–2	265.886	25.5	8.36×10^{-4}
HCO^+	1–0	89.188	4.3	4.25×10^{-5}
	2–1	178.375	12.9	4.08×10^{-4}
	3–2	267.558	25.7	1.48×10^{-3}

Gas-Phase Formation of H₂

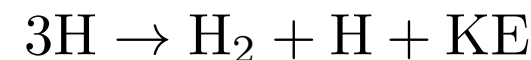
- ***Direct Radiative Association***

- When two free H atoms collide with each other, they create an excited hydrogen molecule that is unbound.



- It must emit a photon carrying away enough energy to leave it a bound state, or it will break apart again. There is no electric dipole moment. As a result, there is no dipole radiation that could remove energy from the system and leave the two H atoms in a bound state. Electric quadrupole transitions are possible, but the rates are very low.
 - As a consequence, the rate coefficient for direct radiative association of H₂ is so small that **this reaction can be ignored in astrochemistry**.

- ***Three-body reaction***



- The reaction can occur, when the third body carrying off the energy released when H₂ is formed, but the rate for this three-body reaction is negligible at interstellar or intergalactic densities.
 - At the high densities of a protostar or protoplanetary disk, the three-body reaction is able to convert H to H₂.

- ***Formation of negative hydrogen ion by radiative association followed by formation of H₂ by associative detachment:***
 - First step:
$$\text{H}^0 + e^- \rightarrow \text{H}^- + h\nu$$
 - Second step:
$$\text{H}^- + \text{H} \rightarrow \text{H}_2 + e^- + \text{KE}$$
This is an exothermic ion-molecule reaction.
 - The density of negative H ion is very low because the formation rate of H⁻ (first step) is slow while there are many, rapid processes that destroy H⁻.
- ***In the absence of dust (e.g., in the early universe), H⁻ + H → H₂ + e⁻ is the dominant channel for forming H₂.***

Grain Catalysis of H₂

- The dominant process of H₂ formation in the Milky Way and other galaxies is via grain catalysis.

- The surface of a dust grain acts as a lab of chemical activity.

- Adsorption:**

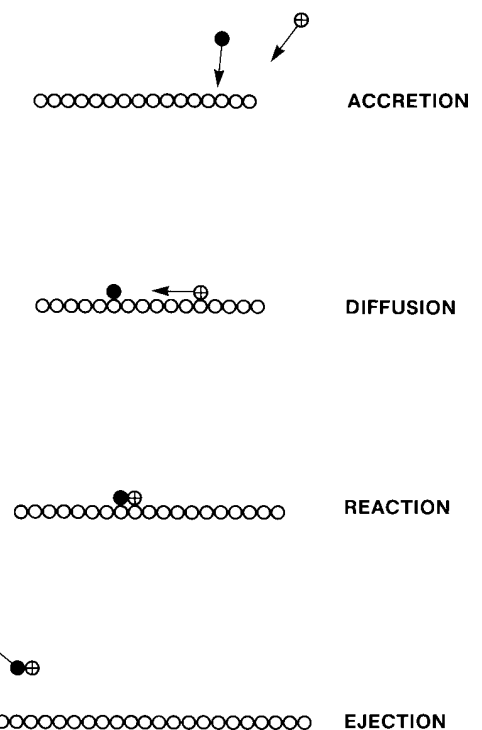
- A H atom colliding with a dust grain has some probability of sticking (bounding) to the grain.
- Sticking probability: $p_s \approx 0.3$ for grains with $a \sim 0.1\mu\text{m}$

- Diffusion & Reaction:**

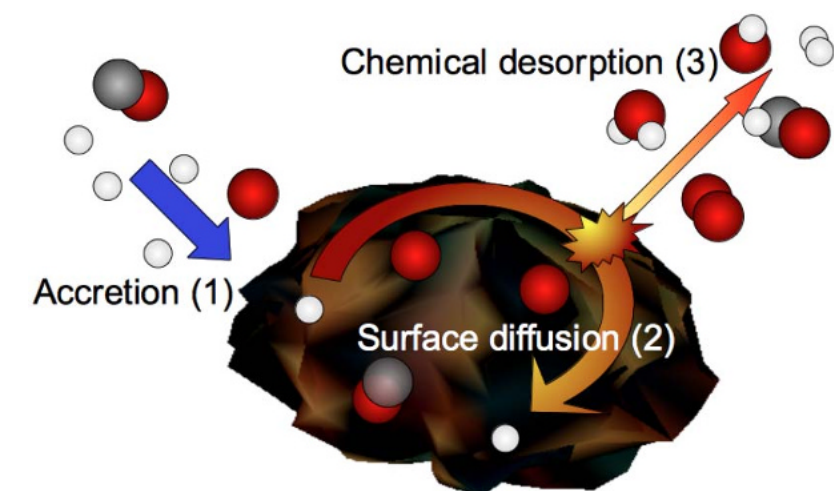
- Initially, the binding may be weak enough that the H atom is able to diffuse (i.e., random-walk) some distance on the grain surface, until it happens to arrive at a site where it is bound strongly enough that it becomes “trapped.”
- Subsequent H atoms arrive at random locations on the grain surface and undergoes their own random walks until they also become trapped, but eventually one of the newly arrived H atoms encounters a previously bound H atom before itself becoming trapped.
- When the two H atoms encounter one another, they react to form H₂.

- Desorption:**

- The energy released when two free H atoms react to form H₂ in the ground state is $\Delta E = 4.5 \text{ eV}$. This energy is large enough to overcome the forces that were binding the two H atoms to the grain, and the H₂ molecule is ejected from the grain surface.



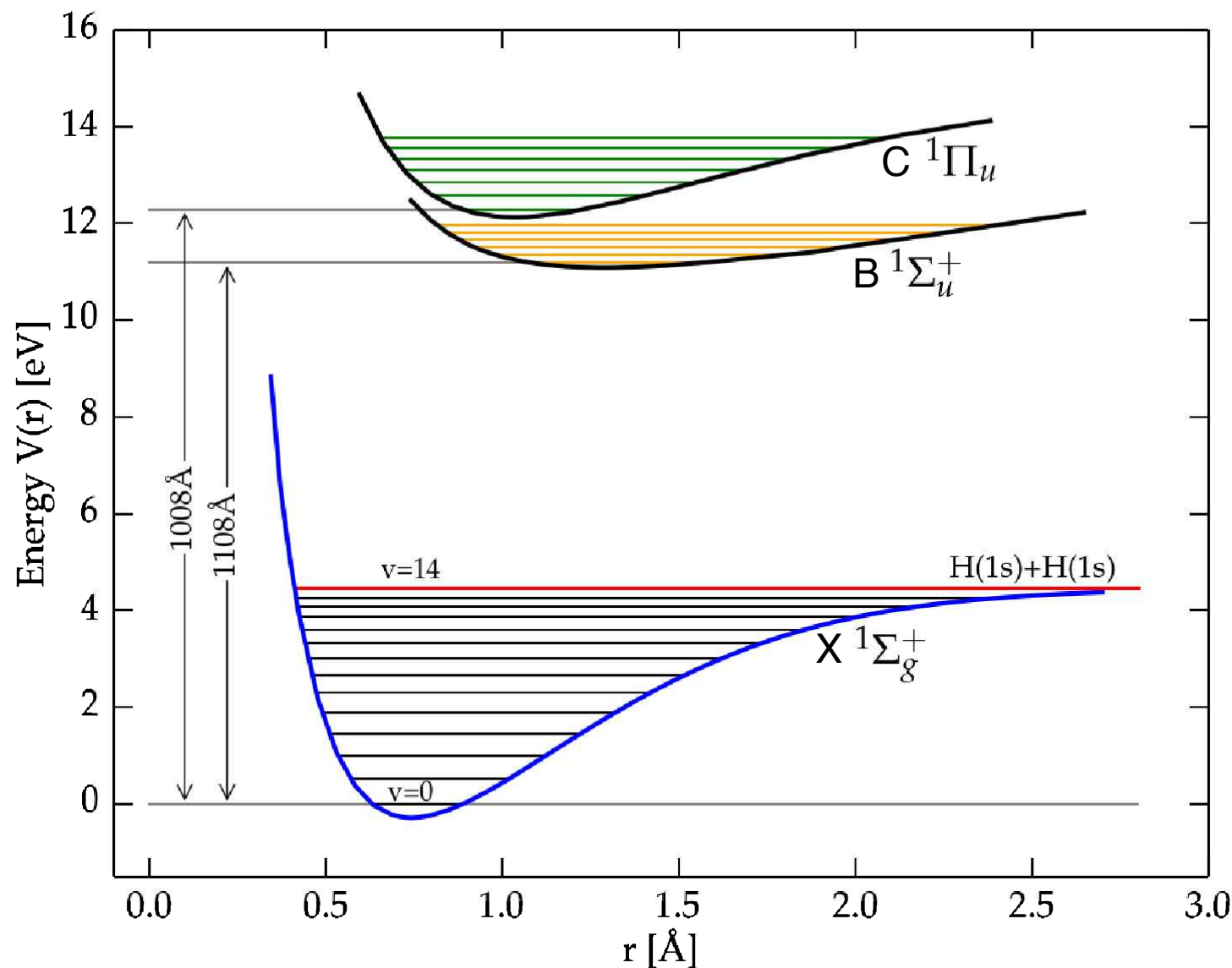
A schematic of the formation of molecules on grain surfaces. [Fig 4.1, Tielens]



Sketch that illustrates the chemical desorption process.
[Fig 1, Dulieu, 2003, Scientific Reports]

Photodissociation of H₂

- Photodissociation: $\text{H}_2 + h\nu \rightarrow \text{H} + \text{H} + \text{KE}$
 - Photodissociation is the principal process destroying interstellar H₂.



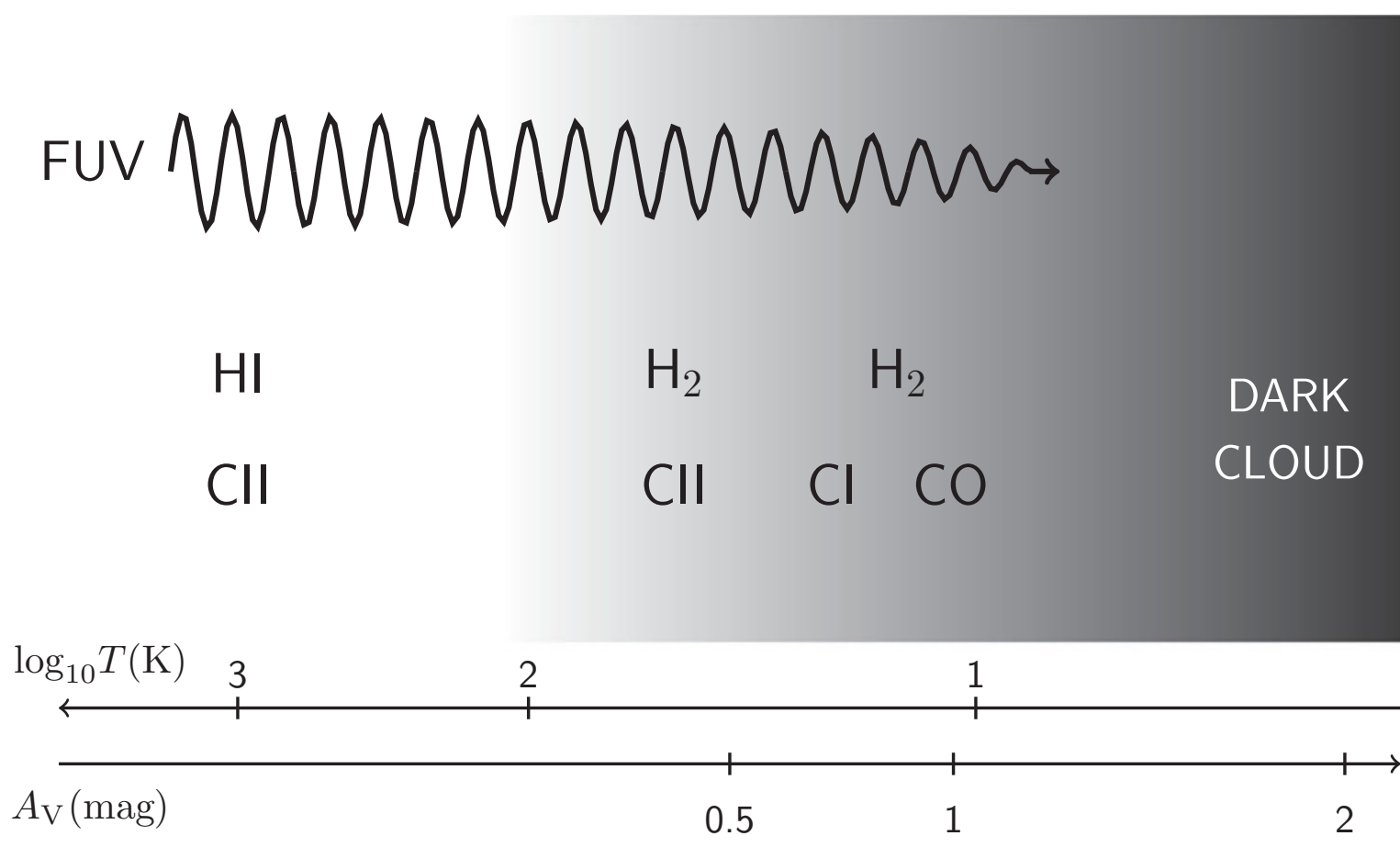
In the left potential energy curves, you might think that photodissociation of H₂ is a simple task; if H₂ absorb a photon of energy $h\nu > 4.52$ eV, it will be excited to a vibrational state (**vibrational continuum**) with quantum number $v > 14$, which will be unbound.

However, absorbing a photon to lift the molecule to a $v > 14$ vibrational state requires a quadrupole transition, which has a very small transition probability.

Schematic drawing of the potential energy curves of molecular hydrogen [Figure 7.4, Ryden]

PhotoDissociation Regions (PDRs)

- The edge of a molecular region, where molecules turn to atoms, is termed a **photodissociation region** or interchangeably a **photon dominated region**, both with the same PDR abbreviation.
 - Far-ultraviolet (FUV) radiation (91.2nm-200nm) can dissociate molecular hydrogen, ionize carbon, and broadly affect the physical properties and chemical composition of the gas.



The structure of a PDR. The FUV radiation enters from the left hand side into a neutral atomic cloud and is attenuated by dust to the point where molecular hydrogen begins to form in sufficient numbers to self-shield. Deeper in, carbon becomes neutral and then reacts with oxygen to form CO. Very little radiation penetrates further and more molecules form in the cold, dark interior.

[Fig. 7.11. J. P. Williams]

Molecular Clouds: Observations

- Cloud Structure
 - Local density estimates using line ratios often give larger densities than global mean densities found by averaging the observed molecular column densities along the line of sight.
 - The interpretation of this is that the ***clouds are very clumpy***, with the dense cores having typical sizes of < 1 pc or smaller, and densities $> 10^6 \text{ cm}^{-3}$.
 - The overall cloud extends for 3–20 pc on average, with a mean density of 10^{3-4} cm^{-3} .
 - Most molecular clouds show a number of discernible cores. These are often detected as sources of molecular lines with high critical densities (e.g., CS), while the general cloud is mapped using lines of lower critical density (mainly CO).
 - Within the galaxies, molecular clouds are most often seen organized into complexes with sizes from 20 pc to 100 pc, and overall H₂ masses of $10^{4-6} M_{\text{sun}}$. The distinction between “clouds” and “complexes” in terms of sizes and masses is somewhat artificial. A more precise statement would be that ***we see a wide range of structures***, from single small clouds to large complexes of clouds, with many complexes arrayed along the spiral arms of the Galaxy.

Molecular Clouds: Cloud Categories

- Cloud Categories (based on the total surface density)
 - Individual clouds are separated into categories based on their optical appearance: **diffuse, translucent, or dark**, depending on the visual extinction A_V through the cloud.

Category	A_V (mag)	Examples
Diffuse Molecular Cloud	$\lesssim 1$	ζ Oph cloud, $A_V = 0.84^a$
Translucent Cloud	1 to 5	HD 24534 cloud, $A_V = 1.56^b$
Dark Cloud	5 to 20	B68 ^c , B335 ^d
Infrared Dark Cloud (IRDC)	20 to $\gtrsim 100$	IRDC G028.53-00.25 ^e

^a van Dishoeck & Black (1986).

^b Rachford et al. (2002).

^c Lai et al. (2003).

^d Doty et al. (2010).

^e Rathborne et al. (2010).

[Table 32.1, Draine]

- **Diffuse and translucent clouds** have sufficient UV radiation to keep gas-phase carbon mainly photo-ionized throughout the cloud.
 - ▶ Such clouds are usually pressure-confined, although self-gravity may be significant in some cases.
- The typical **dark clouds** have $A_V \sim 10$ mag, and is self-gravitating. Some dark clouds contain dense regions that are extremely opaque, with $A_V > 20$ mag.
- **Infrared Dark Clouds** are opaque even at 8 μm , and can be seen in silhouette against a background of diffuse 8 μm emission from PAHs in the ISM.

- Terminology for Cloud Complexes and Their Components

Categories	Size (pc)	n_{H} (cm^{-3})	Mass (M_{\odot})	Linewidth (km s^{-1})	A_V (mag)	Examples
GMC Complex	25 – 200	50 – 300	$10^5 – 10^{6.8}$	4 – 17	3 – 10	M17, W3, W51
Dark Cloud Complex	4 – 25	$10^2 – 10^3$	$10^3 – 10^{4.5}$	1.5 – 5	4 – 12	Taurus, Sco-Oph
GMC	2 – 20	$10^3 – 10^4$	$10^3 – 10^{5.3}$	2 – 9	9 – 25	Orion A, Orion B
Dark Cloud	0.3 – 6	$10^2 – 10^4$	5 – 500	0.4 – 2	3 – 15	B5, B227
Star-forming Clump	0.2 – 2	$10^4 – 10^5$	$10 – 10^3$	0.5 – 3	4 – 90	OMC-1, 2, 3, 4
Core	0.02 – 0.4	$10^4 – 10^6$	$0.3 – 10^2$	0.3 – 2	30 – 200	B335, L1535

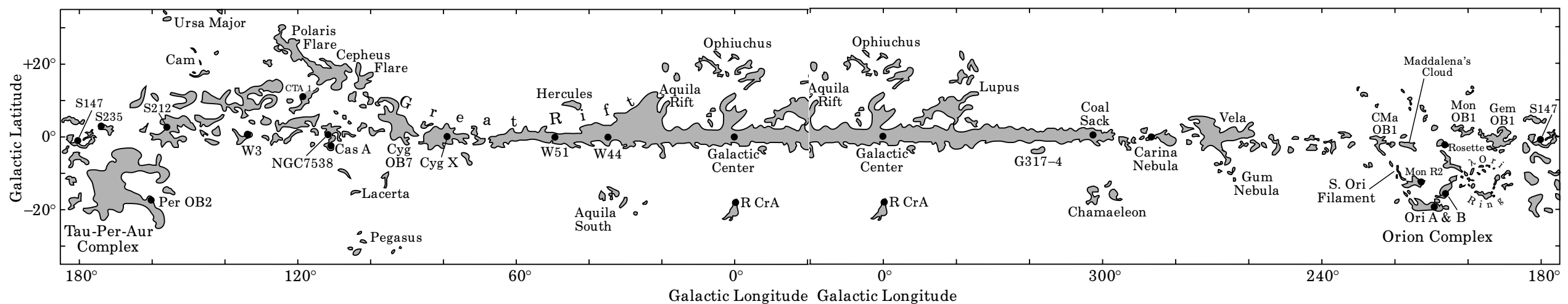
[Table 32.2, Draine]

- The **giant molecular cloud (GMC)** and **dark cloud** categories are distinguished mainly by total mass.
- Groups of distinct clouds are referred to as **cloud complexes**.
 - ▶ Molecular clouds are sometimes found in isolation, but in many cases molecular clouds are grouped together into complexes.
 - ▶ Since large clouds generally have substructure, the distinction between “cloud” and “cloud complex” is somewhat arbitrary.
 - ▶ Delineation of structure in cloud complexes is guided by the intensities and radial velocities of molecular lines (e.g., CO J = 1-0) as well as maps of thermal emission from dust at submm wavelengths.

Categories	Size (pc)	n_{H} (cm^{-3})	Mass (M_{\odot})	Linewidth (km s^{-1})	A_V (mag)	Examples
GMC Complex	25 – 200	50 – 300	10^5 – $10^{6.8}$	4 – 17	3 – 10	M17, W3, W51
Dark Cloud Complex	4 – 25	10^2 – 10^3	10^3 – $10^{4.5}$	1.5 – 5	4 – 12	Taurus, Sco-Oph
GMC	2 – 20	10^3 – 10^4	10^3 – $10^{5.3}$	2 – 9	9 – 25	Orion A, Orion B
Dark Cloud	0.3 – 6	10^2 – 10^4	5 – 500	0.4 – 2	3 – 15	B5, B227
Star-forming Clump	0.2 – 2	10^4 – 10^5	$10 - 10^3$	0.5 – 3	4 – 90	OMC-1, 2, 3, 4
Core	0.02 – 0.4	10^4 – 10^6	$0.3 - 10^2$	0.3 – 2	30 – 200	B335, L1535

[Table 32.2, Draine]

- Structures within a cloud (self-gravitating entities) are described as **clumps**.
 - ▶ Clumps may or may not be forming stars; in the former case they are termed **star-forming clumps**. **Cores** are density peaks within star-forming clumps that will form a single star or a binary star.
- GMC and GMC complex
 - ▶ Much of the molecular mass is found in large clouds known as “giant molecular clouds”, with masses ranging from $\sim 10^3 M_{\odot}$ to $\sim 2.5 \times 10^5 M_{\odot}$. These have reasonably well-defined boundaries.
 - ▶ A GMC complex is a gravitationally bound group of GMCs (and smaller clouds) with a total mass $\gtrsim 10^{5.3} M_{\odot}$.



Locations of prominent molecular clouds along the Milky Way

[Fig 32.2, Draine, Dame et al. (2001)]

Gas Surface Density in the Milky Way

- The most common way to study molecular gas is through molecular line emission, and the primary line used is the $J = 1-0$ transition (2.6 mm) of CO.
 - ▶ This transition is often optically thick, but the CO 1-0 luminosity of a cloud is approximately proportional to the total mass.
 - ▶ ***Velocity-resolved mapping of CO 1-0 together with an assumed rotation curve and an adopted value of the “CO to H₂ conversion factor” X_{CO} have been used to infer the surface density of H₂ over the Milky Way disk.***

Gas surface densities as a function of galactocentric radius. The Sun is assumed to be at $R = 8.5$ kpc.

- Surface density of H₂ estimated from CO 1-0 observations (Nakanishi & Sofue 2006), assuming
 $X_{CO} = 1.8 \times 10^{20} \text{ H}_2 \text{ cm}^{-2}/\text{K km s}^{-1}$
- Surface density of H II derived from pulsar dispersion measures (Cordes & Lazio 2003).
- Surface density of H I from 21-cm studies (Nakanishi & Sofue 2003)

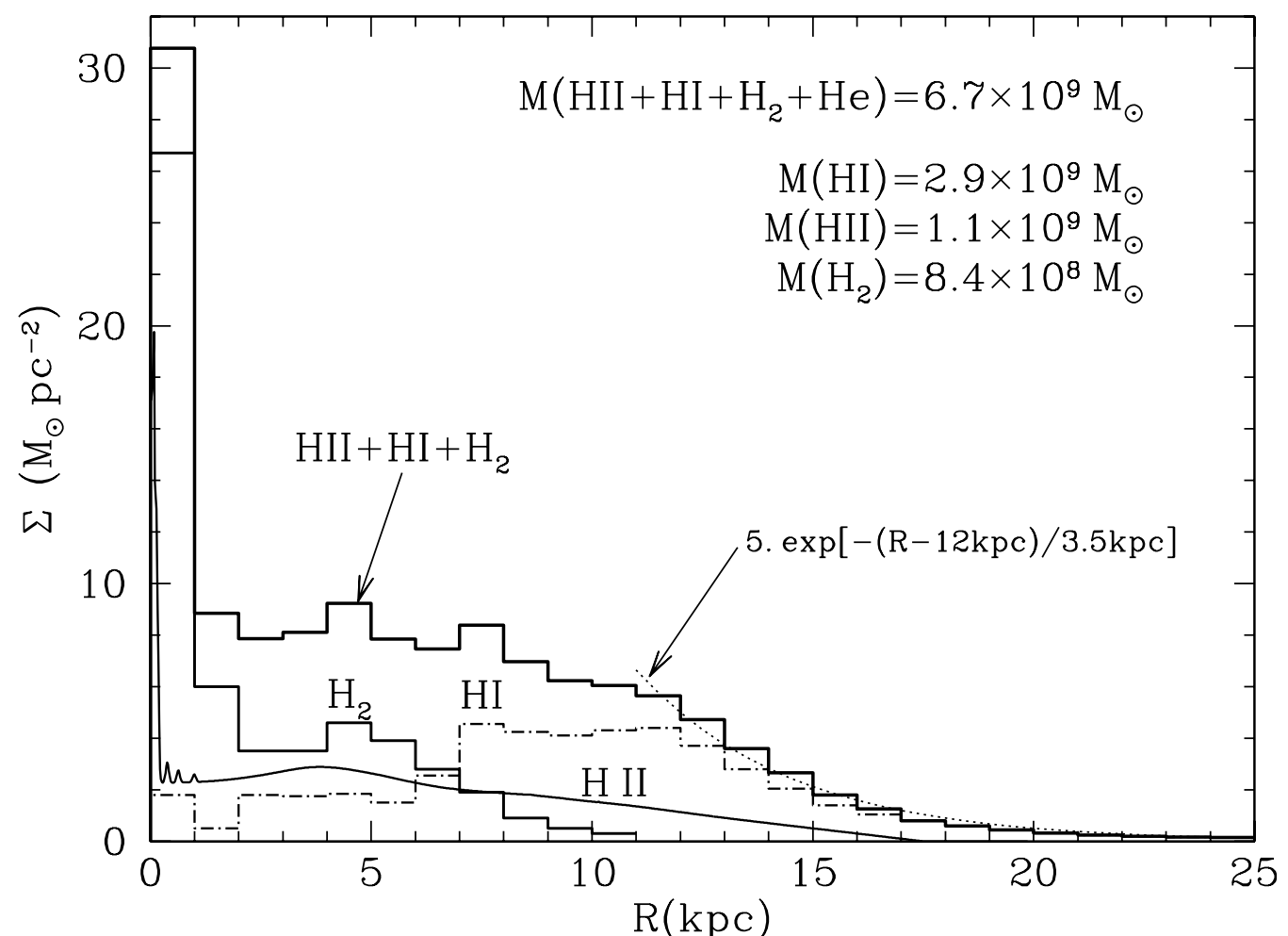


[Fig 32.4, Draine]

Size-Linewidth Relation in Molecular Clouds

- Larson (1981) noted that observations of molecular clouds in spectral lines of CO, H₂CO, NH₃, OH, and other species, were broadly consistent with a **size-linewidth relation**, where a density peak of characteristic size L tends to have a 3D velocity dispersion given by

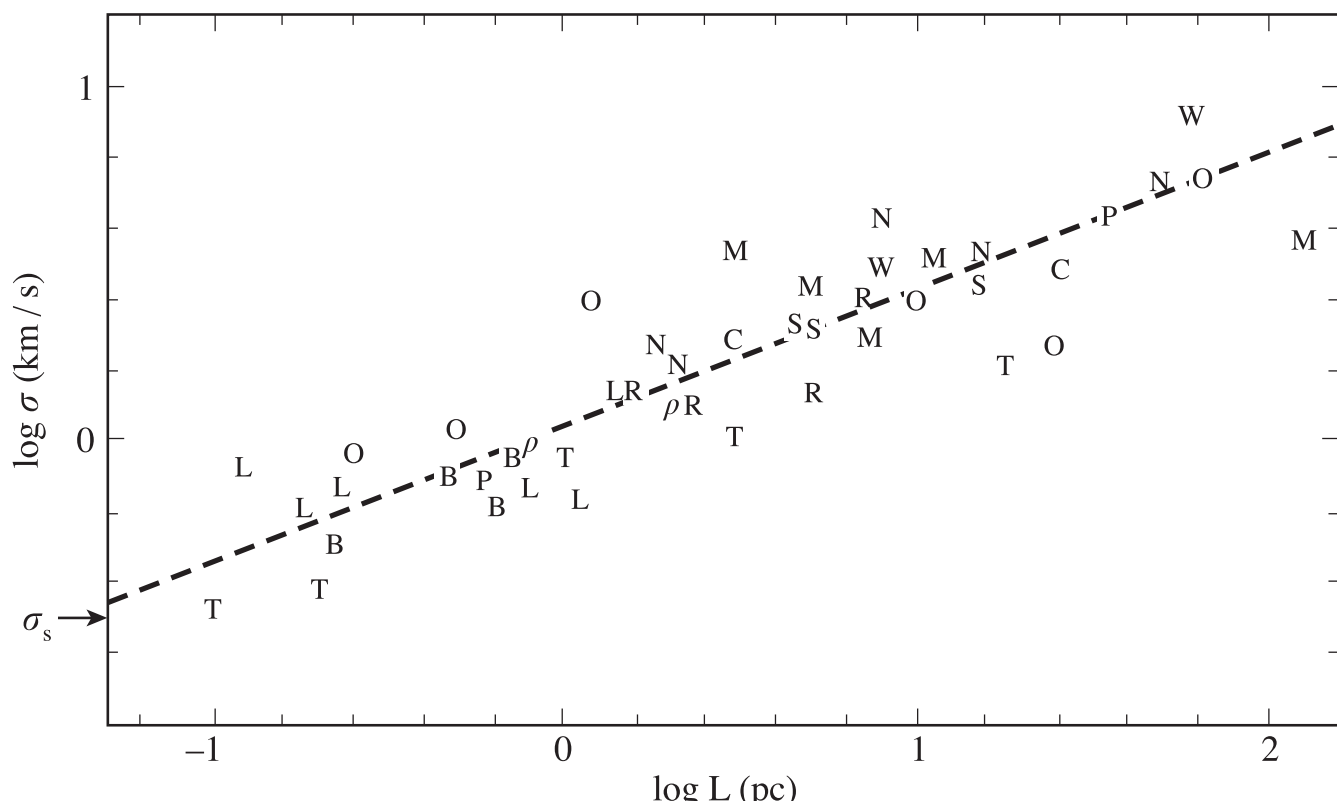
$$\sigma_v^* \approx 1.10 L_{\text{pc}}^\gamma \text{ km s}^{-1}, \quad \gamma \approx 0.38 - 0.5 \quad \text{for } 0.01 \lesssim L_{\text{pc}} \lesssim 10^2 \quad (L_{\text{pc}} = L/\text{pc})$$

where L is the maximum projected dimension of the density peak.

- ▶ Larson noted that the power-law index $\gamma \approx 0.38$ is curiously close to the index 1/3 found by **Kolmogorov** for a turbulent cascade in an incompressible fluid.
- ▶ It therefore is tempting to refer to the observed fluid motion as “turbulence,” although in reality the motions are some combination of thermal motions, rotation, MHD waves, and turbulence.

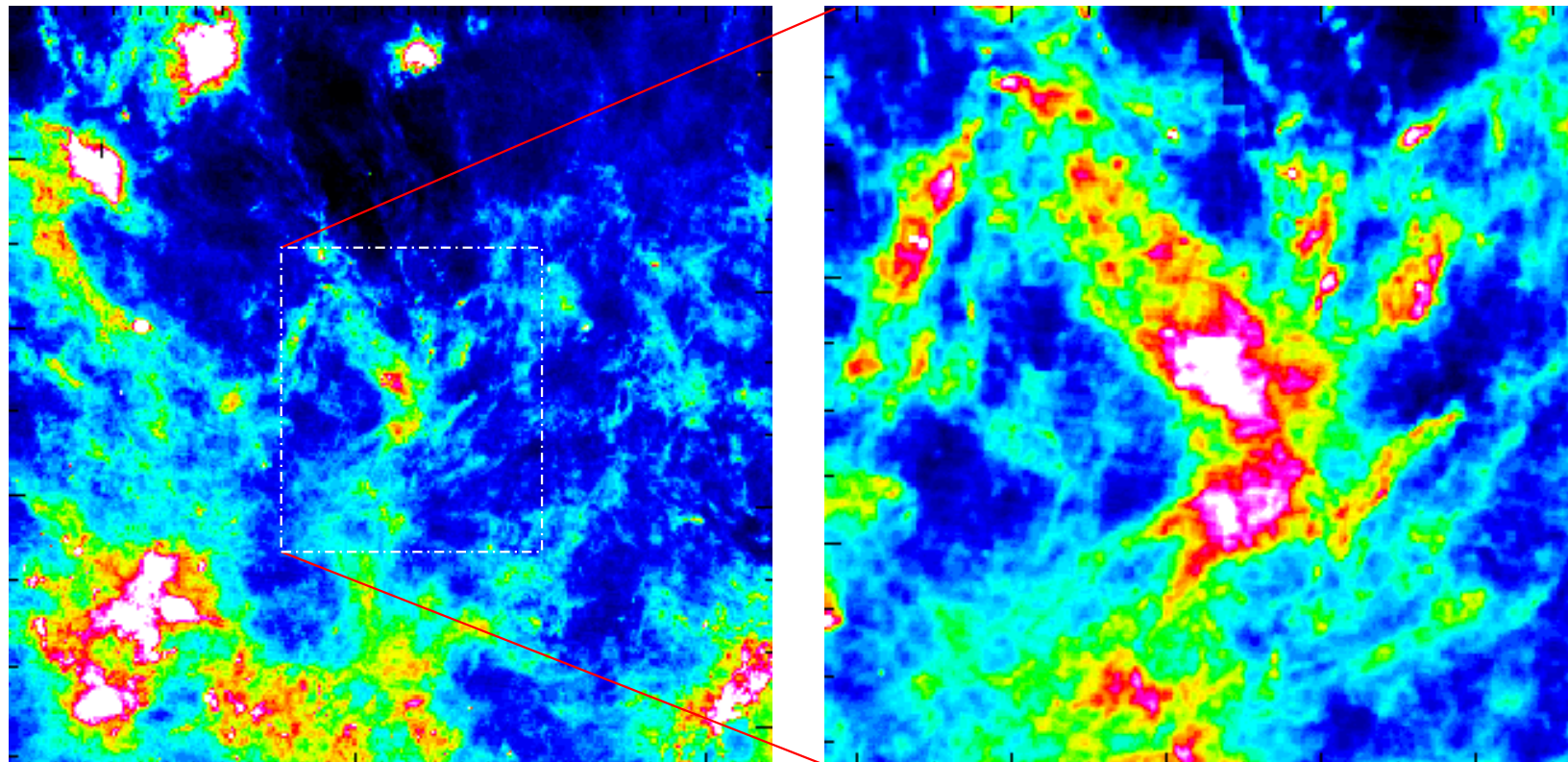
The 3D internal velocity dispersion versus maximum linear dimension L of the density peak.

Fig 32.5, Draine; Larson (1981)



The Fractal Structure of the Molecular Clouds

- Self-similarity of Clouds
 - The molecular interstellar medium is very clumpy and fragmented. Its hierarchical structure can well be described by a fractal, because of its self-similarity.
 - It has no characteristic scale. Fractals by definition are self-similar ensembles, that have a non-integer, i.e., fractional dimension.
 - ***The self-similar structures in the ISM extends over 6 orders of magnitude in scale, from about 10^{-4} to 100 pc.***
 - ▶ These are not observed for the same molecular cloud only because of technical problems, lack of spatial resolution on one side, and difficulty of mapping too large areas on the other.
 - ▶ The scaling relations all over the scales are however obtained by comparing various clouds observed with different resolutions.



IRAS 100 μm map of molecular clouds towards the Taurus complex, located at about 100 pc from the Sun. The square is $\sim 4000 \text{ pc}^2$.

Fig 14, Chap 2, Blain, Combes, Draine
[The Cold Universe]

Dust

Dust matters!

- Importance of Dust
 - In our Galaxy, the gas-to-dust ratio is about 100:1 by mass. Since the ISM is about 10% of the baryonic mass of the Galaxy, dust grains comprise roughly 0.1% of the total baryonic mass.
 - Dust grains absorb roughly 30-50% of the starlight emitted by the Galaxy and re-emit it as far-infrared continuum emission. ***This means that only 0.1% of the baryons are ultimately responsible for a third to a half of the bolometric luminosity of the Galaxy.***
 - Dust grains are central to the chemistry of interstellar gas. ***The abundance of H₂ in the ISM can only be understood if catalysis on dust grains is the dominant formation avenue.***
 - The formation of planetary systems is believed to begin when dust grains in a protostellar disk begin to coagulate into larger grains, leading to planetesimals and eventually to planets, carrying their complex organic molecules with them.

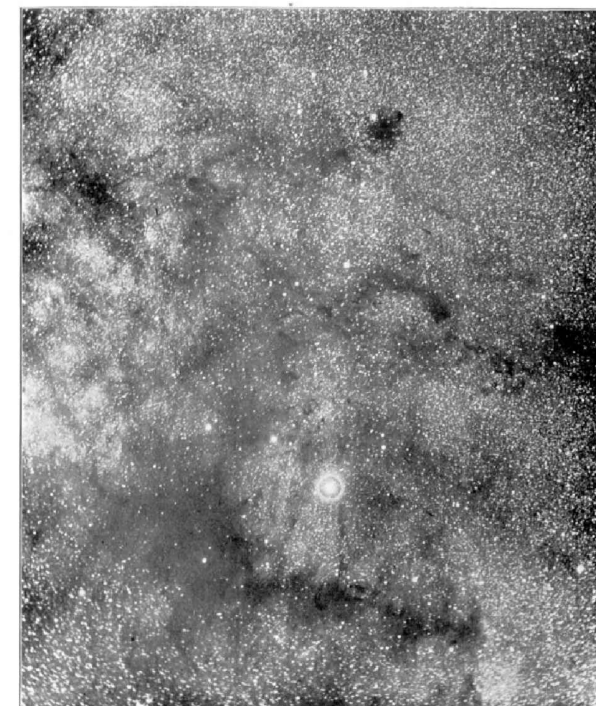
Observed Properties

- Extinction = Absorption + Scattering
 - Dust particles can scatter light, changing its direction of motion. When we look at a reflection nebula, like that surrounding the Pleiades, we are seeing light from the central stars that has been scattered by dust into our line of sight.
 - Dust particles can also absorb light. The relative amount of scattering and absorbing depends on the properties of the dust grains.
- Thermal radiation from Dust
 - When dust absorbs light, it becomes warmer, so dust grains can emit light in the form of thermal radiation. Most of this emission is at wavelengths from a few microns (near IR) to the sub-mm range (Far-IR).
- Polarization
 - The polarization of starlight was discovered in 1949 (Hall 1949).
 - The degree of polarization tends to be larger for stars with greater reddening, and stars in a given region of the sky tends to have similar polarization directions.



The Pleiades cluster and surrounding reflection nebulae (Fig. 6.3, Ryden)

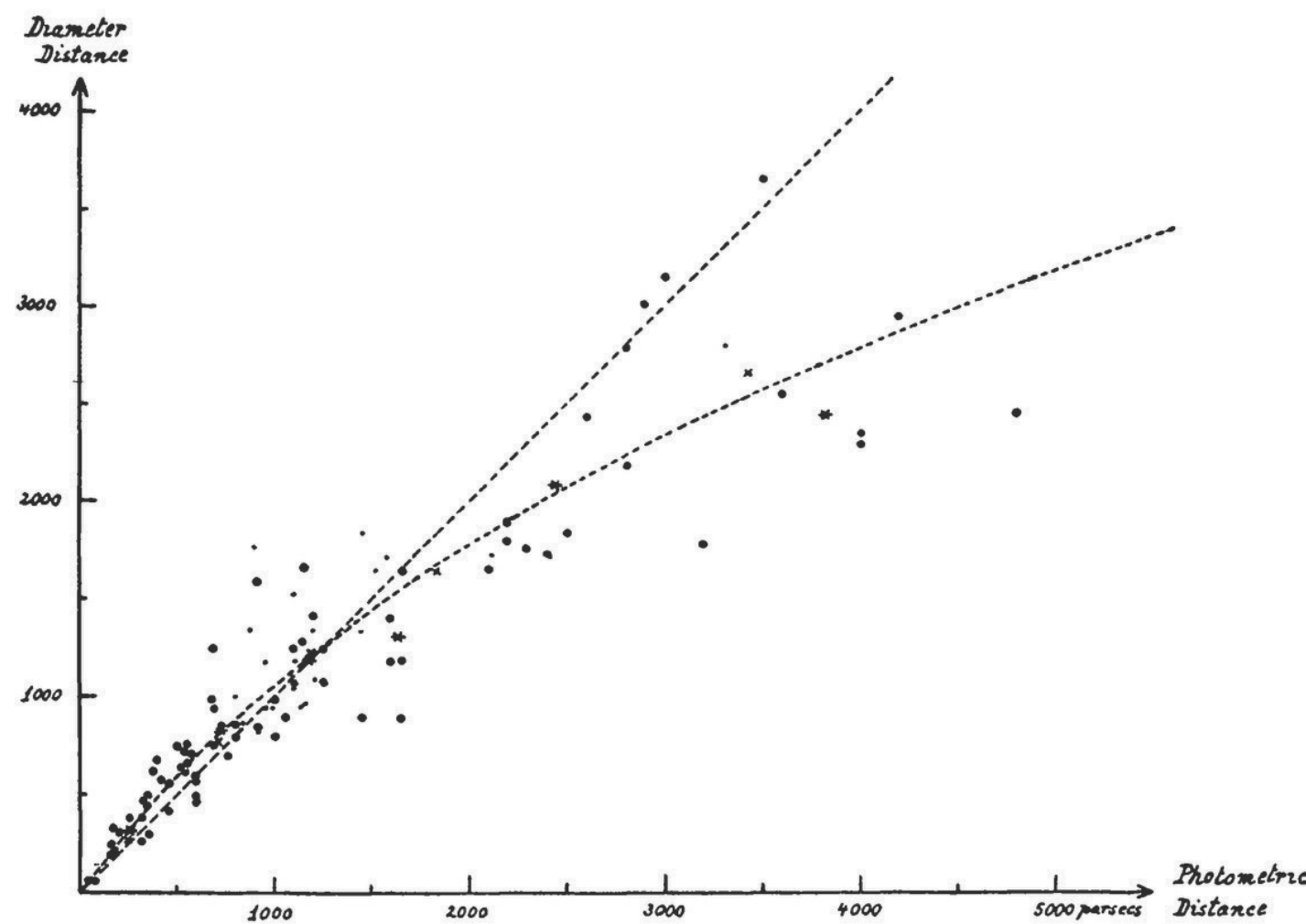
PLATE II.



PHOTOGRAPH OF THE MILKY WAY NEAR THE STAR THETA OPHIUCHI.

The dark structures near θ Ophiuchi
(Barnard 1899; Fig. 6.1, Ryden)

-
- Evidence for extinction. The correlation of distance determined from the angular size with the distance determined from the flux.



Extinction

- ***Extinction***

- Astronomers characterize the attenuating effects of dust by the “extinction” A_λ at wavelength λ . The extinction at a particular wavelength λ , measured in “magnitudes” is defined by the difference between the observed magnitude m_λ and the unabsorbed magnitude m_λ^0 :

$$\begin{aligned} A_\lambda \text{ [mag]} &= m_\lambda - m_\lambda^0 \\ &= -2.5 \log_{10} \left(\frac{F_\lambda}{F_\lambda^0} \right) \end{aligned}$$

F_λ = the observed flux from the star

F_λ^0 = the flux that would have been observed if the only attenuation had been from the inverse square law.

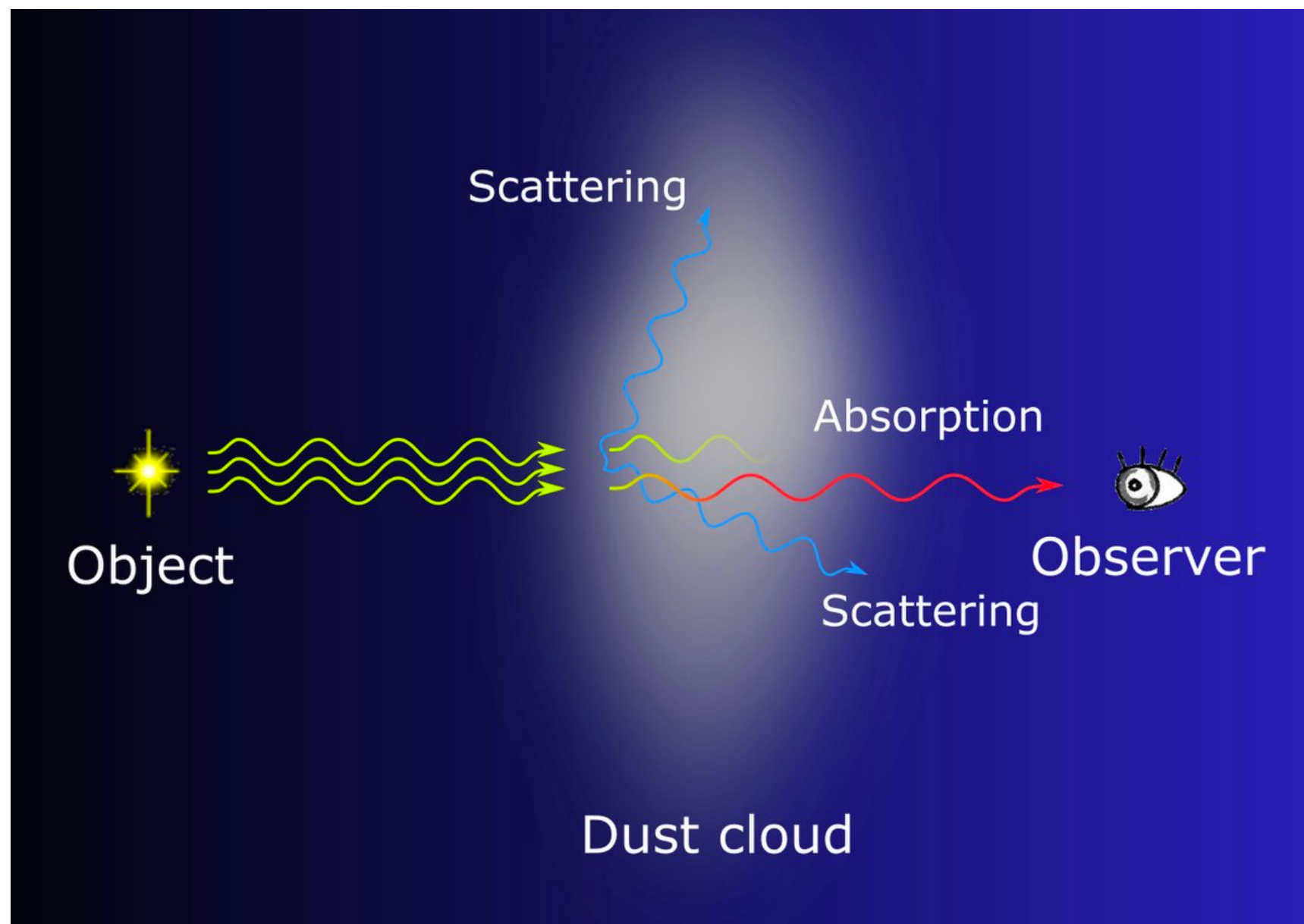
- The extinction measured in magnitudes is proportional to the optical depth:

$$F_\lambda = F_\lambda^0 e^{-\tau_\lambda} \quad \longrightarrow \quad A_\lambda = 2.5 \log_{10} (e^{\tau_\lambda}) = 2.5 \log (e) \times \tau_\lambda = 1.086 \tau_\lambda$$

Reddening

- ***Reddening***

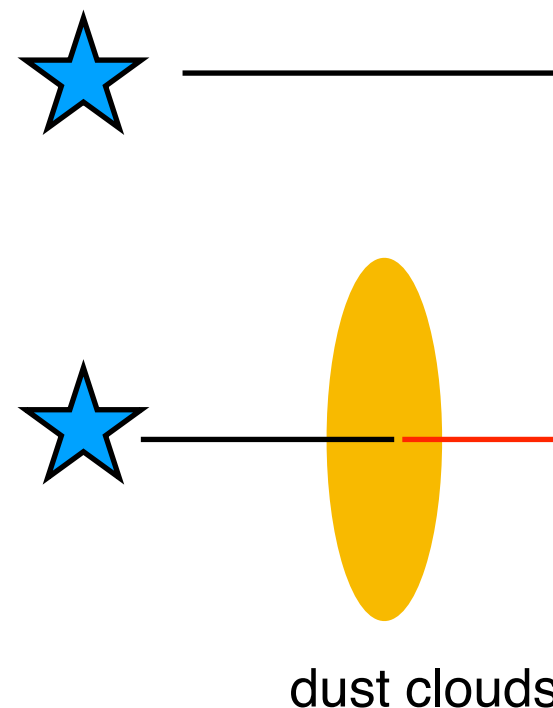
- Reddening is the phenomena of the color of a visible astronomical object (e.g., star) appearing more red from a distance than from nearby. Within the visible wavelength range, the absorption/scattering by dust increases with frequency, absorbing more of the blue light than red. This effect leads to the reddening.



How to measure the Interstellar Extinction

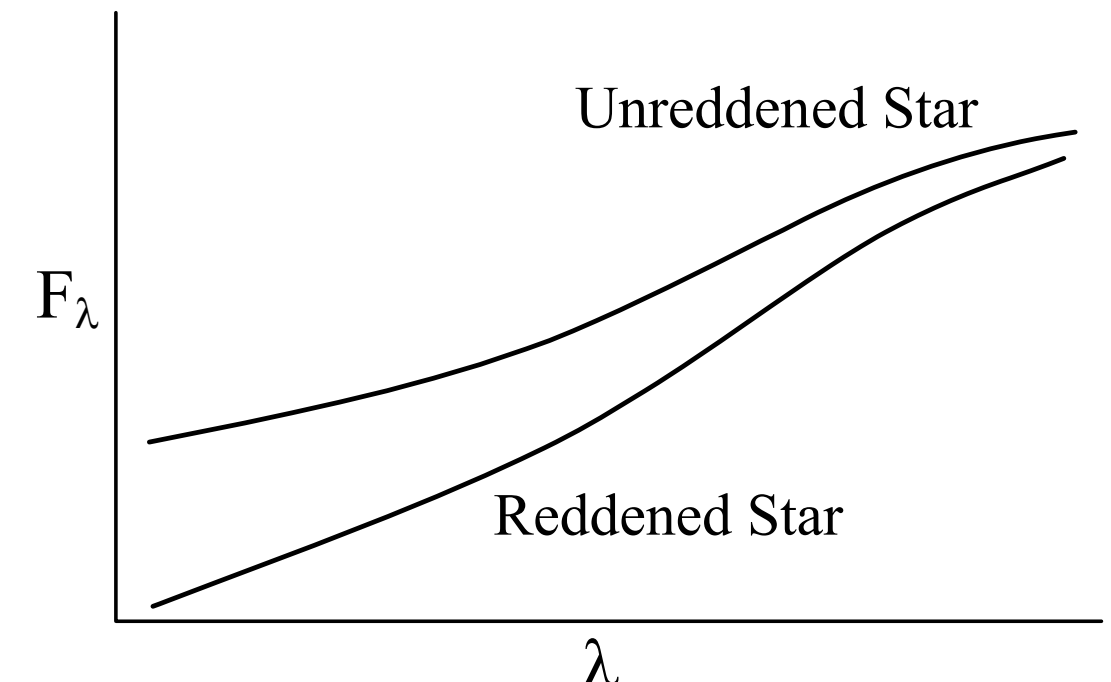
- Pair method
 - Trumpler (1930) compared the spectra of pairs of stars with identical (or similar) spectral type, one with negligible obscuration and the other extinguished by dust along the line of sight. This method remains our most direct way to study the “selective extinction” or “reddening” of starlight by the interstellar dust.

two stars
with the same spectral type



$$F(\lambda) = \frac{F_0(\lambda)}{4\pi d_1^2}$$

$$F(\lambda) = \frac{F_0(\lambda)}{4\pi d_2^2} e^{-\tau_\lambda}$$



- ***The Reddening Law, Extinction Curve***

- Extinction curve - the extinction A_λ as a function of wavelength or frequency
 - ▶ A typical extinction curve shows the ***rapid rise in extinction in the UV.***
 - ▶ ***The extinction increases from red to blue,*** and thus the light reaching us from stars will be “reddened” owing to greater attenuation of the blue light.
 - ▶ The reddening by dust is expressed in terms of a color excess; for instance,

B-V color excess:

$$E(B - V) \equiv A_B - A_V$$

$$\lambda_B \sim 4400 \text{ \AA}$$

$$\lambda_V \sim 5500 \text{ \AA}$$

in general,

$$E(\lambda_1 - \lambda_2) \equiv A_{\lambda_1} - A_{\lambda_2} \quad (\lambda_1 < \lambda_2)$$

- ▶ The detailed wavelength dependence of the extinction - the “reddening law” - is sensitive to the composition and size distribution of the dust particles.
- ▶ The slope of the extinction at visible wavelengths is characterized by the dimensionless ratio, the ratio of total to selective extinction:

$$R_V \equiv \frac{A_V}{A_B - A_V} \equiv \frac{A_V}{E(B - V)}$$

- ▶ R_V ranges between 2 and 6 for different lines of sight. Sightlines through diffuse gas in the Milky Way have $R_V \approx 3.1$ as an average value. ***Sightlines through dense regions tend to have larger values of R_V .*** In dense clouds, the value $R_V \approx 5$ is typically adopted.

- ▶ ***Observed extinction curves vary in shape from one line of sight to another.***
- ▶ Extinction curve, relative to the extinction in the I band ($\lambda = 8020\text{\AA}$), as a function of inverse wavelength, for Milky Way regions characterized by different values of R_V .

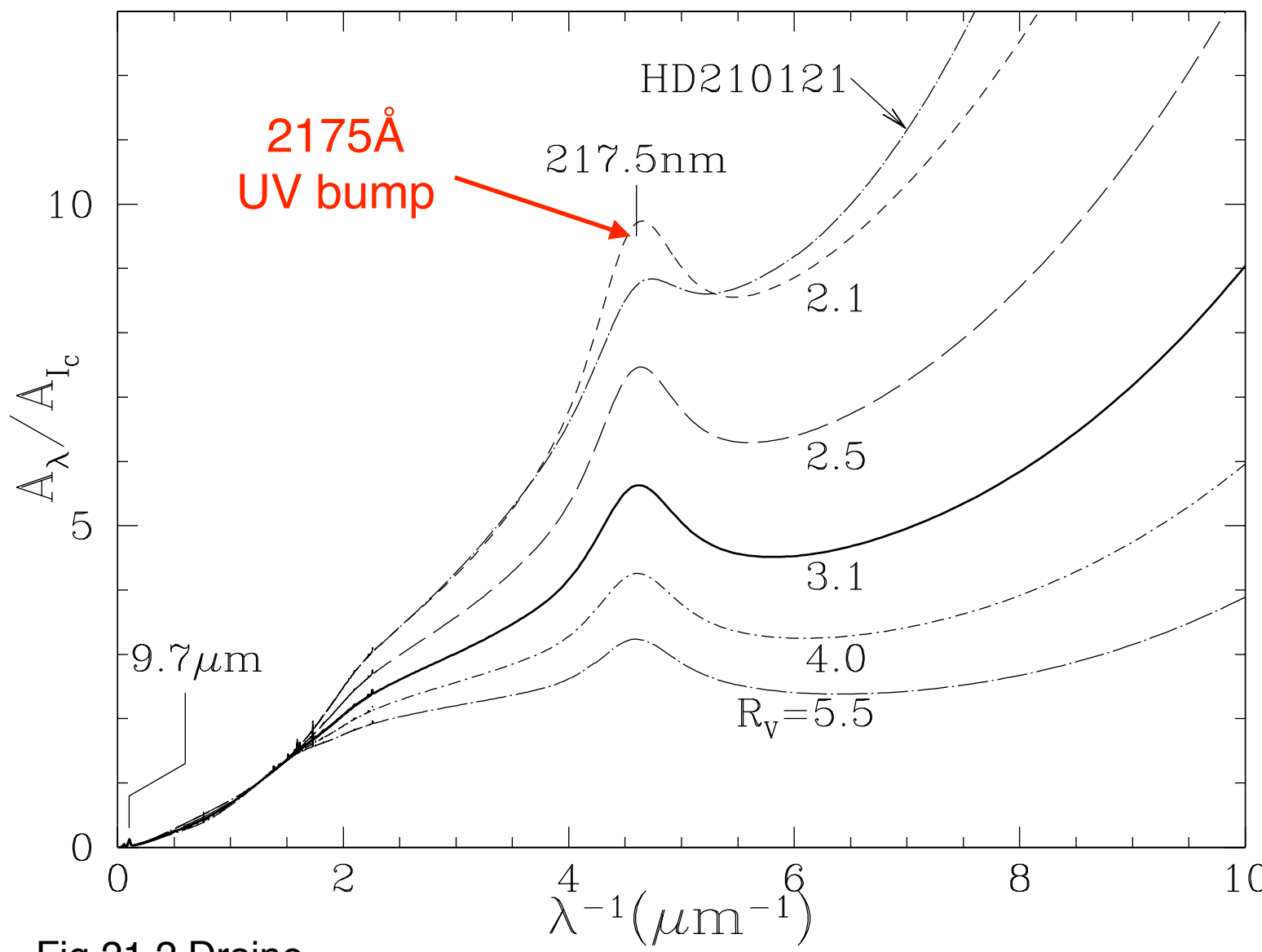


Fig 21.2 Draine

Parameterization of the extinction curve.

Cardelli et al. (1989)

Fitzpatrick (1999)

Gas-to-dust ratio

- If the dust grains were large compared to the wavelength, we would be in the “geometric optics” limit, and the extinction cross section would be independent of wavelength (gray extinction).
 - ▶ The tendency of the extinction to rise with decreasing λ , even at the shortest ultraviolet wavelengths tells us that grains smaller than the wavelength must be making an appreciable contribution to the extinction at all observed wavelengths, down to $\lambda = 0.1 \mu\text{m}$.
 - ▶ According to the Mie theory, “small” means (approximately) that $2\pi a/\lambda \lesssim 1$. Thus interstellar dust must include a large population of small grains with $a \lesssim 0.015 \mu\text{m}$.
- The dust appears to be relatively well-mixed with the gas (Bohlin et al. 1978; Rachford et al. 2009):

$$\frac{N_{\text{H}}}{E(B-V)} = 5.8 \times 10^{21} \text{ H cm}^{-2} \text{ mag}^{-1}$$

$N_{\text{H}} \equiv N(\text{HI}) + 2N(\text{H}_2)$
column density of total hydrogen nuclei

- ▶ For sightlines with $R_V \approx 3.1$, this implies that

$$\frac{A_V}{N_{\text{H}}} \approx 5.3 \times 10^{-22} \text{ mag cm}^2 \text{ H}^{-1}$$

- ▶ Thus, even at high galactic latitudes, where the column density of hydrogen is $\sim 10^{20} \text{ cm}^{-2}$, there is still some foreground extinction when looking at extragalactic sources; ~ 0.05 magnitudes in the V band.

- **Mean ratio of visual extinction to length in the Galactic plane**

$$\left\langle \frac{A_V}{L} \right\rangle \approx 1.8 \text{ mag kpc}^{-1}$$

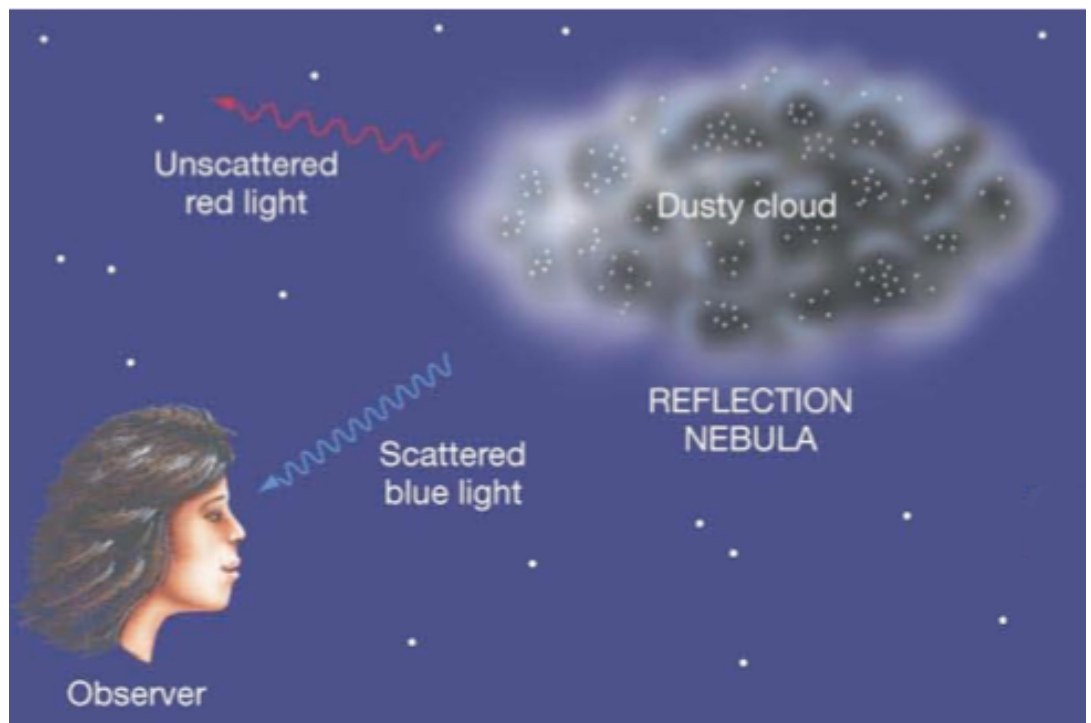
- **Scattering of Starlight**

- When an interstellar cloud happens to be unusually near one or more bright stars, we have a reflection nebula, where we see starlight photons that have been scattered by the dust in the cloud.

- **The spectrum of the light coming from from the cloud surface shows the stellar absorption lines**, thus demonstrating that scattering rather than some emission process is responsible.

- Given the typical size of interstellar dust grains, blue light is scattered more than red light.

A reflection nebulae is typically blue (so for the same reason that the sky is blue, except it's scattering by dust (for the reflection nebula) vs by molecules (for the earth's atmosphere)).



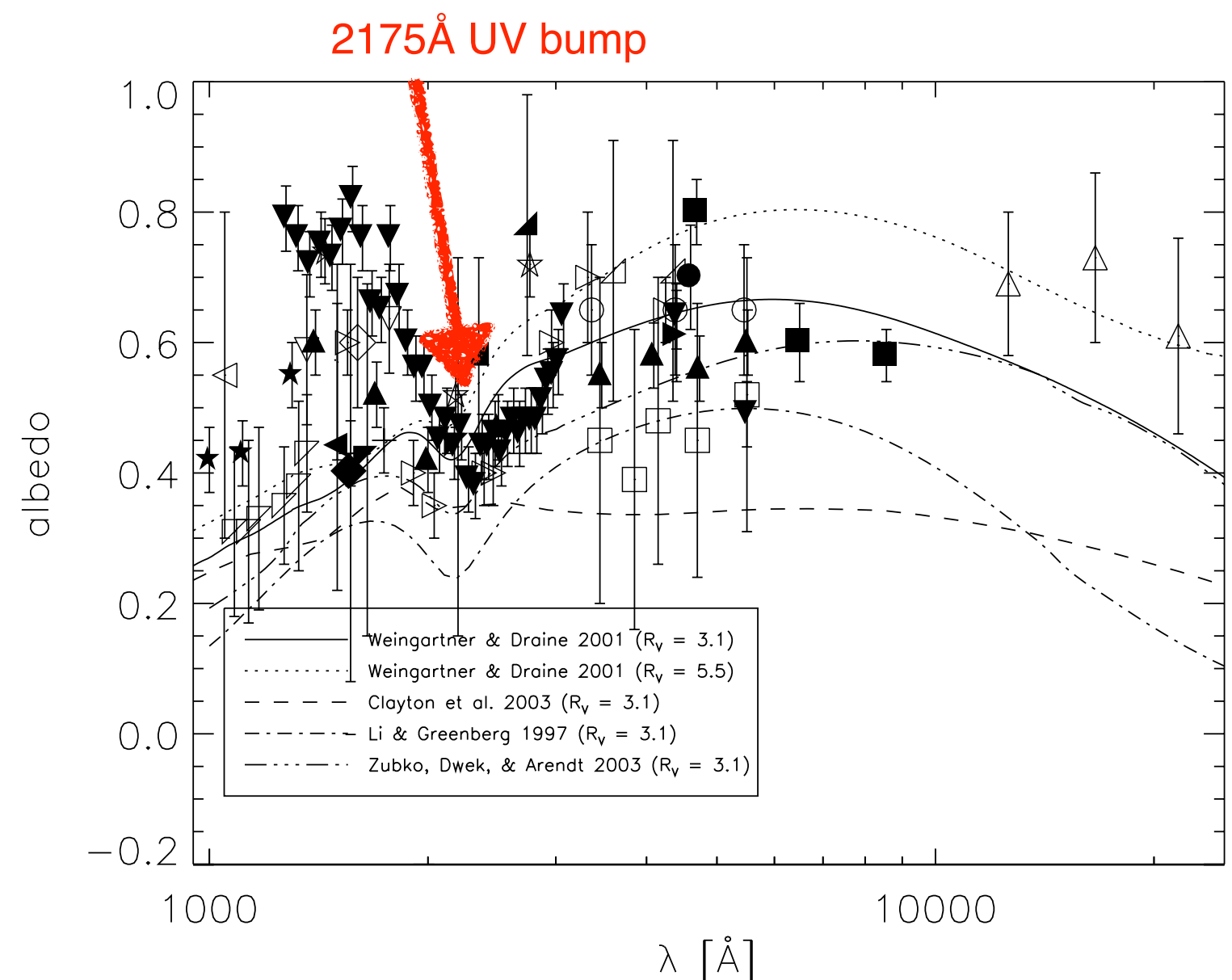
UV bump

- The study of dust scattering properties has shed light on the nature of the 2175Å bump and the far-ultraviolet rise features of extinction curves.
- Lillie & Witt (1976) and Calzetti et al. (1995) showed that ***the 2175Å bump was likely an absorption feature with no scattered component.***

The determinations of the albedo in reflection nebulae, dark clouds, and the diffuse Galactic light are plotted versus wavelength.

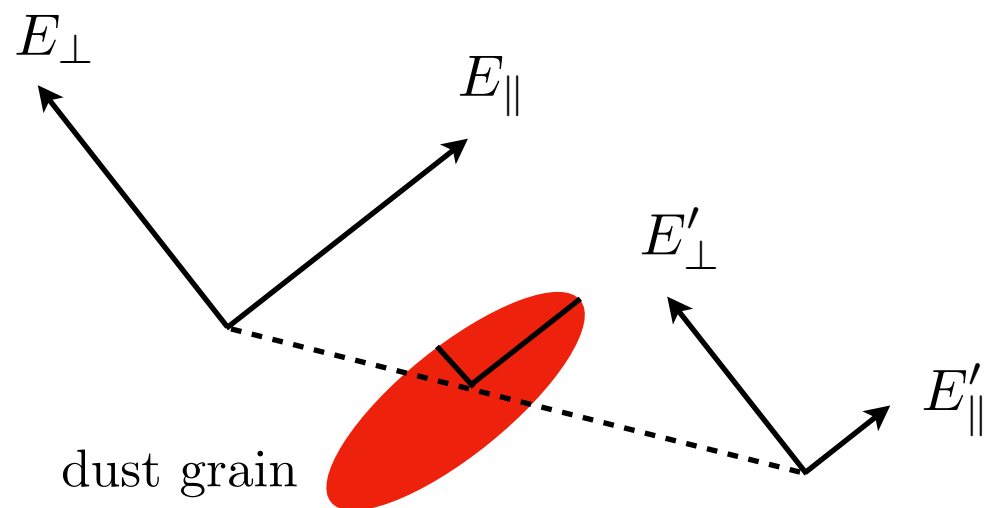
Predictions from dust grain models are also plotted for comparison.

Karl D. Gordon,
2004, ASPC, 309, 77



- **Polarization of Starlight by Interstellar Dust**

- Initially unpolarized light propagating through the ISM becomes linearly polarized as a result of ***preferential extinction*** of one linear polarization mode relative to the other.



$$E_{\parallel} = E_{\perp}$$

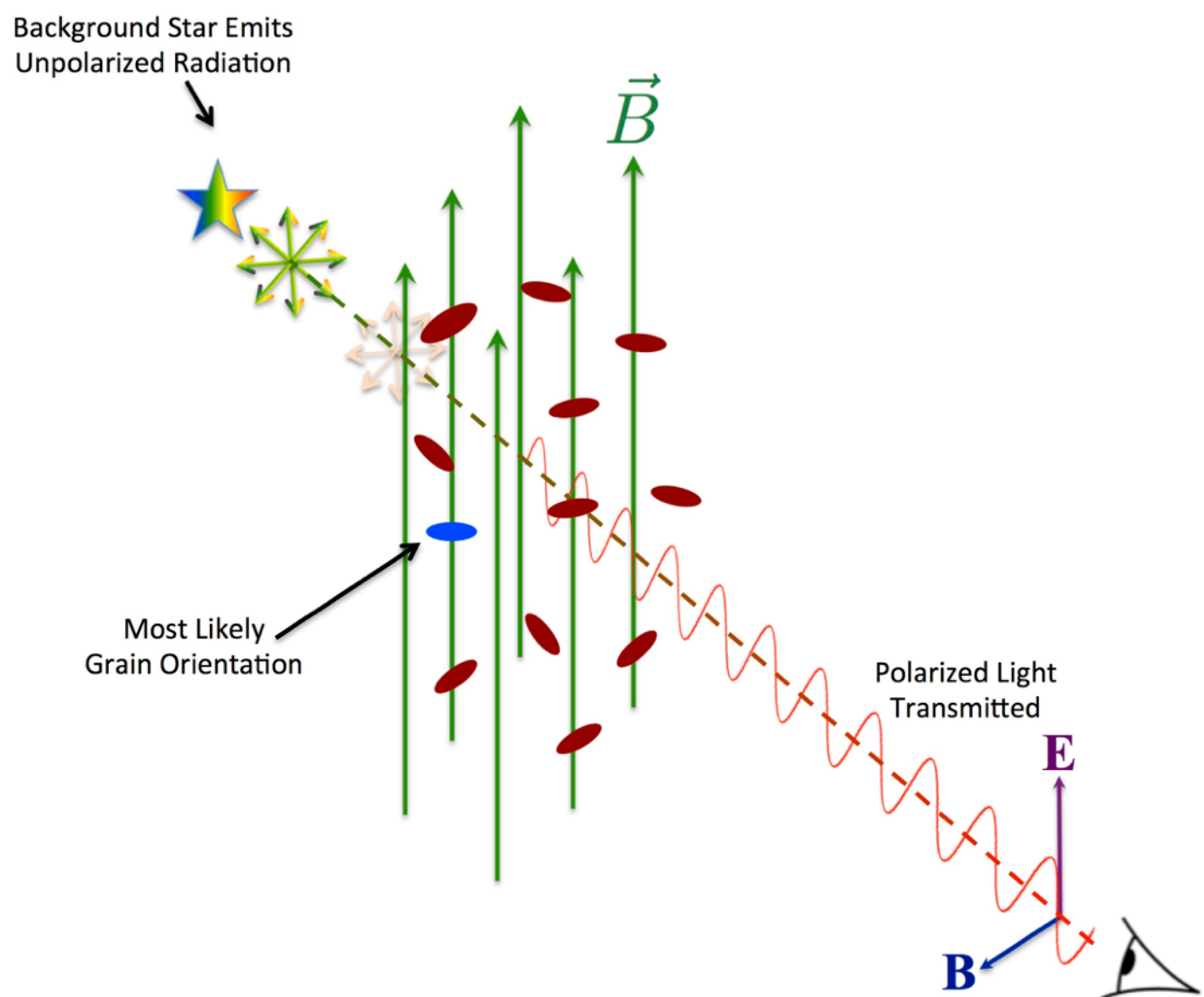
$$E'_{\parallel} < E'_{\perp}$$

$$E'_{\parallel} = E_{\parallel} e^{-\tau_{\parallel}}$$

$$E'_{\perp} = E_{\perp} e^{-\tau_{\perp}}$$

$$\tau_{\parallel} > \tau_{\perp}$$

The starlight is slightly more blocked along the long axis of the grains than along the short axis. This give rise to the polarization of starlight.



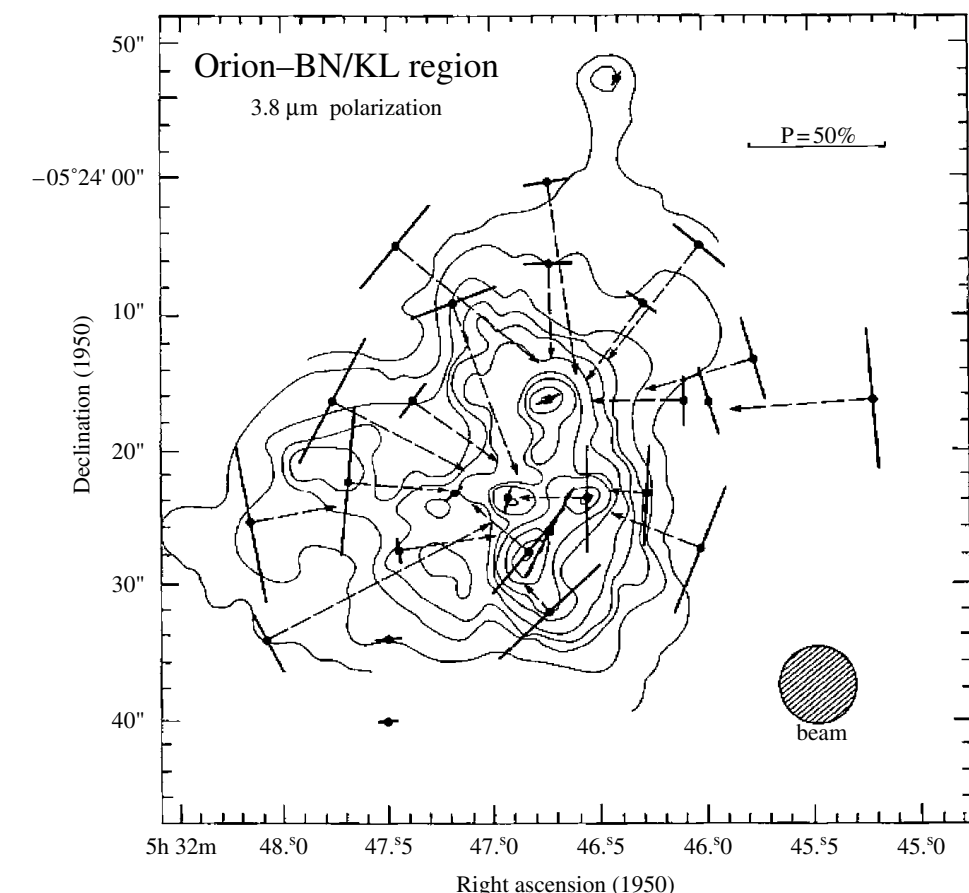
credit: B-G Andersson

- **Polarized Infrared Emission**

- The far-IR emission from aligned dust grains will also be polarized, this time with a direction along the long axis of the grains. Far-IR polarization has been observed for a large number of molecular clouds that have “high” dust emission optical depths at long wavelengths ($\sim 0.1\text{-}1$ mm).

- **Polarization due to scattering**

- Scattering of light by dust grains generally also lead to polarization.
- For single scattering, the polarization vector is perpendicular to the line connecting the light source and the scattering grain.
- The degree of polarization and its distribution provide information on the characteristics of the scattering grains and the geometry of the nebula.



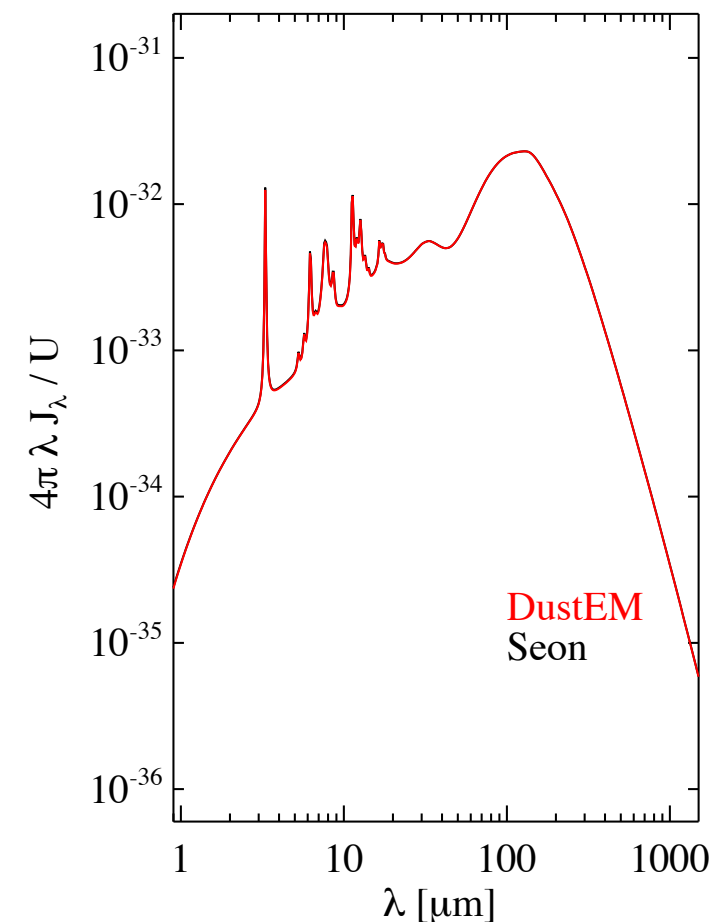
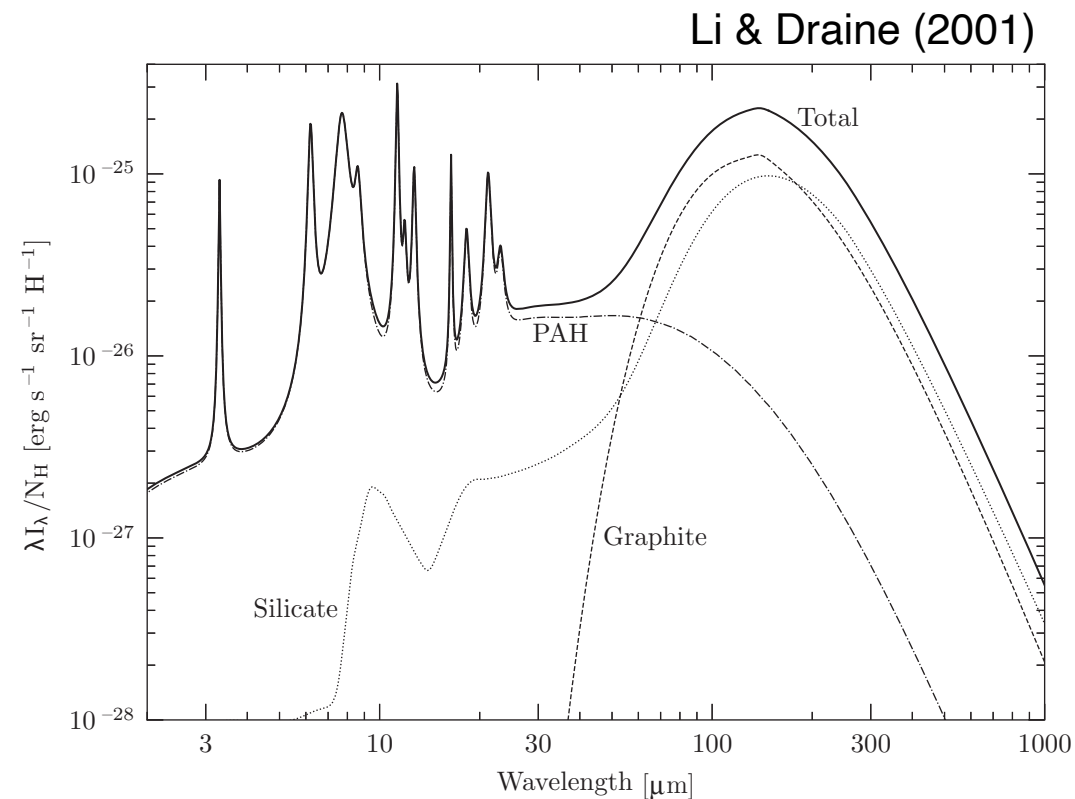
Linear polarization of the IR reflection nebula associated with the region of massive star formation in Orion.
The linear polarization vectors measured at K are superimposed on a map of the scattered light intensity.

[Werner et al. 1983, ApJ, 265, L13]

Infrared Emission

- ***Infrared Emission***

- Dust grains are heated by starlight, and cool by radiating in the infrared.
- The IR spectrum provides very strong constraints on grain models.
- There are two components: ***a cold ($T \sim 15\text{-}20 K$) component*** emitting mainly at long wavelengths (far-IR) and ***a hot ($T \sim 500 K$) component*** dominating the near- and mid-IR emission.
 - ▶ The **cold component** is due to **large dust grains** in radiative equilibrium with the interstellar radiation field.
 - ▶ The **hot component** is due to **ultra small grains and PAH species** that are heated by a single UV photon to temperatures of $\sim 1000 K$ and cool rapidly in the near- and mid-IR.



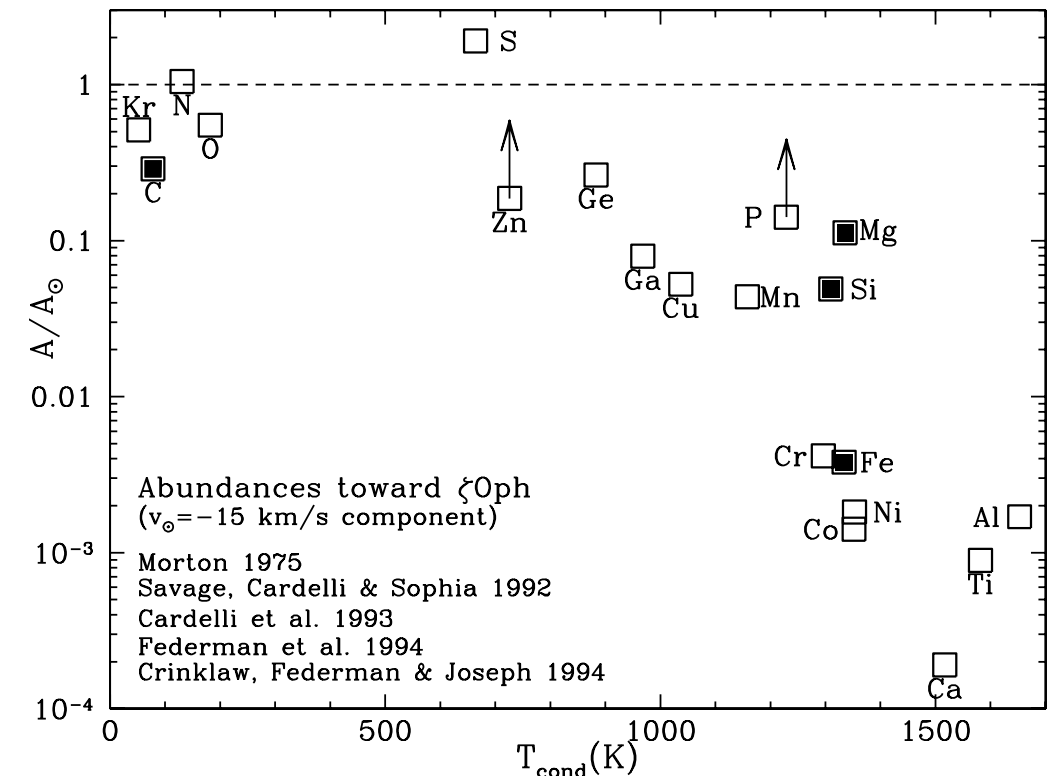
What are the dust grains made of?

- Observational Constraints
 - **Interstellar Depletion:** Certain elements appear to be underabundant or “depleted” in the gas phase. The observed depletions tell us about the major elemental composition of interstellar dust.
 - **Spectroscopy:** We would observe spectroscopic features that would uniquely identify the materials, and allow us to measure the amounts of each material present. But, it is difficult to apply this approach to solid materials because: (1) the optical and UV absorption is largely a continuum; and (2) the spectral features are broad, making them difficult to identify conclusively.
 - **Extinction:**
 - ▶ The wavelength dependence of the extinction curve provides constraints on the interstellar grain size distribution.
 - ▶ What materials could plausibly be present in the ISM in quantities sufficient to account for the observed extinction? A Kramers-Kronig integral over the observed extinction indicates that the total grain mass relative to total hydrogen mass:

$$M_{\text{dust}}/M_{\text{H}} \gtrsim 0.0083$$

Interstellar Depletion

- Condensable elements:
 - ▶ Hydrogen: There is no way to have hydrogen contribute appreciably to the grain mass (even polyethylene (CH_2)_n is 86% carbon by mass).
 - ▶ The noble gases (He, Ne, Ar, Kr, Xe...) and nitrogen(N), zinc (Zn), and sulfur (S) are examples of species that generally form only rather volatile (휘발성) compounds. They are observed to be hardly depleted at all.
volatile = easily evaporated at normal temperature
 - ▶ The only way to have a dust/H mass ratio of 0.0056 or higher is to build the grains out of the most abundant condensable elements: C, O, Mg, Si, S, and Fe (refractory materials; 내열성물질).
refractory = stubborn or unmanageable
- Abundance Constraints toward ζ Oph
 - ▶ Nitrogen is present at its solar abundance.
 - ▶ C abundance is at $\sim 35\%$ of its solar value.
 - ▶ O abundance is at $\sim 55\%$ of its solar value.
 - ▶ Mg is at $\sim 11\%$.
 - ▶ Si is at $\sim 5\%$.
 - ▶ Fe is at $\sim 0.4\%$.



Gas-phase abundances (relative to solar) in the diffuse cloud toward ζ Oph, plotted versus “condensation temperature”

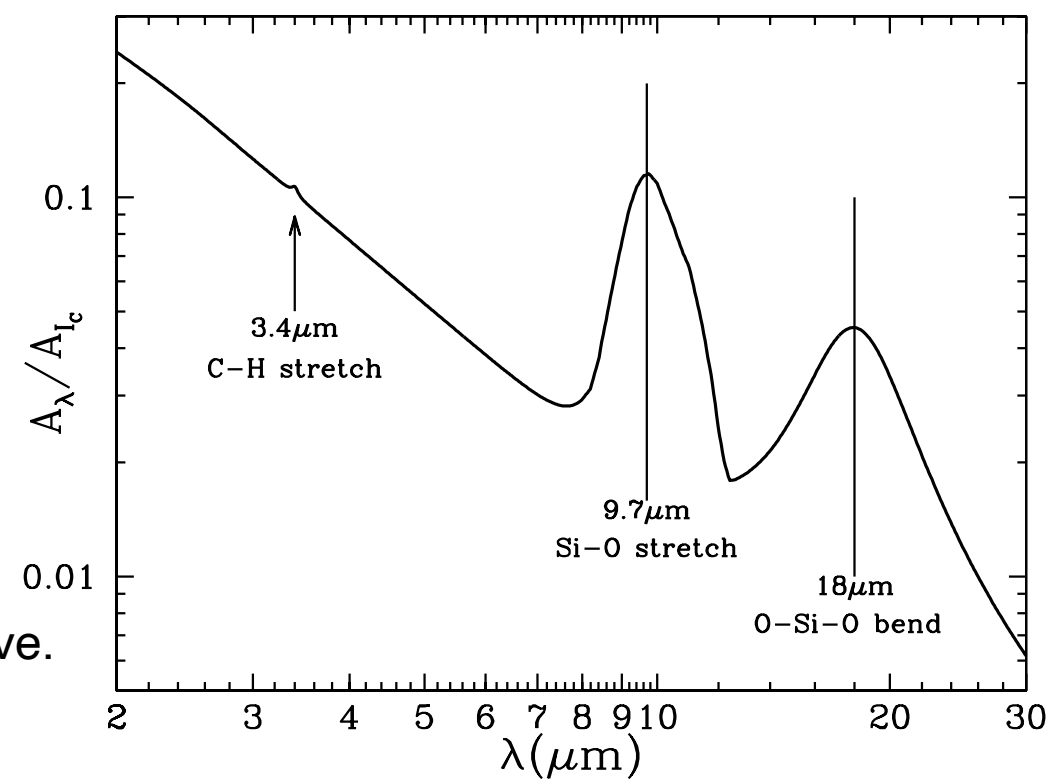
Observed Spectral Features of Dust

- The 2175Å Feature (UV bump)
 - The strongest feature in the interstellar extinction curve is a broad “bump” centered at $\sim 2175\text{\AA}$ where there is additional absorption above the rough $1/\lambda$ behavior at adjacent wavelengths.
 - ▶ The feature is well-described by a Drude profile.
- $$S(\lambda) = \frac{2}{\pi} \frac{\gamma_0 \lambda_0 \sigma_{\text{int}}}{(\lambda/\lambda_0 - \lambda_0/\lambda)^2 + \gamma_0^2} \quad \text{where } \sigma_{\text{int}} = \int S(\lambda) d\lambda^{-1}$$
- ▶ The central wavelength is nearly identical on all sightlines, but the width varies significantly from one region to another.
 - ▶ The strength of the feature is a strong function of the metallicity of the gas, with the UV bump appearing slightly weaker in the LMC extinction curve (metallicity $\sim 50\%$ solar), but essentially absent in the SMC extinction curve (metallicity $\sim 10\%$ solar).
 - The strength of this feature implies that the responsible material must be abundant: it must be made of H, C, N, O, Mg, Si, S, or Fe.

- Mid-Infrared Silicate Features:

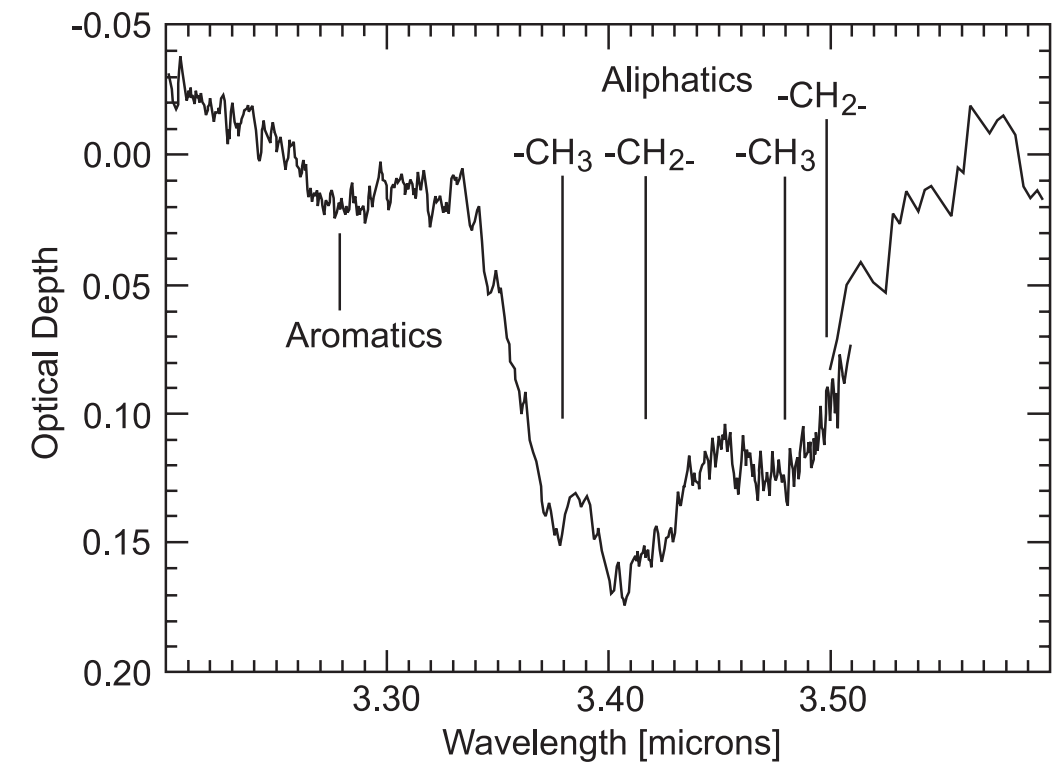
The fact that the $9.7\mu\text{m}$ band is fairly featureless, unlike what is seen in laboratory silicate crystals, suggests that this “astrophysical” silicate is primarily amorphous rather than crystalline in nature.

IR extinction curve.
[Fig 23.2 Draine]



- The $3.4\mu\text{m}$ Feature

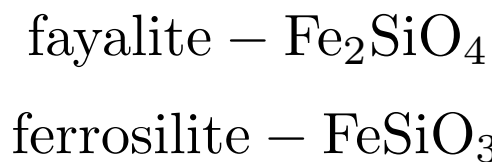
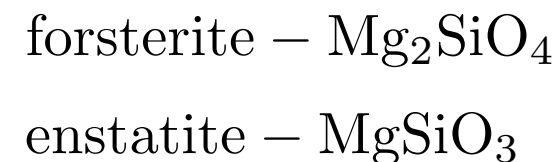
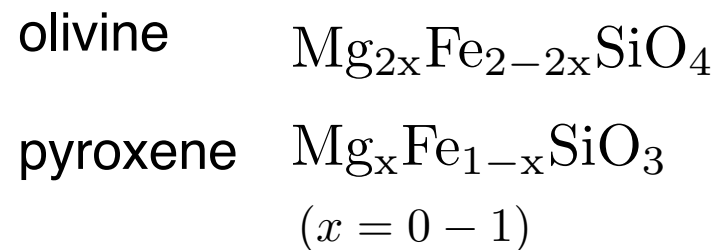
- There is a broad absorption feature at $3.4\mu\text{m}$ that is almost certainly due to the C-H stretching mode in “aliphatic” hydrocarbons (organic molecules with carbon atoms joined in straight or branched chains).



The source GCS3 in the
Galactic Center
Chiar et al. (2000, ApJ)

Dust Materials

- Silicates
 - The two main types of silicates in dust are pyroxene and olivine.



[Left] Olivine is the simplest silicate structure, which is composed of isolated tetrahedra bonded to iron and/or magnesium ions. No oxygen atom is shared to two tetrahedra.

[Middle] In pyroxene, silica tetrahedra are linked together in a single chain, where one oxygen ion from each tetrahedra is shared with the adjacent tetrahedron.

[Right] Other types are possible. In amphibole structures, two oxygen ions from each tetrahedra are shared with the adjacent tetrahedra.

In mica structures, the tetrahedra are arranged in continuous sheets, where each tetrahedron shares three oxygens with adjacent tetrahedra.

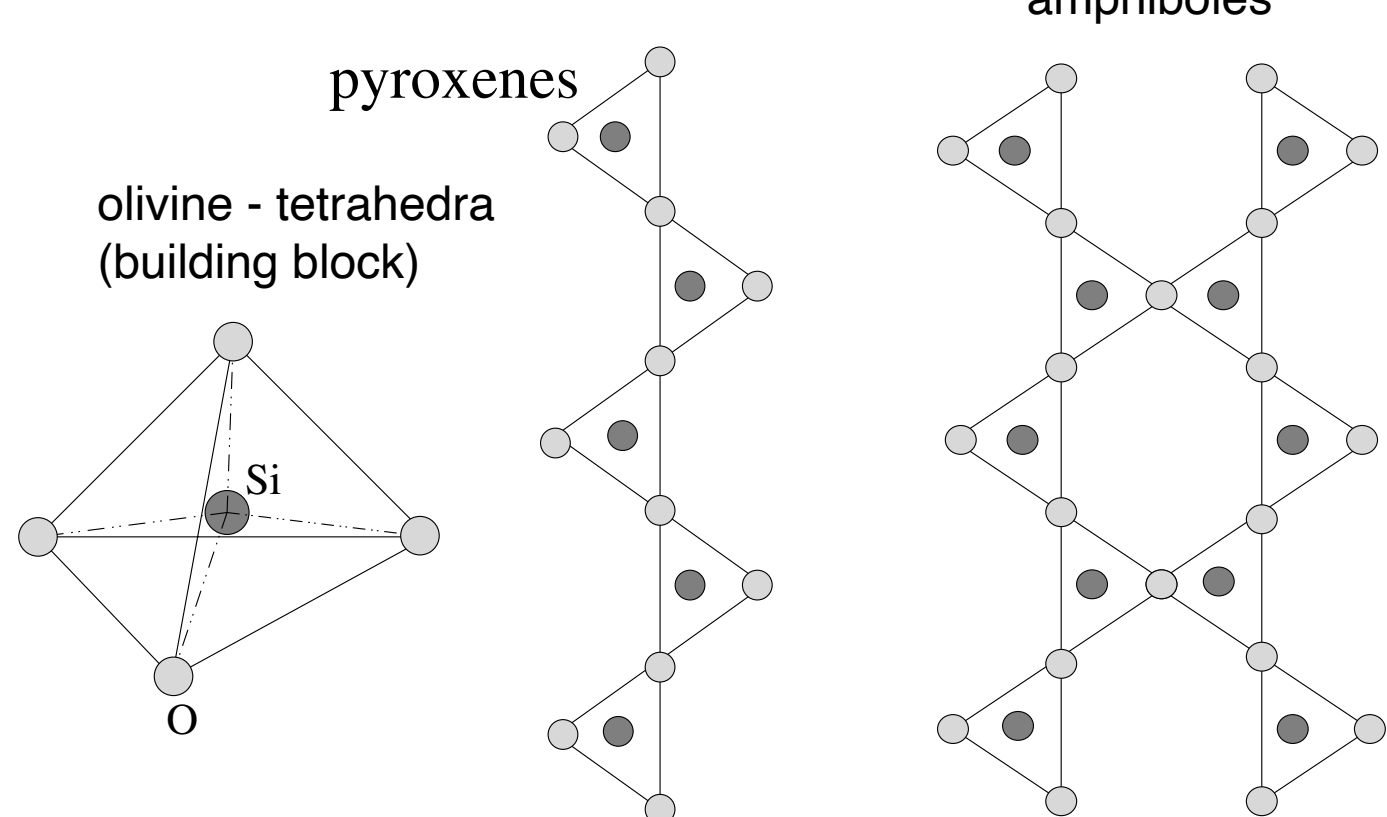
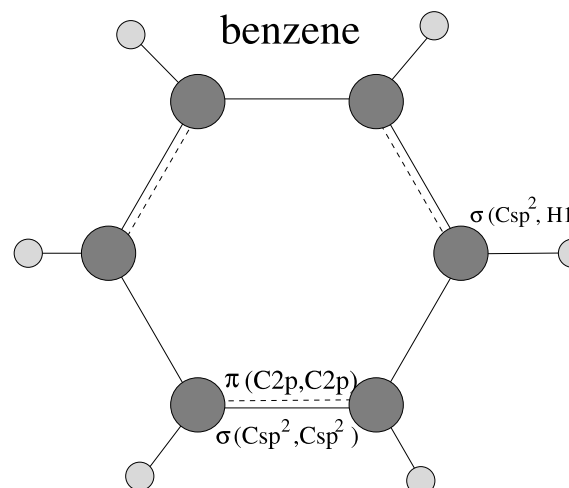


Fig 5.9 Krugel
[An Introduction to the Physics of Interstellar Dust]

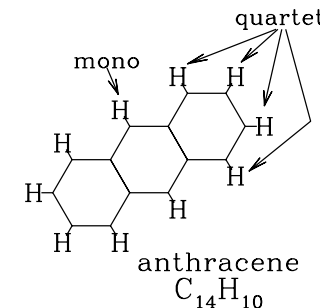
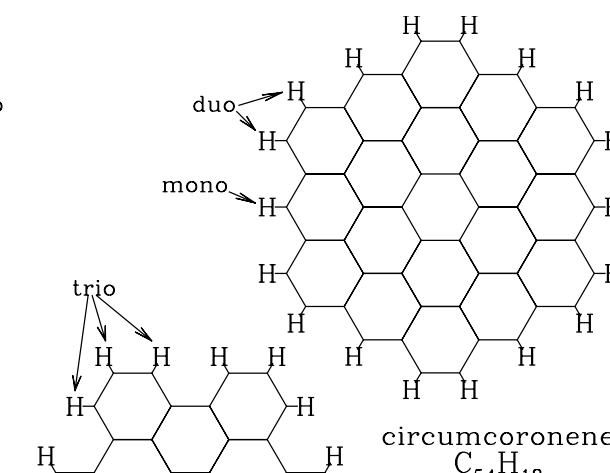
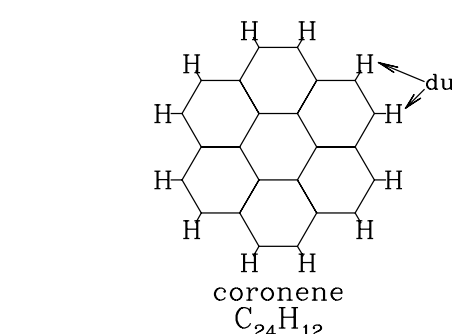
• Polycyclic Aromatic Hydrocarbons

- The IR emission spectra of spiral galaxies show emission features at 3.3, 6.2, 7.7, 8.6, 11.3, and 12.7 μm that are attributable to vibrational transitions in polycyclic aromatic hydrocarbon (PAH) molecules.
- PAH molecules are planar structures consisting of carbon atoms organized into hexagonal rings, with hydrogen atoms attached at the boundary.

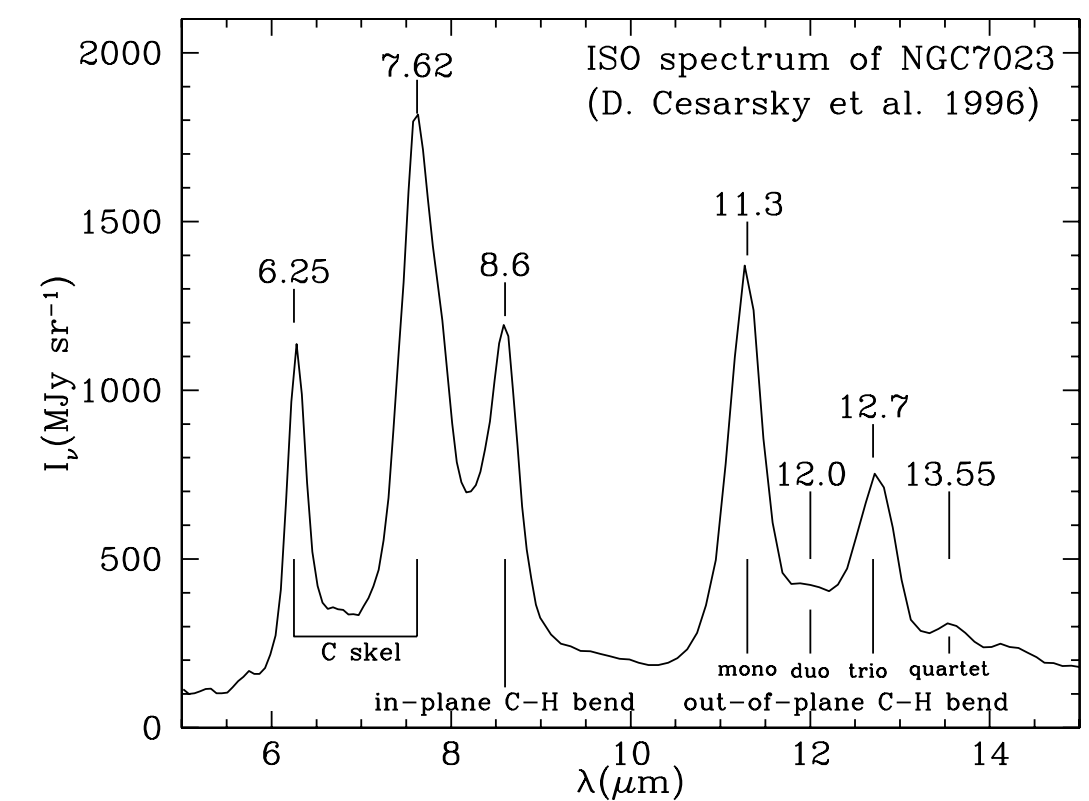


Bezene ring:
The simplest type of PAHs.

[Fig 5.6 in Krugel]



Structure of four PAHs.
[Fig 23.9 in Draine]



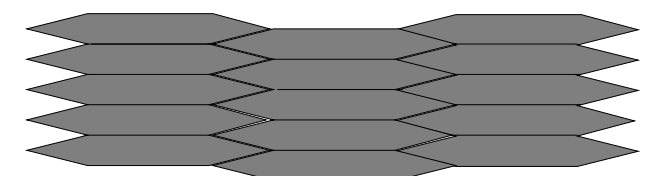
The IR spectrum of the reflection nebula NGC 7023 (Cesarsky et al. 1996)

- Graphite (흑연)

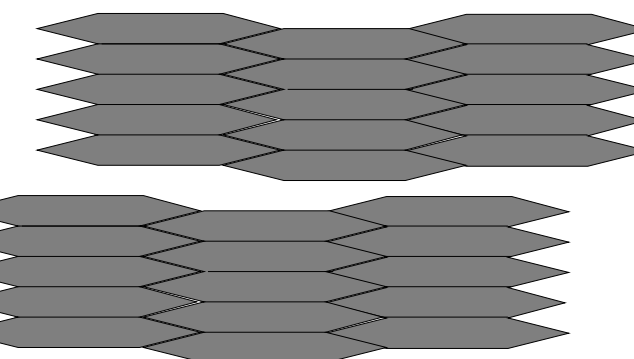
- Graphite is the most stable form of carbon (at low pressure), consisting of infinite parallel sheets of sp^2 -bonded carbon.
 - ▶ A single (infinite) sheet of carbon hexagons is known as graphene. Each carbon atom in graphene has three nearest neighbors, with a nearest-neighbor distance of 1.421\AA .
 - ▶ Crystalline graphite consists of regularly stacked graphene sheets.
 - ▶ The sheets are weakly bound to one another by van der Waals forces.



graphite sheets

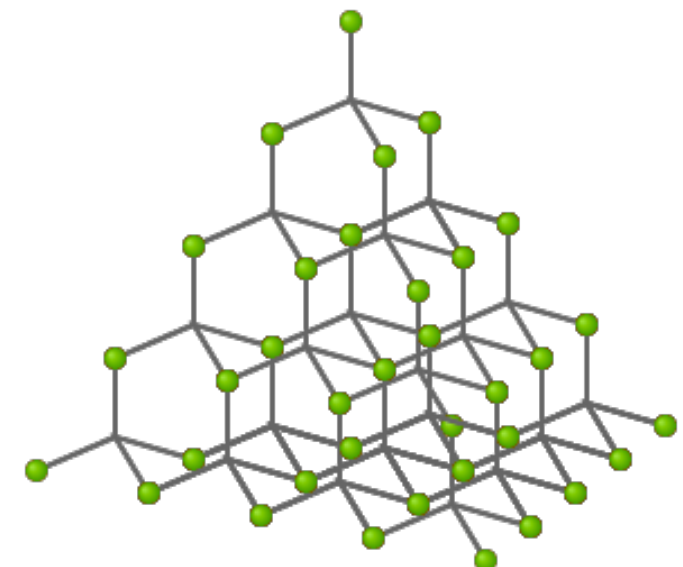


3.35\AA



- Nanodiamond

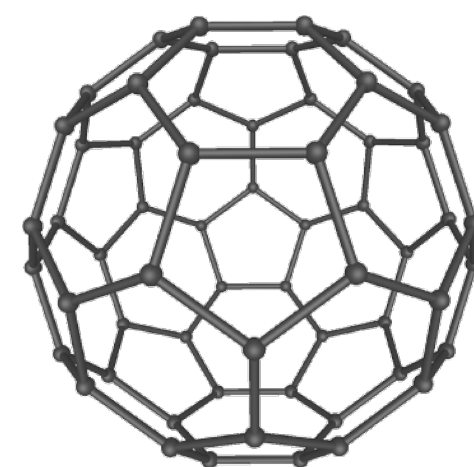
- Diamond consists of sp^3 -bonded carbon atoms, with each carbon bonded to four equidistant nearest neighbors (enclosed angles are 109.47°).
- Diamond nanoparticles are relatively abundant in primitive meteorites. Based on isotopic anomalies associated with them, we know that some fraction of the nanodiamond was of premolar origin.
- But, its abundance in the ISM is not known.



- Armorphous carbon

- Hydrogenated amorphous carbon (HAC)

- Fullerenes



Buckminsterfullerene (C_{60})

Structure of diamond.

Dust Theory: cross section and efficiency factors

- **Cross Sections:**

- A dust grain has wavelength-dependent cross sections for absorption and scattering. Extinction is the sum of absorption and scattering processes.

$$C_{\text{ext}}(\lambda) = C_{\text{abs}}(\lambda) + C_{\text{sca}}(\lambda)$$

- For a population of dust grains with number density n_d , the extinction cross section is related to the extinction coefficient and the dust optical depth by:

$$\kappa_\lambda = n_d C_{\text{ext}}(\lambda)$$

$$\begin{aligned} \tau_\lambda &= n_d C_{\text{ext}}(\lambda) L && L = \text{pathlength} \\ &= 1.086 A_\lambda \end{aligned}$$

- **Efficiency Factors:**

- The cross section is often expressed in terms of efficiency factors, normalized to the geometric cross section of an equal-solid-volume sphere:

$$Q_{\text{ext}}(\lambda) = \frac{C_{\text{ext}}(\lambda)}{\pi a^2}, \quad Q_{\text{abs}}(\lambda) = \frac{C_{\text{abs}}(\lambda)}{\pi a^2}, \quad Q_{\text{sca}}(\lambda) = \frac{C_{\text{sca}}(\lambda)}{\pi a^2}$$

$$V = \frac{4\pi}{3} a^3 \quad a = \text{the radius of an equal-volume sphere}$$

- Albedo and Scattering phase function

- The **albedo** is defined by

$$\omega(\lambda) = \frac{C_{\text{sca}}(\lambda)}{C_{\text{ext}}(\lambda)}$$

In many cases, the albedo is denoted by a or ω .

- Scattering is a function of the scattering angle and thus expressed in terms of the differential scattering cross section:

$$C_{\text{sca}}(\lambda) = \int_0^{2\pi} \int_0^\pi \frac{d\sigma_{\text{sca}}(\theta, \phi; \lambda)}{d\Omega} \sin \theta d\theta d\phi$$

- The **scattering asymmetry factor** is defined by:

$$g \equiv \langle \cos \theta \rangle = \frac{1}{\sigma_{\text{sca}}} \int_0^{2\pi} \int_0^\pi \cos \theta \frac{d\sigma_{\text{sca}}}{d\Omega} \sin \theta d\theta d\phi$$

- The scattering phase function can be described by the Rayleigh function or Henyey-Greenstein function:

$$\mathcal{P}(\theta) \equiv \frac{1}{\sigma_{\text{sca}}} \int_0^\pi \frac{d\sigma_{\text{sca}}}{d\Omega} d\phi \rightarrow$$

$\mathcal{P}_{\text{Ray}}(\theta) = \frac{1}{2} (1 + \cos^2 \theta)$ $\mathcal{P}_{\text{HG}}(\theta) = \frac{1}{2} \frac{1 - g^2}{(1 + g^2 - 2g \cos \theta)^{3/2}}$	for $\frac{2\pi a}{\lambda} \ll 1$ \longrightarrow $\langle \cos \theta \rangle = 0$	for $\frac{2\pi a}{\lambda} \gg 1$ \longrightarrow $\langle \cos \theta \rangle = g$
--	--	--

- ▶ The Henyey-Greestein phase function is only introduced for computational convenience and has no physical meaning.

Theoretical Model of the Extinction Curve

- Scattering Theory: How to calculate the theoretical extinction curve.
 - **Mie scattering** (Gustave Mie), the general solution for (absorbing or non-absorbing) spherical particles without a particular bound on particle size. ==> complex
- A model for interstellar dust must specify the **composition** of the dust as well as the geometry (**shape and size**) of the dust particles.
 - If the model is to reproduce the polarization of starlight, at least some of the grains should be nonspherical and aligned.
 - However, it is not yet possible to arrive at a unique grain model.

Models for Interstellar Dust

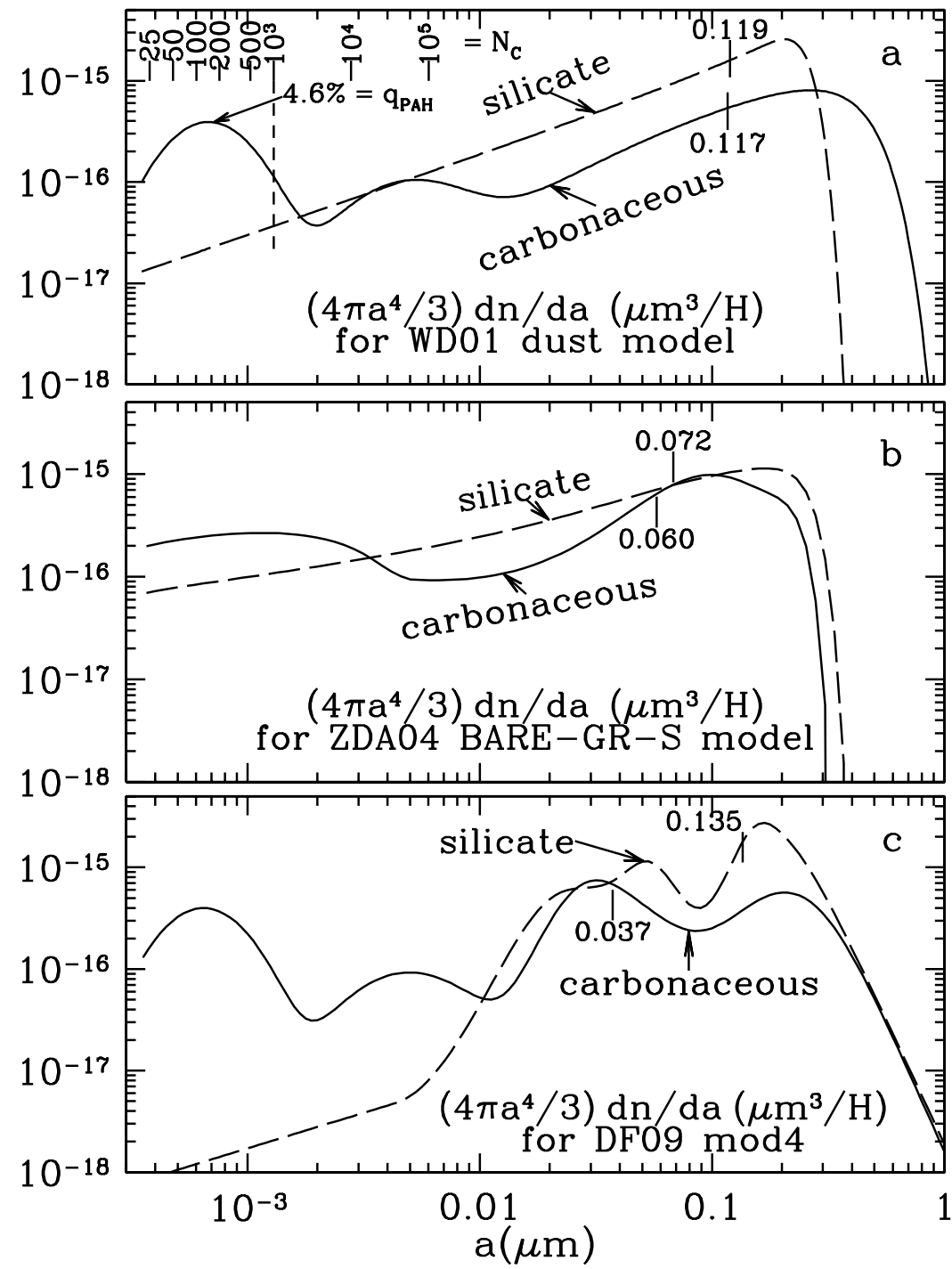
- A class of models that has met with some success assumes the dust to consist of two materials: (1) amorphous silicate, and (2) carbonaceous material.
 - ***Mathis, Rumpl, and Nordsieck (1977; MRN)*** found that models using two components, silicate and graphite spheres with power-law size distributions, could reproduce the observed extinction from the near-IR to the UV ($\lambda = 0.11\mu\text{m} - 1\mu\text{m}$).

$$\frac{dn_{\text{gr}}}{da} da = A_i n_{\text{H}} a^{-3.5} da \quad \text{for } a_{\min} \leq a \leq a_{\max}$$

$a_{\min} \approx 0.025\mu\text{m}$
 $a_{\max} \approx 0.25\mu\text{m}$

$$A_{\text{sil}} = 7.8 \times 10^{-26}, \quad A_{\text{gra}} = 6.9 \times 10^{-26} \text{ cm}^{2.5} (\text{H atom})^{-1}$$

- ▶ Graphite was a necessary component. The other could be silicon carbide (SiC), magnetite (Fe_3O_4), iron, olivine, or pyroxene.
- ***Draine and Collaborators***
 - ▶ Draine & Lee (1984) presented self-consistent dielectric functions for graphite and silicate, and showed that the graphite-silicate model appeared to be consistent with what was known about dust opacities in the Far-IR. (extended the MRN model to the Far-IR).
- ***Zubko et al. (2004)***
 - ▶ The size distribution of the “BARE-GR-S” model of Zubko et al. (2004), composed of bare graphite grains, bare silicate grains, and PAHs, differs significantly from the WD01 size distribution.



A “typical” grain size may be taken as the half-mass grain size $a_{0.5}$, defined so that half the mass of dust is in grains of radius $a_{0.5}$ or greater.

Size distributions for silicate and carbonaceous grains for dust models from (a) Weingartner & Draine (2001), (b) Zubko et al. (2004), and (c) Draine & Faisse (2009).

In each case, tick-marks indicate the “half-mass” radii for the silicate grains and carbonaceous grains.

[Fig 23.10 Draine]

Temperatures of Interstellar Grains

- The “temperature” of a dust grain is a measure of the internal energy present in vibrational modes and possibly also in low-lying electronic excitations.
- Grain Heating
 - In diffuse regions, where ample starlight is present, grain heating is dominated by absorption of starlight photons.
 - In dense dark clouds, grain heating can be dominated by inelastic collisions with atoms or molecules from the gas (grain-grain collisions are too infrequent).
- When an optical or UV photon is absorbed by a grain, an electron is raised into an excited electronic state; three cases can occur.
 - If the electron is sufficiently energetic, it may be able to escape from the solid as a **“photoelectron.”**
 - In most solids or large molecules, however, the electronically excited state will deexcite nonradiatively, with the energy going into ***many vibrational modes - i.e., heat.***

Temperature of Large Grains and Small Grains

- Large Grains
 - Grains with radii $a \gtrsim 0.03 \mu\text{m}$, can be considered “classical.” These grains are macroscopic
 - absorption or emission of single quanta do not appreciably change the total energy in vibrational or electronic excitations.
 - The temperature of a large dust grain can be obtained by equating the heating rate to the cooling rate.
- Very Small Grains
 - For ultra-small particles, ranging down to large molecules, quantum effects are important (this include the “spinning” dust grains responsible for microwave emission).
 - When a dust particle is very small, its temperature will fluctuate. This happens because whenever an energetic photon is absorbed, the grain temperature jumps up by some not negligible amount and subsequently declines as a result of cooling.
 - To compute their emission, we need their optical and thermal properties.
 - ▶ The optical behavior depends in a sophisticated way on the complex index of refraction and on the particle shape.
 - ▶ The thermal behavior is determined more simply from the specific heat.
 - We need to calculate the distribution function of temperature.

Heating & Cooling

- Radiative Heating rate (for a single particle):
 - the rate of heating of the grain by absorption of radiation can be written.

$$\begin{aligned} \left(\frac{dE}{dt} \right)_{\text{abs}} &= \int \frac{u_\nu d\nu}{h\nu} \times c \times h\nu \times Q_{\text{abs}}(\nu) \pi a^2 \\ &= \int d\nu 4\pi J_\nu Q_{\text{abs}}(\nu) \pi a^2 \end{aligned}$$

Here, $u_\nu d\nu/h\nu$ is the number density of photons; the photons move at the speed of light c and carry energy $h\nu$.

- Radiative Cooling rate (for a single particle)

- Kirchhoff's Law in LTE

j_ν = emissivity per unit volume

κ_ν = absorption coefficient per unit length

j_ν/n_d = emissivity per particle

$\kappa_\nu/n_d = C_{\text{abs}}(\nu)$ = absorption cross section

n_d = number density of dust particles

$$\frac{j_\nu}{\kappa_\nu} = B_\nu(T) \Rightarrow \frac{j_\nu}{n_d} = C_{\text{abs}}(\nu) B_\nu(T)$$

[$B_\nu(T)$ = Planck function, $\kappa_\nu = n_d C_{\text{abs}}(\nu)$]

- Grains lose energy by infrared emission at a rate:

$$\left(\frac{dE}{dt} \right)_{\text{emiss}} = \int d\nu 4\pi j_\nu / n_d = \int d\nu 4\pi B_\nu(T_d) C_{\text{abs}}(\nu)$$

- In general, the absorption cross section in the far-IR can be approximated as a power-law in frequency,

$$Q_{\text{abs}}(\nu) = Q_0(\nu/\nu_0)^\beta = Q_0(\lambda/\lambda_0)^{-\beta} \quad (1 \lesssim \beta \lesssim 2)$$

in the far-IR

then the Planck average can be obtained analytically:

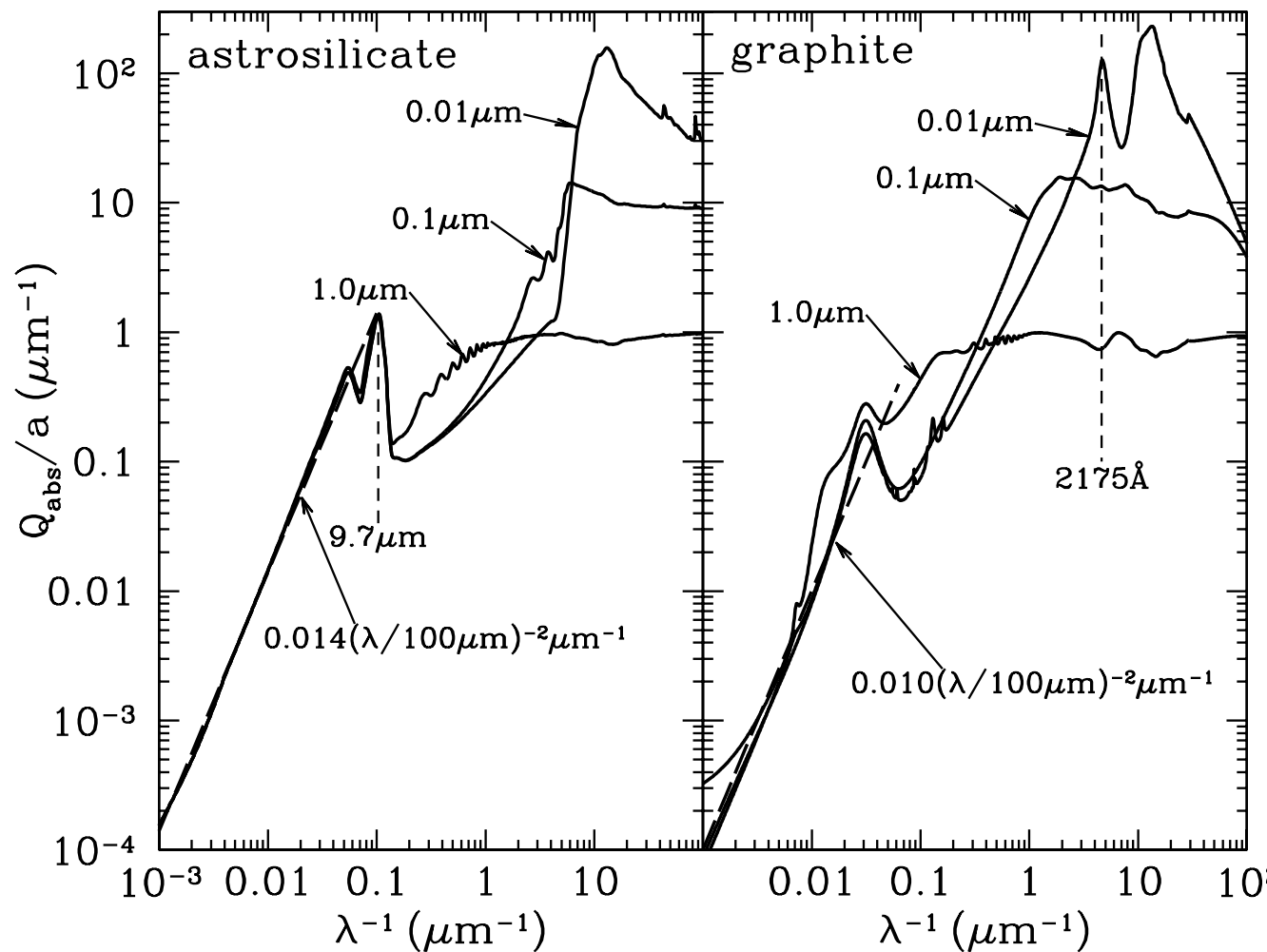


[Fig 24.1, Draine]

$$Q_{\text{abs}} \approx 1.4 \times 10^{-3} \left(\frac{a}{0.1 \mu\text{m}} \right) \left(\frac{\lambda}{100 \mu\text{m}} \right)^{-2}$$

silicate, $\lambda \gtrsim 20 \mu\text{m}$

$$\approx 1.0 \times 10^{-3} \left(\frac{a}{0.1 \mu\text{m}} \right) \left(\frac{\lambda}{100 \mu\text{m}} \right)^{-2}$$

graphite, $\lambda \gtrsim 30 \mu\text{m}$

Using the power-law approximation is valid because we are interested only in the Far-IR.

Equilibrium Temperature

- Steady state temperature of large grains
 - The balance equation between the heating and cooling is:

$$\left(\frac{dE}{dt} \right)_{\text{abs}} = \left(\frac{dE}{dt} \right)_{\text{emiss}} \Rightarrow \text{calculate the temperature of grains.}$$

- As a result, the temperature of a large grain is given by:

$$T_d \approx 16.4 (a/0.1 \mu\text{m})^{-1/15} U^{1/6} \text{ K, silicate } (0.01 \lesssim a \lesssim 1 \mu\text{m})$$

$$\approx 22.3 (a/0.1 \mu\text{m})^{-1/40} U^{1/6} \text{ K, graphite } (0.005 \lesssim a \lesssim 0.15 \mu\text{m})$$

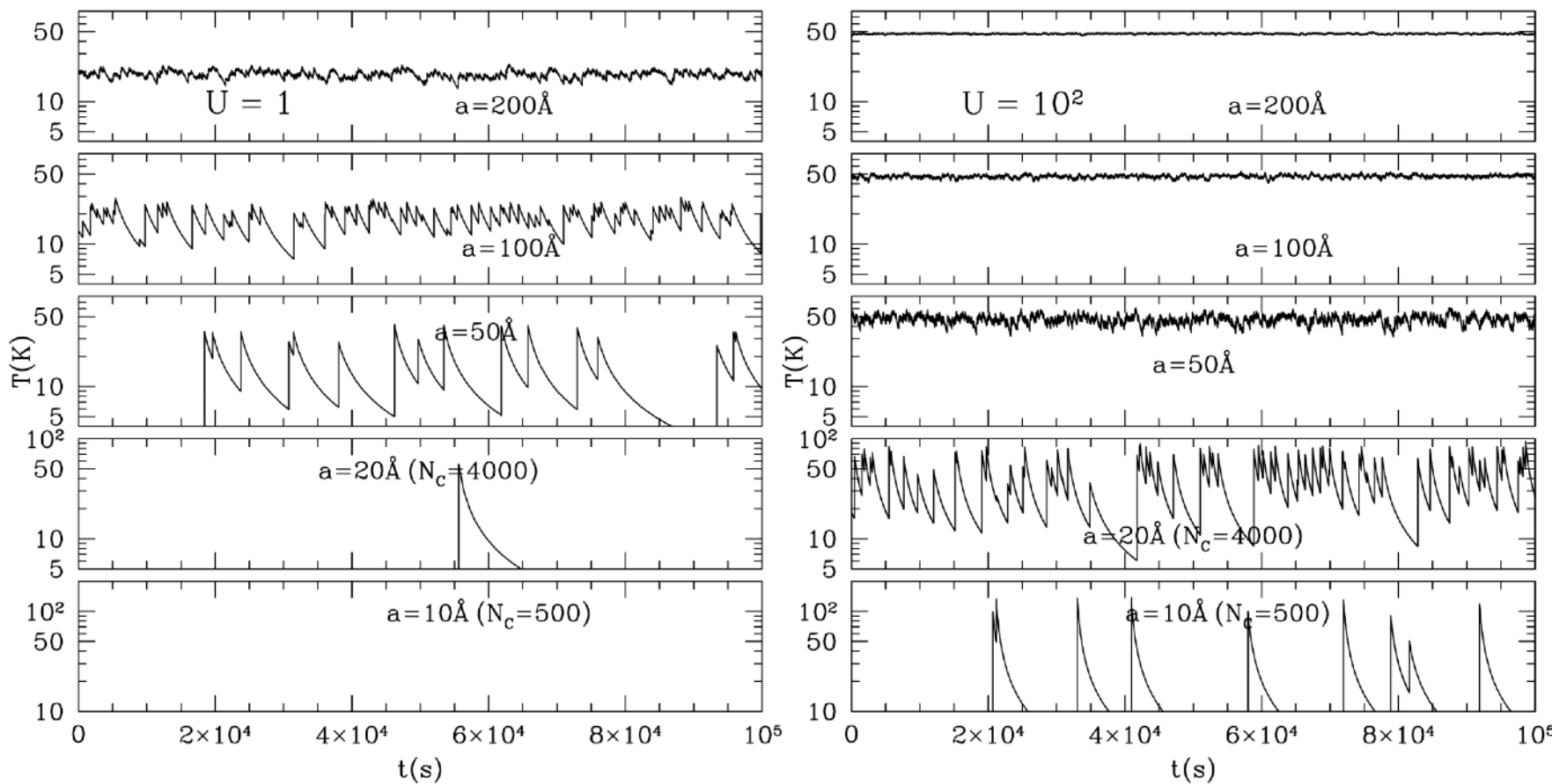
U = strength of the interstellar radiation field in units of Mathis model.

- Implications
 - ▶ If the ISRF is doubled, the grain temperature increases by $\sim 12\%$. In order to increase the temperature by a factor of 2, 64 times stronger radiation is required.
 - ▶ ***There is also little dependence of the grain temperature on grain radius. Therefore, large grains can be regarded to be grains with a single size.***

Stochastic Heating of Very Small Grains

- Temperature History:

- ▶ Two effects become increasingly important with diminishing grain size: (1) the heat capacity of the dust becomes sufficiently small that single-particle hits can cause large spikes in the dust temperature and (2) the absorption rate with photons becomes sufficiently low that the cooling of the dust between successive collisions becomes important.
- ▶ ***Therefore, for very small dust grains, it is clear that one cannot speak of a representative grain temperature under these conditions - one must instead use a temperature distribution function.***



Monte-Carlo simulations of the temperature fluctuation: Temperature versus time during 10^5 s (~ 1 day) for five carbonaceous grains in two radiation fields: the local starlight intensity ($U = 1$; left panel) and 10^2 times the local starlight intensity ($U = 10^2$; right panel). The importance of quantized stochastic heating is evident for the smallest sizes.

[Fig 24.5, Draine]

-
- [Q3]
 - Suppose that we observe a radio-bright QSO and detect absorption lines from Milky Way gas in its spectra. The 21 cm line is seen in optically-thin absorption with a profile with $\text{FWHM}(\text{H I}) = 10 \text{ km s}^{-1}$. We also have high-resolution observations of the Na I doublet lines referred to as D_1 (5898Å) and D_2 (5892Å) in absorption. The Na I D_2 5892Å line width is $\text{FWHM}(\text{Na I } D_2) = 5 \text{ km s}^{-1}$. The line profiles are the result of a combination of thermal broadening plus turbulence with a Gaussian velocity distribution with one-dimensional velocity dispersion $\sigma_{v, \text{turb}}$.

You will want to employ the following theorem: If the turbulence has a Gaussian velocity distribution, the overall velocity distribution function of atoms of mass M will be Gaussian, with one-dimensional velocity dispersion:

$$v_{\text{rms}}^2 = \sigma_v^2 = \sigma_{v, \text{turb}}^2 + \frac{2kT}{M}$$

- If the Na I D_2 line is optically thin, estimate the kinetic temperature T and $\sigma_{v, \text{turb}}$. Note that for a Gaussian function, $\text{FWHM} = 2\sqrt{2 \ln 2}\sigma$.

Homework (due date: 03/31)

[Q4]

Look up (google) the absolute magnitude of the Sun at V band. What would the apparent magnitude be for a solar twin at the Galactic center? What would it be with dust assuming that the extinction along the Galactic plane is 1 mag/kpc?

[Q5]

If the dust extinction A_λ were a power law in the wavelength, $A_\lambda \propto \lambda^{-\alpha}$, what would be R_V as a function of α ?

What value of α would give $R_V = 3.1$?